TECHNICAL MEMORANDUM

40

The production of a new orography, land sea mask and associated climatological surface fields for operational purpose

S. Tibaldi and J.-F. Geleyn

Research Department

August 1981

European Centre for Medium-Range Weather Forecasts
Europäisches Zentrum für mittelfristige Wettervorhersage
Centre européen pour les prévisions météorologiques à moyen

1. Introduction

The production of a more realistic orography and associated climatological surface fields, and the assessment of their impact on medium range weather forecasts has been a major undertaking for the research department since 1979 and has involved the effort of several people.

This technical memorandum serves the purpose of explaining how these fields have be prepared (Part 2), how their impact on the operational suite has been assessed (Part 3), and also what the plans for future work are (Part 4).

2. Preparation of the fields

The fields that have been produced, at various stages and by different people, are the following:-

a) Surface geopotential (so-called "orography") (Geleyn-Tibaldi).

b) Land-sea mask (0 on water and ice, 1 on land) (Geleyn-Tibaldi).

c) Roughness length (Geleyn).

d) Albedo (annual climatology) (Geleyn).

e) Surface temperature (monthly climatology) (Tibaldi).

f) Surface soil water content (monthly climatology) (van Maanen).

g) Snow cover (monthly climatology) (van Maanen).

2.1 Orography

Orography (in m) was derived from the US Navy 10' lat-lon regularly gridded orography, provided by NCAR. A program was written that computes the average heights on any user-supplied lat-lon grid with resolution coarser than the original 10' (~20km) data resolution.

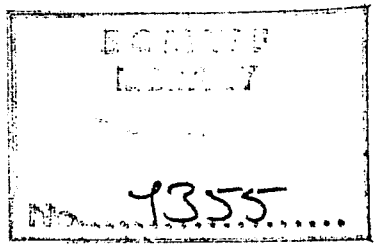

After having produced an N48 version of this orography, we passed a grid point filter with bi-dimensional normalised gaussian weights of the type

$$W_{ij} = n_i e^{-(d_{ij}^2 / 2D^2)}$$

d_{ij} = distance between centre point and surrounding points

n_i = normalisation factor: $1/\sum_j e^{-(d_{ij}^2 / 2D^2)}$

D = radius of filter: ≃ 100 km

2.2 Land-sea mask

The N48 coastline field (0 on water and ice, 1 on land) was similarly obtained from the same US Navy tape using the percentage of area covered by water for all tye 10' grid and averaging on the N48 grid. No filter was applied.

It should be noted that from the moment this new set of surface parameters has been brought into operation, the concept of soil nature (land/sea or sea ice) was disconnected from the physical height of the topography. Some partially land-covered ocean grid points are catalogued as sea, but the effective geopotential assigned to them is $\neq 0$. Values less than zero are also possible (e.g. Caspian area).

2.3 Roughness length

The procedure to decide z_o (roughness length in meters) was the following):

a) z_o data on vegetation obtained on a 5^o x 5^o grid from Munich University (Baumgartner et al., 1976) were interpolated using bicubic splines to an N48 grid. Information about land/sea was used during interpolation.

b) Information was extracted, as previously for topography and water covered area, about urbanisation. A value proportional to 2.5 meters for 100 % town area was assumed.

c) Information was also extracted from the same source about the number of significant ridges and of topography maximum excursion in a 10' x 10' box. This was combined with an analysis of the variance and number of

extremes of the 10' grid topography with respect to the main N48 value into the following formulæ for z_o (roughness height ∝ to variance x slope) :

$$z_o = \sqrt{\frac{N}{F}} \left(\sum p_i h_i^{-2} - \left(\sum p_i h_i\right)^2\right)$$

$$+ \sum \sqrt{\frac{n_i}{f_i}}\ p_i\ \frac{(\bar{h}_i - h_i^{min})\ (h_i^{max} - \bar{h}_i)}{4}$$

where : N = number of relative $\bar{h}_i$ maximum in the user-defined grid square

F = surface area of the user-defined grid square

n_i = number of significant ridges in the 10' grid square

$\bar{h}_i$ = mean height in the 10' grid square

h_i^{max} = maximum height in the 10' grid square

h_i^{min} = minimum height in the 10' grid square

f_i = surface area of the 10' grid square

p_i = proportion of the user-defined grid square occupied by the i^{th} 10' grid square

A provisional z_o value was derived using a pythagoric combination of a), b) and c) values. On sea and sea ice this was reset to .001 m. The logarithm of this field was, in turn, smoothed with the same filtering operator as used for the orography, but with $D \tilde{=} 200$ km. The final z_o was then obtained by the exponentiation of the smoothed log field plus a second resetting of sea and sea ice values to .001 m. Of course, on open sea this value is only used by the model as a background, since the Charnock formula is used to diagnose an effective (time-dependent) value of z_o.

2.4 Albedo

Values (0 ÷ 1) were derived from Nimbus 3 data following the method of Preuss (Preuss and Geleyn, 1980).

The values were smoothed with a 9 grid point cross operator:

$$\begin{matrix} 1 & 2 & 1 \\ 2 & 4 & 2 \\ 1 & 2 & 1 \end{matrix}$$

Sea values were set to .07, sea ice to .55 and land values were bound within the interval .07 - .80.

This, of course, is only a background yearly climatological field that the model alters, while running, over snow-covered areas, values being then closer to .8 .

2.5 Surface Temperature

The monthly climatological fields of surface temperature have been computed with the following procedure:

Over land the surface has been assumed to have the same temperature as the air temperature for the same geopotential height as interpolated from the NCAR 5^{o} x 5^{o} standard pressure level monthly temperature climatology (Alexander and Mobley, 1974). The horizontal grid-to-grid bilinear interpolation (using routine LINTRP by Rex Gibson) was carried out first, then vertical interpolation (or, occasionally, extrapolation when the climatological surface pressure was higher than 1000 mb) was carried out linearly in height, using height climatology along with temperature climatology. Since 1000 mb height climatology was not available, it was derived from MSLP and 1000 mb T climatology.

Over water, the surface temperature has been derived by bilinear interpolation (see above) of the monthly sea surface temperature RAND 1^{o} x 1^{o} climatology (Crutcher and Jenne, 1970).

Over ice (as specified by the same RAND source) the surface tempereture was taken as the minimum between the temperature as defined by the land procedure and $0^{o}C$.

2.6 Soil water content (J. van Maanen)

The soil water content climatology is determined from the climatological rainfall and temperature. It is assumed that the rain falls as a continuous process. Water is removed from the soil layer considered by evaporation and the sinking into deeper layers. The amount of water thus removed is dependent on the amount already present, and by equating the removal and the precipitation, a solution for the soil water content results.

2.7 Snow (J. van Maanen)

For each month of the year the snow climatology is obtained by considering the climatological snow depth of the previous month, the precipitation amount and the temperature. The precipitation is divided into rain or snow, depending on the temperature. The snow is added to the snow cover of the previous month, and an assumption on the amount of snow melt depending on temperature is made. The snow depth thus obtained is then converted into water content. In areas with eternal snow, however, a value of 50 m water content is assigned.

For further details on 2.6 and 2.7, see van Maanen, 1981 (in preparation).

3. Evaluation of the impact of the new orography on the operational suite

Several orographies were tried, at different stages, before the final choice was made (see section 2.1).

These orographies were the following:

OØ Old (operational) orography (from GFDL, Berkofsky and Bertoni, 1955), see Fig. 1.

O1 Unfiltered orography

O2 Ridge-saving filtered orography, see Fig. 2

O3 Gaussian filtered orography, D = 100 km (light filter), see Fig. 3

O4 " " " , D = 200 km (heavy ")

O5 T32 Spectral Truncation of O1 (noise up to 6 Δ x filtered)

Fig. 4 shows the spectral behaviour of two (O2 and O3) of the "new" orographies compared to the old OØ.

The spectra are computed using the amplitudes of the spectral harmonic coefficient and are, therefore, strictly isotropic.

For orographies O1 and O3 tests were made to assess the impact of the land-sea mask alone: in one case the new coastline field was imposed (DØ2), in the other the old coastlines were left operation (DØ6). Maps of the experiments and objective verifications showed a negligible impact (see, for example, Fig. 5 and Fig. 6). For the sake of simplicity, we will, therefore, from now on refrain from specifying the coastlines used in experiments.

Despite errors and inconsistencies that prevented most of our comparisons from being absolutely clean, the assessment procedure can be schematically divided into three parts:

a) Assessment of old (very smooth and unrealistic) orography against a new, very realistic (but also rough) one. This showed that the impact of a "new" orography on a 10-day forecast was positive enough to justify the search for an "optimal" realistic orography to be put in operation.

b) Choice of new operational orography among various filtered versions of O1. The choice was made to put O3 through a final set of benchmark tests.

c) Benchmark Tests of O3 VS OØ in a quasi-operational environment (several data assimilation cycles + 10d test). Errors and unforeseen problems with the interaction between orography and data assimilation system transformed this apparently simple operation into a major research effort.

We will now expand on these three points.

3.1 Assessment of the old (OØ) versus a new (O2) orography)

The exact procedure by which O2 was produced is lengthy and irrelevant to the point we are making, since the differences between O2 and O3 are minor and have later been assessed as of almost negligible impact. It should suffice to say that the general criterion used to produce O2 was to smooth O1 with a local grid point filter everywhere, apart from major ridges and valleys where the actual unsmoothed values were kept unmodified.

Differences appear obvious to the eye looking at Figs. 1 and 2. Larger scale features, although heavily smoothed OØ, are not substantially different, but synoptic and subsynoptic topographical features (such as the Alps, the Scandinavian mountains, the Atlas mountains, etc.) are almost absent in OØ while they are well described by O2. (See also Fig. 4 for an objective estimate of the different small scale content of the two orographies).

This comparison took place in the following set of cases:

- 16th January 1979 (two different analyses, BØ3 and B93)
- ensemble of four operational cases (24.10.79., B17, 8.11.79., B18, 15.11.79., B20, 13.12.79., B45)
- one more operational case (29.1.80., B96)
- one "climatological" (50 day) run (16.01.79., B53)

All these cases were run starting from p-file analysis and interpolating from p to σ to a newly defined set of σ surfaces (new orography), initializing and then running a 10-day forecast with the same model as the control (old orography) case.

The 16th January case was tried with two different analyses (BØ3 new, BØ4 old and B93 new and B83 old), but both experiments showed that the impact of the new topography on this particular case was not decisive or, if anything, negative (Figs. 7 to 8).

The ensemble of four operational cases, on the contrary, showed a markedly positive impact, mainly on the long waves and, more precisely, on their stationary part (Figs. 9 to 12). The synoptic evaluation of the four cases showed a small but overall positive impact (see, for example, Appendices A and B by Du X-Y).

One of these four cases (13.12.79) was repeated (B54), preceded by five new orography data assimilation cycles, showing a further substantial improvement in the scores and in the synoptic evaluation (Figs. 13 and 14 and Appendix B).

One more operational case (29.01.80, B96) was also run, showing a rather contrasting behaviour of the objective scores of height and temperature (Fig. 15 and 16) but little synoptic impact (see Appendix C).

The climatological run (50 days, B53), besides showing markedly improved 500mb and 1000mb 20 days mean maps (see Figs. 17 and 18) compared with a twin old orography run (B52), showed a somewhat different, if not better, transient waves variance (Figs. 19 and 20) and marginally smaller deviations of U and T from observed (Fig. 21).

A comparison of 25 days mean precipitation maps showed no discernable worsening of the patterns of large scale precipitation (as compared with climatology) (Fig. 22), together with noticeable differences in convective precipitation.

These last differences being mainly confined to SH tropical land areas and being not of worrying amplitude (Fig. 23), although showing, in the same areas, a remarkable reduction of the horizontal scale of the convective rain patterns, were, at the time, (wrongly) considered as tolerable.

Future experience would have shown that different horizontal diffusion (linear rather than non linear) coupled with different synoptic situations (NH spring and summer, rather than winter) and the diversity of the land (and therefore sharp orographic features) distribution in the mid-latitude belt between NH and SH meant major changes in the behaviour of the convective precipitation in the presence of steeper orography.

Work is presently being done to overcome difficulties arising from this detrimental interaction and there are indications that a better diffusion scheme can substantially alleviate this difficulty. (See Burridge and Tibaldi, 1981).

3.2 Choice of the new operational orography

Orographies O1, O3, O4 and O5 were assessed comparatively on two cases, a newly available analysis of the 79.01.16.00 case and on a new "summer" case, the 80.06.05.12 case. This last experiment was also meant to give us some indication of the performance of "new" type orographies in summer cases.

Orography O2 was, at this stage, also compared to orographies O1 and O5 but it was decided to replace it, so to speak, in the list of possible orographies, with the almost equivalent orography O3, since the algorithm to produce O3 (filter) is homogeneous rather than inhomogeneous. The level of noise left in the orography seemed, by eye, slightly lower, while the synoptic features retained were practically the same (see again Figs. 2 and 3).

The overall order of merit was the following:

	orog.	79.01.16.00 exp.	80.06.05.12 case
1st	O3	C 80	D 02
2nd	O5	C 88	D O3
3rd	O1	C 78	D O5
4th	O4	C 79	D O4
reference exp.(old)		C 63	D 14

For the relevant scores see Figs. 24 to 29. Orography O1 (very rough), although not doing badly scorewise in the second case, was marked down on account of generating too much noise. It should be remembered that synoptic sonsiderations also played a part in deciding the final order of merit exposed above.

On the basis of the experiments performed and also on the ground of considerations of principle, it was then decided to go ahead and benchmark the O3 orography together with the new surface and climatological parameters for operational use.

Since we wanted to benchmark all new surface fields in operation at the same time, we had to assess at least in one case the impact of roughness length alone (D60 vs C80, Fig. 30) and all surface fields, orography excluded, together (E40 vs NM2, Fig. 31); z_o getting the preferential treatment because it was the most likely to have a detectable impact.

The results showed very little sensitivity to the specification of these fields, as it can be seen from the scores, but, if anything, the impact was small and positive for both changes.

3.3 Benchmark Tests of O3 (and new surface fields) versus OØ in a quasi-operational environment

Originally five cases were chosen from recent operations with the aim of forming a climatologically coherent picture that could be considered an "ensemble".

These cases were the following:-

case	YY MM DD HH
NMØ	80-10-08-12
NM1	80-10-24-12
NM2	80-11-02-12
NM3	80-11-10-12
NM4	80-12-18-12

The procedure was to repeat the operational sequence for the dates shown, that is to start from 12Z the day before (insert the new topography via a full field p to sigma interpolation), run 4 data assimilation cycles and then a 10-day forecast. For this purpose it was decided to use the Operations Department Test Suite.

Since in the time interval between the last but one date (NM3) and the beginning of the benchmarking experiments, interpolation of full fields (IFF) had been replaced, in the analysis suite, by interpolation of increments (II), we could not have a perfectly clean comparison. This was because we wanted to test the system in the same conditions in which it was meant to operate. However, we felt, on the basis of past experience with the introduction of II (in the presence of the old orography!), that this would not matter very much since the previously observed impact of II was far smaller than the "new orography" one. We also hoped that four data assimilation cycles were enough to reabsorb the shock caused by the insertion of the new orography.

The first set of experiments showed a surprisingly catastrophic impact of the new set of surface fields. An important error was, however, discovered: the ocean was treated like a desert, from the point of view of surface exchanges.

The experiments were repeated but, unfortunately, the error was only partially removed. A few ocean points (along coastal lines) were still ill-treated in the second set of experiments.

The results were far better than in the first set but still not as good as expected and, moreover, presented an almost reversed picture from the previous ensemble set (para. 3.1), (see Figs. 32 and 33). We firstly attributed the difference in behaviour to the remaining land/sea error and re-ran the worst case (NM2) with no error at all (NM6) to see the difference. The results, albeit again improved, remained far below expectations and persisted in presenting us with the above-mentioned reversed behaviour (see Fig. 34).

To explain the remaining difference we only had three possible causes left at our disposal. These were:

(a) O3 was used this time, instead of O2.

(b) II was used in place of IFF.

(c) The additional cumulative impact of z_o, L/S and the other climatology surface fields.

Case (c) having already been ruled out by a few clean experiments (see para. 3.2), we did a clean test to isolate either (a) or (b).

To achieve this we ran three more experiments (E53, E55, E65) and made the following comparisons (all on the same 80.11.02.12 particularly bad case):

ØØ2 old orography, with IFF

NM6 O3 orography, four cycles with II (like previous NM2 but with bugs removed)

E53 O2 orography, four cycles but IFF p to sigma before 10d-forecast

E65 O3 " " " " " " " "

E66 OØ (old) orography, four cycles with II (like NM6 but with old orography).

Fig. 35, comparing ØØ2, NM6 and E53 shows that a p to sigma IFF before the 10day forecast makes a "new" type topography (O2, E53) behave more like an "old" (ØØ2) with IFF rather than like another "new" (O3, NM6) but with II.

Fig. 36, comparing NM6, E53 and E65 shows that orographies O2 and O3 behave similarly; what makes the difference is II or IFF.

Fig. 37, comparing E66 (a 4 cycles old orography II forecast) with ØØ2 (operational IFF forecast) confirms the importance of the role of interpolation,

showing that, even with the old orography, four cycles after a p to sigma IFF are not enough to bring the II data assimilation system back to regime. A "new" orography would, of course, take even longer to settle down or show an even worse impact before reaching regime.

So, to our only partial surprise, the type of new orography used (O3 or O2) turned out to be almost irrelevant, while the interaction between the insertion of the new orography and either II or IFF was shown to be crucial. This interaction was considered big enough to explain all major differences in behaviour between the two "ensemble" set of cases.

The last (known) question left to be answered was whether this detrimental interaction would, in fact, disappear with protracted data assimilation cycling or not. To discover this was the purpose of the last test (81-02-12-12-, Exp E76, this date being chosen because it was inside the period of II being operational). The test involved three preceding days of data assimilation before running the 10-day forecast. Results of this test are shown in Figs. 38 to 43.

The quality of the results, in terms of both scores (Figs. 38 to 41) and synoptic assessment (Figs. 42 and 43), looked good enough to justify the operational switch to new orography and new surface fields that took place on 1st April 1981 (!).

A note should be added; during the second ensemble, one case (NM2) showed a highly noisy 500 mb height field up and downstream of a very strong cross-Greenland flow. A re-run of the same experiment with no total tendency chopping of prognostic fields showed a totally changed situation, with no detrimental effects on the synoptic quality of the forecast.

Past experience had already shown that, with the introduction of the implicit linear ∇^4 diffusion, the total tendency chopper was no longer needed and, if anything, that its impact was slightly negative on scores (and computer time lost). It was, therefore, decided to remove it from operations a few days in advance of the insertion of the new topography.

4. Plans for future work

Plans for future work on the specification of orography in numerical models include:

(a) Quantitative assessment of the impact on long waves of small-scale topographically generated noise, due to either steep-orography induced truncation errors, or due to spurious feedback processes

via physical parameterization.

(b) More case studies on different orographies (e.g. of the ridge-saving type or or the Shapiro-filtered type) for the GP model to achieve a better balance between small scale detail and 2 & 3 grid interval noise generation.

(c) Studies on the sensitivity of spectral integrations to the specification of the orography field before the spectral truncation (e.g. unfiltered vs envelope-type).

(d) Possible incorporation of an Egger-type orography to include stronger low-level blocking effects.

Acknowledgments

Several people were involved in this long exercise and provided us with assistance with various problems - Jan Haseler and Rex Gibson with model and post-processing problems, Dave Shaw with rejections and interactions with the data assimilation suite, Jan van Maanen with the creation of some climatological fields, Gerard Cats with the creation of new climatological tapes and, most of all, Brian Norris with repeated assistance in the use of the Test Suite - we gratefully acknowledge their help. We are also indebted to Dr. Du Xing-Yuan for his synoptic assessment of some of the experiments (Appendices A to C). We should also mention the kind and efficient assistance we always receive from the Printing Office staff.

REFERENCES

Alexander, R.C. and Mobley, R.L., 1974 Monthly average sea-surface temperatures and ice-pack limits on a 1° global grid. RAND Rep. R-1310-ARPA.

Baumgartner, A., Mayer, H. and Metz, W., 1977 Weltweite Verteilung des Rauhigkeitsparameters Z_o mit Anwendung auf die Energiedissipation an der Erdoberfläche. Meteorol. Rdsch.,30, 43-48.

Berkofsky, L., and Bertoni, E.A., 1955 Mean topographic charts for the entire earth. Bull. Amer. Meteor. Soc., 36, 350-353.

Burridge, D. and Tibaldi, S. 1981 On a spurious feedback between horizontal diffusion and parameterization of convection triggered by sharp orographic features. ECMWF Technical Memorandum No.41.

Crutcher, H.L. and Jenne, R.J., 1970 An interim note on Northern Hemisphere climatological grid data tape NOAA Environmental Data Service, NWRC, Asheville.

Preuss, J.H. and Geleyn, J-F., 1980 Surface Albedos Derived from Satellite Data and their Impact on Forecast Models. Arch. Met. Geoph. Biokl. A, 29, 345-356.

van Maanen, J., 1981 ECMWF Internal Memorandum (in preparation).

SYNOPTIC ASSESSMENT OF THE NEW OROGRAPHY: EXPERIMENT B17

by

Du Xing-Yuan

Abbreviations

ECA: verification (ECMWF Analysis, 24-10-1979 to 5-11-1979)
024: predictions with old mountain produced by Operations
B17: predictions with new mountain

Comparisons of the 10-day forecasts by B17 and 024

The ECA are made up by using the old mountain. Therefore, these comparisons have a bias towards the 024. In the initial fields, the 024 are identical with ECA. But for B17, on 500 mb, the closed low centre over the Bering Strait is rather smaller; and on 1000 mb, the cold centre over the Plateau of Tibet is lost.

For ECA and 024, over the Plateau of Tibet, there are always existing strong cold centres on 1000 mb level, not only at the initial time (24 October 1979, 12 GMT) but also in the other ten forecasts up to 3 November. It seems to us that this anomalous phenomenon is not connected with the forecasting model, and is purely a consequence of the interpolation from sigma-coordinates to p-coordinates. Anomalous temperature fields may be obtained as a result of such interpolation if an unsuitable temperature lapse rate is used. Recently, Chinese researchers had shown that in the region of the Qinghai-Tibet Plateau it is better to use a mean lapse-rate of $0,45^{\circ}C/100$ m instead of $0.6^{\circ}C/100$ m in reducing ground level data to sea level to obtain a consistent thermal field.

DAY 1

The B17 and 024 are more similar to each other than they are to ECA. For 500 mb, some prediction deficiencies can be easily found in the temperature field. A few newly generated thermal centres have not been predicted. For example, in the bottom of the Icelandic trough a cold centre with two isolines is formed, and a cut-off low is likely to appear. In the upwind side of the Rocky Mountains a cold centre is formed, and over the Tibet plateau a warm centre is formed.

On the contrary, for 1000 mb forecasts the deficiency is more evidently reflected on the pressure field. A high pressure centre over Iran has not been predicted. In the predicted charts over Tunisia one can see a low pressure centre with two isolines which is not present on ECA. The differences between B17 and 024 are not discernable yet. But one can see the influence of the initial analyses on the forecasts. For example, over the Bering Strait, the shape of a 500 mb low pressure pattern in 024 is more similar to ECA than that on B17. The above-mentioned facts suggest that barotropic processes are caught fairly well by the model.

The main efforts to improve the forecast should be focussed on baroclinic processes, especially those caused by the mountain ranges.

DAY 2

One can see more clearly differences between B17 and 024. Some of them go one way, others go the opposite way; a definite superiority of B17over 024 has not been displayed yet. This may be due to the influences of the initial fields, which is favourable to the 024.

The main common shortcomings for both B17 and 024 are as follows: On ECA 500 mb the low pressure centre near the Black Sea has disappeared and the low temperature centre is strongly weakening. But the predicted centre remains unchanged. On the other hand, the predicted low pressure pattern over the Gulf of Alaska is too weak compared with ECA. On ECA 1000 mb the Icelandic low is stagnant, but the

predicted one is moving to the east.
The 500 mb low pressure centred on New Hampshire predicted by B17 is too weak. In this case 024 gives a better forecast, but still the associated low temperature centre is missed. On 024,500 mb near Seattle, there is a cold centre with two closed isothermals which is not present on either ECA or B17. The trough over Eastern Europe on ECA is much weaker than the troughs of both day 1 and day 3. This sharp discontinuity may suggest that something went wrong with the analysis.

DAY 3 (See Fig. A1)

Although the difference between 024 and B17 is still smaller than the difference between any one of them and ECA, the superiority of B17 over 024 is becoming more evident. The weakening process of the 500 mb low pressure system over the Sea of Okhotsk is well predicted by B17, while on 024 its intensity remains unchanged.
On ECA 500 mb the Greenland low is disappearing; but the predicted one; especially that one by 024, is too strong and moving too fast.
Generally speaking, the predicted 500 mb pressure systems are too weak compared with those on ECA. This statement applies in particular to the following pressure systems: low over Eastern Spain, low over the Volga basin, low over the Gulf of Alaska and high over Scandinavia. This shortcoming may be due to the insufficient generation by the model of available potential energy by diabatic process. We will return to this point later.

Speaking of the 1000 mb pressure systems, some of them are predicted too weak, others too intense. The low over the Sea of Okhotsk has rapidly intensified on ECA, but the predicted one has weakened. The predicted lows over the Aleutian Islands and over the Gulf of Alaska are too strong, particularly the latter.

DAY 4

The 500 mb forecasts are much better than the 1000 mb forecasts. The main changes in 500 mb weather systems are well predicted, especially by 024; this is contrary to what could be expected. As examples, we may mention the high pressure centre over the Barents Sea and the low pressure centre over Eastern Spain. Inspecting the 1000 mb forecasts, one may conclude that there is little similarity between ECA and the predicted, either by 024 or by B17. If the 500 mb forecasts are still valuable up to day 6, then the period for which the 1000 mb forecasts are meaningful is only half of it. The 1000 mb forecasts either by B17 or by 024 are very similar to each other. The striking pecularity of both of them are the strong pressure gradients, in particular of the Aleutian Low and of the Icelandic Low.

DAY 5

On 500 mb, the low over the Western Mediterranean is markedly weakening, its closed centre has disappeared and only a trough remains. On the whole this process has been predicted by both B17 and 024. But the predicted orientation of the remaining trough is NE-SW, while in ECA its orientations are N-S.

On ECA the Ural Mountains Low has split into two centres. One of them has remained north of the Caucasus Mountains, the other one has moved eastward and is located over the southern part of the West Siberian Plain. This splitting process is predicted only by B17. But the prediction of the low centre over the Sea of Okhotsk by 024 is rather better than that by B17. Its closed centre has been missing in ECA. The Icelandic Low is overestimated by both B17 and 024, but especially by 024. With reference to the 1000 mb weather systems, the Sachalin Low in ECA is disappearing, partly merged with the Aleutian Low. But in both forecasts, and especially in 024, the Sachalin Low even

intensified. Over the Norwegian Sea a very deep low is found, both in 024 and B17, but in ECA there is only a very weak trough. Over Eastern Europe ECA shows a trough, but a false high pressure centre has been predicted by both, B17 and 024.

DAY 6

On 500 mb, over Kamchatka, a false ridge has been predicted by 024, but over Central Asia a weak ridge has been lost by the B17. For the remaining systems, the forecasting deficiencies by both B17 and 024 are very alike. The pressure high over Iceland and Novaja Zemla, which position had already been predicted too eastward, retreated westwards, while in the prediction it continued to move eastward. As a consequence, the phase prediction error reaches 30^{o}E. The two Ural Mountain lows merged again into one and located just south of the above-mentioned high along the same longitude. But on B17 and 024 this low is located to the south-west of the high. In America and the western Atlantic along 40^{o}N, the mean wavelength is near 45^{o} of longitude on ECA. But on B17 and 024 it is 30^{o} of longitude. The 1000 mb forecasts by B17 and 024 are similar to each other. Both the Aleutian low and the Icelandic low are predicted too deep; in addition to this the position of the latter one is predicted to the north-east of the ECA.

DAY 7 (See Fig. A2)

The superiority of B17 over 024 is obvious for 500 mb as well as for 1000 mb. As usual, at first we describe the 500 mb. The main deficiency of 024 is that there is a false intense ridge over the North Pacific Ocean. This false ridge was already mistakenly predicted on day 6, and has now moved eastwards. Connected with this, downstream, the trough over Alaska is too deep. In the upper half of the NH chart (i.e. from 90^{o}E anti-clockwise to 90^{o}W) the major characters of the synoptic evolution are very well predicted by B17. For all other aspects, the B17 and 024 are rather alike. Over west Siberia a ridge is erroneously predicted,

but to its south, over Tibet, the temperature ridge is underestimated, especially by 024. In most parts of the lower half of the chart (from 90° E clockwise to 90°W) the predicted waves are in general ouf of phase with ECA. On 1000 mb, the upper half of the B17 chart, more closely resembles ECA. The mistakenly predicted very deep lows over the Facific Ocean are to some extent filled up and the geopotential gradients there become loose on B17. But they all remain the same on 024. In the lower half of the chart, B17 looks more like 024, but both have little similarity with ECA.

DAY 8

In America the cyclone on the lee side of the Rocky Mountains intensified. Its centre, at 1000 mb, is located 5° longitude to the east of the 500 mb centre. This main feature of the synoptic development has not been predicted, neither by B17 nor by 024. The trough over the Gulf of Alaska is also intensified and a closed centre appeared. This tendency is well predicted by both B17 and 024. The general shape of 024 is more similar to ECA than B17. But the forecasting ability is by no means proved by this phenomenom.

One day earlier on 024 there was a false closed low, while on B17 and ECA only a trough was present.

ON ECA over the Central Siberian Plateau there is a low on 500 mb and a cold center on 1000 mb. Over the Barents Sea there is a high centre. To the south of it there is a cut-off low. Over Iceland there is a huge low. All these major situations have not been predicted. On some occasions, due to the phase-error of the forecast, pressure systems of opposite sign are obtained in certain regions.
On ECA over the European part of the USSR on 1000 mb there is a warm centre, and to the south of this centre stretches a frontal zone. All these features are lost on B17 and 024.

DAY 9 and DAY 10

On day 9 of ECA the two pressure lows on 1000 mb in the Atlantic sector are joined together. Aloft, at 500 mb, the Greenland trough becomes more intense and evident, and the transverse trough over Iceland weakens. The closed low centre on the lee side of the Ural Mountains has disappeared.

On day 10 of ECA the 500 mb huge trough over the Atlantic sector is broken off. Its southern part is cut off and a cut-off low is built up over the Azores on the 500 mb chart as well as on the 1000 mb chart. The northern part of the trough is deepening while it moves eastwards. A new, deep, low is formed over Scandinavia. In the North Pacific Oceanic sector the Aleutian low is clearly divided into two centres. These low centres have intense gradients, associated to them, especially on the 1000 mb chart.

Both in B17 and 024 there is little similarity to ECA. It would be meaningless to compare the individual weather systems in detail. But one can still notice that the main East Asia trough located to the east of Japan predicted by B17 is markedly better than 024.
Inspecting the hemispheric prediction as a whole, one may mention the following : the predicted gradients in both temperature and pressure fields are weaker than that in ECA. That is to say that the predicted frontal zone and jet are less intense than in reality. These kinds of deficiencies are especially grave for 024. All this implies that the transformation of available potential energy into finite energy is over balancing its generation in the model. The gradients in B17 are a little stronger than those in 024. This fact supports the idea that one of the possible ways to improve the forecasts is to describe the mountains more accurately. See also the differences in transient wave activity (Fig. A3).
It is interesting to notice that the day 6 forecasts are more similar to the day 10 ECA. This might suggest a 5 day cycle in the process.

SYNOPTIC ASSESSMENT OF THE NEW OROGRAPHY : EXPERIMENTS B45 AND B54

by Du Xing-Yuan

Abbreviations

ECA: ECMWF analyses from December 13 1979 to December 23 used for verification.

013: Operational forecasts (with old mountains).

B45: Forecasts with new mountains but without analysis cycle (p to σ only).

B54: Forecasts with new mountains and four analysis cycles.

DAY 0

On the initial conditions, on 500 mb, the centre of the polar vortex is shifted away from the North Pole, towards North America. Over the Gulf of Anadyr there is a blocking high. To its south there is a huge cut-off low: the Aleutian low. On 1000 mb the Aleutian low has two centres. Due to the deviation of the polar vortex, the circulation index in the western hemisphere is higher than in the eastern hemisphere. There are four main troughs: European, East Asian, Alaska and Iceland troughs.

On 1000 mb over the Tibet Plateau there is a "permanent" cold centre. There are a few differences in B45 and/or B54. In these two experiments on 1000 mb over the Tibet Plateau there is no longer a cold centre. And on 500 mb over Iceland a small closed low centre is present. In addition to this, in B54, over Davis Strait, there is a separate closed low centre. And on 1000 mb over Tibet the analysed high by B54 is a little weaker.

.../2

DAY 1

All the three forecasts are very alike and evolution of the weather systems is predicted well enough, especially at 500 mb. The European and East Asian troughs have developed rapidly. A cut-off low with two closed isolines has appeared over East Europe, and another cut-off low has appeared over the Amur Basin. For the latter, 013 is rather better. The deepening of the East Asian trough had not been predicted either by B45 or by B54.

On 1000 mb two strong low pressure centres were located over Scandinavia and Eastern Siberia. Generally speaking, the predicted weather systems are too strong compared with ECA. This especially applies to the newly generated low over Germany, the high over the New Siberian Islands, the high over Alaska, the high over the Colorado Plateau, and the low over East Europe. The eastern centre of the Aleutian low was, however, missing in all the three forecasts.

DAY 2

All three forecasts still remain very similar to each other, and the main synoptic changes, especially on 500 mb, are well predicted. The European and the East Asian troughs deepened considerably and moved eastward. Two cut-off lows are situated over the Caucasian Mountains and over the Japan Sea.

The transverse trough over Western America is weakening a little. All the above mentioned features have been predicted fairly well, but the splitting of the Aleutian low is not predicted, and the predicted transverse trough is too weak, so that no closed isoline appears in it. On B45 and B54 over southern Scandinavia there is a low centre with a closed isoline, but on ECA only a transverse trough appears. For this system 013 gives a slightly better forecast.

.../3

On 1000 mb the predicted high over Alaska and the predicted (huge) Iceland low with three centres are too strong compared with ECA. On the other hand the predicted Aleutian low is too weak, its eastern centre is missing, just as for the day 1 forecast. The predicted temperature trough over the Caucasian Mountains is also too strong; to its west a false high pressure centre appears on the predicted charts. But to its east the low pressure centre is predicted too deep only by 013. The temperature trough over the Japan Sea is also predicted too deep by the three versions.

Over Tibet there is a closed temperature low on ECA and 013, that we have discussed for the B17 synoptic assessment.

DAY 3 (See Figs. B1 and B5)

On 500 mb the eastward movement of the Rocky Mountains trough, the Davis Strait trough, the Caucasian trough, and the trough over the Japan Sea is predicted fairly well by all the three versions. The retreat of the Northern European low is also portrayed by the predicted charts; this to a large extent is due to the fact that on the previous date the predicted location of this low is too far to the west of its real position. The predicted blocking high over Barents Sea is too strong, a closed centre has appeared in it that does not show on ECA. The low over Europe is predicted too weak and two of its three centres are lost on the predicted charts. While the geopotential contours are very similar, the thickening of the isothermals over east Asia is underestimated by the forecasts.

The 1000 mb forecasts are worse than that of 500 mb. But B45 and B54 remain very similar to each other with the only small differences that both the western centre of the Azores high and the low centre over the Rocky Mountains are one isoline stronger on B45. On ECA the intensity of the western centre of the Azores high is identical with 013 and B45. The low centre over the Rocky Mountains is missing on ECA.

As regards the eastern centre of the Azores high, its predicted position is to the east of its actual position, as this has happened for day 1 and day 2. The predicted low over Iran is too deep, especially for 013 which is 80 geopotential meters lower than ECA. As far as the geopotential gradients over Tibet are concerned, those predicted by B45 and B54 are too strong, while that by 013 is too weak. The low over Germany predicted by 013 is too deep, the lowest isoline has the value of -120 geopotential meters, while that on ECA, B45, and/or B54 is only -40.

So, we may draw the conclusion that for 1000 mb forecasts, B45 and/or B54 is better than 013.

DAY 4 (See Figs. B2 and B6)

For 500 mb, the predicted ridge over the Rocky Mountains is too weak, and the predicted ridge over western Europe is too strong. On the predicted charts over the Barents Sea there is a blocking high centre, while on ECA there is only a ridge. The closed low centre over the Norwegian Sea and the associated jet at its southern edge have not been predicted by any of the three forecasting versions. The intensity of the low over Northern America has been underestimated by 013 and, to a lesser degree by B45. But the secondary centre located to the south-east of the main centre is predicted only by 013.

As far as the 1000 mb is concerned, we firstly notice that the low centre over the eastern coast of Northern America is not predicted by 013, but has been predicted by B45 and /or B54, though its intensity is underestimated. The main (eastern) centre of the Aleutian low is also underestimated by all the three forecasts, but the subsidiary (western) centre is a little overestimated by B54. The predicted eastward movement of the Iceland low is too slow.

.../5

DAY 5

On 500 mb the Iceland low is underestimated by B45 and/or B54, but a closed centre still exists, while on 013 it is entirely missing. A false blocking high over the Barents Sea is produced by 013. Another false blocking high over the East Siberian Sea is present in both 013 and B45. Therefore the best forecast is B54. Its main deficiency is the underestimation of the East American trough and the downstream ridge, which is also existing in 013 and B45.

On the 1000 mb chart on ECA there is a deep low south of Greenland. This situation has not been predicted by any of the three variants. Over Tibet the isolines of both geopotential and temperature are too sparse on 013.

DAY 6

The large meridionality of the 500 mb flow over the Atlantic sector has not been predicted by any of the three forecasting variants; but we still can see that B45 and/or B54 is better than 013, especially if we examine the orientation of the 576 isoline.

The orientation of the Azores high on 1000 mb is north-south on ECA, but the predicted is still east-west oriented. North of 40°N over Asia there is a huge high, but the predicted ones are variegated. In addition to this over Tibet on 013 the geopotential isolines are very sparse, the pressure low has disappeared, notwithstanding the existence of a temperature low.

DAY 7

The main deficiency for 500 mb forecasts is the underestimating of the meridionality over the Atlantic sector and the loss of the cut-off low over the Aral Sea. This deficiency is especially serious for 013. The consequence, or rather the cause of this phenomenon is that the heat interchange between high and low latitudes has not been sufficiently

considered in the Model.

The main characters in the 6 day 1000 mb forecasts remain unchanged.

DAY 8 (See Figs. B3 and B7)

On ECA the meridionality has been further increased,the trough over West Europe deepened intensely and a strong cut-off low was formed over the Iberic peninsula. All this large development of meridionality in the 500 mb flow has not been predicted. In the lower half part of the chart (i.e. from 90° W clockwise to 90°E) B45 and B54 are better than 013. The European trough is deeper on B45 and B54, and a small cut-off low is newly formed on B45 or likely to be formed on B54.

But in the upper half part of the chart 013 is better than B45 and/or B54. Over the Pacific Ocean the orientation of the 013 flow is very similar to ECA and has a much higher meridionality.

On 1000 mb two main members of the weather system, the Iberic low and the Okhotsk low, have been lost in the three forecasts, and this leads to the 1000 mb forecasts being meaningless. But, still, there are many similarities among the three forecasts. The common deficiency is that the forecast gradients are more loose than the observed. (See also Fig. B4).

DAY 9 and DAY 10

In addition to 1000 mb, 500 mb forecasts also lost their meaning. But there are still many similarities among the three variants of forecasting, especially B45 and B54. Generally speaking, the predicted distribution of iso-geopotentials is more or less more even than ECA. The concentration of iso-geopotentials over East Asia and Northern Europe is not present in the forecasting charts.

APPENDIX C

SYNOPTIC ASSESSMENT OF THE NEW OROGRAPHY: EXPERIMENT B96

Abbreviations

by Du Xing-Yuan

ECA: ECMWF analyses, Jan. 29, 1980 to Feb. 8, 1980, used for verification.

029: Operational forecasts with old mountains.

B96: Forecasts with new mountains.

DAY 0

For 500mb analysis there is no discernible difference between B96 and 029, which is identical to ECA. As far as 1000 mb is concerned, there are a few small differences.

Over Tibet on B96 there is a closed low temperature centre, but on 029 only a temperature trough is presented. Over Afghanistan a reverse picture is observed: a temperature trough locates over Tibet, but closed temperature lows locate over Afghanistan-Iran. On 029 over the Rocky Mountains and over Northern Greenland closed iso-geopotential are located, but these closed low centres do not appear on B96. On the other hand, on B96 over Algeria there exists a closed high centre which is not on 029. As we can see later, however, these differences have little influence on the future development.

DAY 1

The 500 mb forecasts are quite similar to one another. The only one trivial difference is that on B96 in the trough over Libya, a closed low temperature centre is lost.

The 1000mb forecasts begin to diverge from ECA. Although there is some diversity between 029 and B96, it is quite small as compared wtih the diversity from ECA. The huge low in the Atlantic section has only one centre on ECA, but on 029 and B96 there are two centres. Over the Rocky Mountains a deep low with two closed iso-geopotentials is predicted, but on ECA there locates only a transverse trough. Over Tibet

on 029 the temperature gradient is too strong as compared with ECA or B96. A closed temperature low appears to the north of Tibex on 029, and a closed temperature high appears to the east of Tibet on B96; both of them have not been presented on ECA.

DAY 2

For 500 mb B96 is very similar to 029, and their disagreements with ECA are also small. The predicted low over Sakhalin is one closed line deeper than ECA; but the predicted low to the north of Canada is one line weaker th8n ECA. The low over the Gulf of Alaska has not been predicted by 029, and on B96 there still remains a small centre. The low over Northern Siberia, however, has not been predicted at all by B96, and a little better results are obtained by 029 in this region.

The 029's and B96's 1000 mb are still very much alike. The predicted Okhotsk low is too deep and its centre is located to the east of ECA. The predicted Aleutian low has an elongated shape in the NE-SW direction, while on ECA its shape is rather circular. On the other hand, on ECA the Okhotsk low is elongated in the E-W direction, but the predicted low has a circular shape. On ECA the Rueopean huge low has two centres, but the predicted only one, the eastern secondary centre is missing. Over Tibet the predicted pressure gradients by 029 are too loose and the low centre is lost. Contrary to this, the predicted temperature gradients are stronger than ECA and/or B96.

DAY 3

The 500 mb forecasts both by 029 and B96 are quite good, and we can hardly say which one of them is better (or worse). Their deficiency is still not very important. In the Atlantic sector the predicted Iceland low has only one center, but on ECA there are two centres. The predicted Alaska low is left to the SW behind that on ECA. The low centre to the north of Siberia was lost in the predictions.

On 1000 mb there are six main synoptic systems, four of them are lows: Iceland low, low over the Baltic, low over Siberia and the Alaska low. The other two are highs: Siberia high and North America high. These main figures still remain in the predicted charts but the lows as predicted are too deep. The orientation of the N. American high, being S-N on ECA, has not been predicted. On the other hand, the predicted Siberia high has rather a S-N orientation, but on ECA it is not so clear.

Examining the pressure topography near Tibet, one can see that B96 is more similar to ECA than 029, but the temperature topography on 029 is more similar to ECA than B96. This again infers that the thermal patterns over the plateau are a consequence of interpolating from a p-coordinate to a σ-coordinate and vice versa.

DAY 4 (See Fig. C1)

The 500mb forecasts by 029 and B96 are still very much alike. The predicted Sachalin low remains too deep. The newly formed slender closed high centre over the Bering Sea has not been predicted. The troughs, both over Western Europe and the Eastern Pacific are predicted too deep. On ECA these two lows are getting through.

The 1000 mb forecasts by 029 and B96 in general are still alike. On ECA over the Pacific there is a huge low with two centres. Between these two centres, at the southern edge, only a very weak ridge is located, but the predicted ridge is very strong and on 029 a closed high centre even appears. The predicted Siberia high is located too far to the north. The strengthening of the North America high and its northward movement has not been predicted at all, especially for 029. The closed low over north Greenland was predicted by B96, but not by 029. So, we can see some of the advantages and preferences for B96 over 029.

DAY 5 (See Fig. C2)

Although the major synoptic systems on 500 mb are predicted in the main, some distinguished differences also appear, On ECA the

western European low and the eastern Pacific low have fully cleared the North Pole. The Bering Sea high is strengthening and moving westward. It turns from a S-N orientation to a W-E orignation, and locates north of the Sachalin low. On O29 and/or B96, however, these changes cannot be observed. There is no Bering Sea high at all, and the eastern Pacific low remains connected with the Sachalin low. The North Pole appears in the saddle region. On B96, over eastern Canada, there is a closed high. This is worse when compared with O29, on which the high centre has no closed iso-geopotential. On ECA there is only a ridge without any high centre.

For the most part, on 1000 mb forecasts the O29 and B96 are still very alike. Their difference with ECA is still increasing. In the main, we may say that the predicted weather systems are too strong and too big. On ECA the Sachalin has moved eastward into the central Pacific, and locates near the position of the permanent Aleutian low with the Alaska low at its N-E, but the predicted movement of the Sachalin low is very slight. Again, over Tibet the temperature fields on ECA and on O29 are more alike, but if we examine the geopotential orientation, we can see that B96 is more similar to ECA. Over North America on ECA a huge high is located, which is completely lost by O29. On B96 this high also exists, although its intensity is insufficient. On the whole, therefore, one can say that B96 is better than O29.

DAY 6 (See Fig. C3)

At 500 mb on ECA to the south of Greenland there is a cut-off low, which is lost by O29. This cut-off low is also presented on B96, although its position is a bit too far to the east, but the blocking high over Baffin Island is only predicted by O29. On ECA in the Asian ridge there appears closed iso-geopotential, which is disappearing on O29. On B96 closed iso-geopotential is presented in the Asian ridge, but its position is to the NE of ECA. The western Pacific low on B96 is too strong.

On 1000mb the Asia high is better predicted by O29, but the situation near Tibet is better predicted by B96. The temperature fields over Tibet on ECA and O29 are very much alike, this

conclusion is valid up to Day 10 inclusive. Over south-west Asia on ECA and/or on B96 there is a huge trough without any cut-off, but on O29 a false cut-off low is presented in it.

DAY 7 - DAY 10

The forecasting significance is rapidly decreasing and one can hardly judge which one is better, even for the 500 mb forecasts. A newly formed cut-off low in the transverse trough over Asia is mistakenly predicted by O29 on day 7.

This mistakenly predicted cut-off low moves westward on day 8 and day 9, and deepens on day 10. This process is completely absent on ECA. On B96 the cut-off low is formed only on day 10. So, according to this process, we may say that B96 is the better one.

On the other hand, however, the orientation of the Pacific low is better predicted by O29. On day 7 the orientation on both O29 and B96 is nearly W-E direction; on the next day, day 8, it becomes roughly N-S, and on day 9 and day 10 it becomes perfectly N-S direction. On ECA the orientation remains N-S direction throughout the whole period, but on B96 it always remains in the W-E direction.

Over the west Atlantic, to the east of Bermuda, on ECA 1000 mb on day 7, a deep low is located. It moves N-E'ward and deepens, and on day 9 and day 10 it becomes a typical permanent Icelandic low. On day 9 a new low is appearing to the east of Bermuda and moves north-eastward . Although this process has more or less been predicted, the predicted intensity is too weak. This is especially true for B96, on which the low to the east of Bermuda is also present one day later.

Examining the 1000 mb as a whole, one can see that the predicted subtropic highs are too strong. On ECA there is only a weak Azores high, but on O29 and /or B96 the area occupied by subtropic highs is more than half of the whole subtropic belt.

5-10 DAYS MEAN

From the above statement we may draw the conclusion that from day 7 on, O29 is better than B96, although before day 6, B96 may be the better of the two. This situation is also reflected in the 5-10 days mean charts. The difference between B96 and ECA is a little greater than that between O29 and ECA. This is true for 500mb as well as 1000mb.

If we take climate as standard and calculate the deviation of the three mean charts from the climate, then we can see that they are of the same order of magnitude. The difference between B96 and climate is by no means larger than the difference between O29 and climate. For 500mb, the difference between B96 and climate is the smallest.

-.-.-.-.-.-

FIGURE CAPTIONS

Fig. 1 World map of orography OØ. Contour interval 500m

Fig. 2 " " " O2. " " "

Fig. 3 " " " O3. " " "

Fig. 4 Bidimensional spectrum of the orographies OØ, O2 and O3 (amplitude in m vs wave number).

Fig. 5 Objective comparisons for Northern Hemisphere tropospheric extra tropical height fields between old coast lines (DØ6) and new coastlines (DØ2) (5.6.80 case).

Fig. 6 Day 5 500 mb (top) and 1000 mb (bottom) Northern Hemisphere maps for experiments (from left to right): DØ6 (old coast lines), D14 (old coast lines and old orography), DØ2 (new coastlines). Note the similarity DØ6-DØ2 when compared to D14.

Fig. 7 Objective comparisons for Northern Hemisphere tropospheric extra tropical height fields between old orography (BO4) and new O2 orography (BO3) (16.1.79. Case A).

Fig. 8 Objective comparisons for Northern Hemisphere tropospheric extra tropical height fields between old orography (B83) and O2 new orography (B93) (16.1.79. Case B).
The repeat of BO3 (see Fig. 7) indicates the extreme similarity of the case to the analysis.

Fig. 9 Objective comparisons for Northern Hemisphere tropospheric extra tropical height fields between old OØ and new O2 orography on an ensemble of 4 cases.

Fig. 10 Objective comparisons for Northern Hemisphere tropospheric extra tropical height fields between old OØ and new O2 orography this time for the standing part of the flow.

Fig. 11 Mean Northern Hemisphere map of forecast errors at day 7 for an ensemble of 4 cases for 500mb. Old topography OØ (top) vs new 02 orography (bottom).

Fig. 12 Mean Northern Hemisphere map of forecast errors at day 7 for an ensemble of 4 cases for 1000 mb. Old topography OØ (top) vs new O2 orography (bottom).

Fig. 13 Objective comparisons for Northern Hemisphere tropospheric extra tropical height fields between old orography (O13), new O2 orography (B45) and new O2 orography with assimilation cycles prior to the forecast (D54) (13.12.79 case).

Fig. 14 Comparison of zonal wind errors (in a latitude/height diagram) between the three forecasts mentioned in Fig. 13.

Fig. 15 Objective comparisons for Northern Hemisphere tropospheric extra tropical height fields between old topography (O29) and new O2 orography (B96) (29.01.80 case).

Fig. 16 Objective comparisons for Northern Hemisphere tropospheric extra tropical temperature fields between old topography (O29) and new O2 orography (B96) (29.01.80).

Fig. 17 Mean 500mb height Northern Hemisphere map for day 7 to 30 from the period starting 16.1.79. B52=old orography, B53=new orography, DWD= DWD analysis as verification.

Fig. 18 Mean 1000 mb height Northern Hemisphere map for day 7 to 30 from the period starting 16.1.79. B52=old orography, B53=new O2 orography, DWD= DWD analysis as verification.

Fig. 19 Mean 500 mb transient waves variance Northern Hemisphere map for day 7 to 30 from the period starting 16.1.79. B52=old orography, B53=new O2 orography, DWD= DWD analysis as verification.

Fig. 20 New 1000 mb transient waves variance Northern Hemisphere map for day 7 to 30 from the period starting 16.1.79. B52-old orography, B53=new orography, DWD= DWD analysis as verification.

Fig. 21 For the same period of the same experiments as Figures 17-20, mean zonal wind and temperature errors expressed in latitude height diagrams.

Fig. 22 For the same period of the same experiments as Figures 17-20, global map of large scale precipitation; contouring in mm/day.

Fig. 23 For the same period of the same experiments as Figures 17-20, global map of convective precipitation; contouring in mm/day.

Fig. 24 Objective comparisons for Northern Hemisphere tropospheric extra tropical height fields between orographies OØ (C63), O1 (C78) and O3 (C80) (16.1.79. case).

Fig. 25 The same as for Fig. 24 but between orographies OØ (C63), O4 (C79) and O5 (C88) (16.1.79. case).

Fig. 26 The same as for Fig. 24 but between orographies OØ (D14), O3 (DØ2) and O5 (DØ3) (5.6.80. case).

Fig. 27 Objective comparisons for Northern Hemisphere tropospheric extra tropical temperature fields between orographies OØ (D14), O3 (DØ2) and O5 (DØ3) (5.6.80. case).

Fig. 28 Objective comparisons for Northern Hemisphere tropospheric extra tropical height fields between orographies O3 (DØ2), O4 (DØ4) and O1 (DØ5) (5.6.80. case).

Fig. 29 Objective comparisons for Northern Hemisphere tropospheric extra tropical temperature fields between orographies O3 (DØ2), O4 (DØ4) and O1 (DØ5) (5.6.80. case).

Fig. 30 Objective comparisons for Northern Hemisphere tropospheric extra tropical height fields between old Z_o (C80) and new Z_o(D60) fields. Please disregard C63 (16.1.79. case).

Fig. 31 The same as for Fig. 30 but between old surface fields (E40) and new surface fields (DØ2). Please disregard NM2 (16.1.79. case).

Fig. 32 The same as for Fig. 30 but between old OØ orography and new O3 orography in an ensemble of 5 cases.

Fig. 33 The same as for Fig. 32 but this time for the standing part of the flow.

Fig. 34 Objective comparisons for Northern Hemisphere tropospheric extra tropical height fields between OØ2 old topography, NM2 new topography but error in coastal areas and NM6 new orography, no error (2.11.80 case).

Fig. 35 The same as for Fig. 34 but between OØ2 old topography, NM6 new O3 orography with interpolation of increments in the analysis cycles and E53 new O2 topography with interpolation of full fields in the analysis cycles (2.11.80. case).

Fig. 36 The same as for Fig. 34 but between OØ2 old topography, NM6 new O3 orography with interpolation of increments on the analysis cycles and E65 new O3 topography with interpolation of full fields in the analysis cycles (2.11.80. case).

Fig. 37 The same as for Fig. 34 but between OØ2 old orography and interpolation of full fields in the analysis cycles and E66 old orography but with interpolation of increments in the analysis cycles (2.11.80. case).

Fig. 38 Objective comparisons for Northern Hemisphere tropospheric extra tropical height fields between new O3 (E76) orography and old orography (O12) (12.2.76. case).

Fig. 39 Objective comparisons for Northern Hemisphere 1000mb extra tropical height fields between new O3 (E76) orography and old orography (O12) (12.2.76 case).

Fig. 40 Objective comparisons for Northern Hemisphere 500mb extra tropical height fields between new O3 (E76) orography and old orography (O12) (12.2.76. case).

Fig. 41 Objective comparisons for Northern Hemisphere tropospheric extra tropical temperature fields between new O3 (E76) orography and old orography (O12) (12.2.76. case).

Fig. 42 Difference maps between forecast and analysis, 500 mb height. E76 corresponds to O3 orography and O12 to old orography.

Fig. 43 Difference maps between forecast and analysis, 1000 mb height. E76 corresponds to O3 orography and O12 to old orography.

Fig. A1 Day 3. 500mb (top) and 1000mb (bottom) map for, from left to right: analysis, old orography forecast, new (O2) orography forecast (24.10.79. case).

Fig. A2 Day 7. The same as for Fig. A2.

Fig. A3 Variance by transient waves during a 10-day period at 500mb (top) and at 1000 mb (bottom) for from left to right: analysis, old orography forecast, new (O2) orography forecast (24.10.79. case).

Fig. B1 Day 3. 500 mb (top) and 1000 mb (bottom) map for from left to right: analysis, old orography forecast, new (O2) orography forecast (13.12.79. case).

Fig. B2 Day 4. The same as for Fig. B1

Fig. B3 Day 8. The same as for Fig. B1.

Fig. B4 Variance by transient waves during a 10-day period at 500mb (top) and at 1000 mb (bottom) for from left to right: analysis, old orography forecast, new (O2) orography forecast (13.12.79. case).

Fig. B5 As Fig. B1 but for analysis, new mountains, new mountains inserted for one day of data assimilation before forecast starts.

Fig. B6 As Fig. B2 but for analysis, new mountains, new mountains inserted for one day of data assimilation before forecast starts.

Fig. B7 As Fig. B3 but for analysis, new mountains, new mountains inserted for one day of data assimilation before forecast starts.

Fig. C1 Day 4. 500mb (top) and 1000mb map for, from left to right: analysis, old orography forecast, new (O2) orography forecast (29.1.80.).

Fig. C2 Day 5. The same as for Fig. C1.

Fig. C3 Day 6. The same as for Fig. C1.

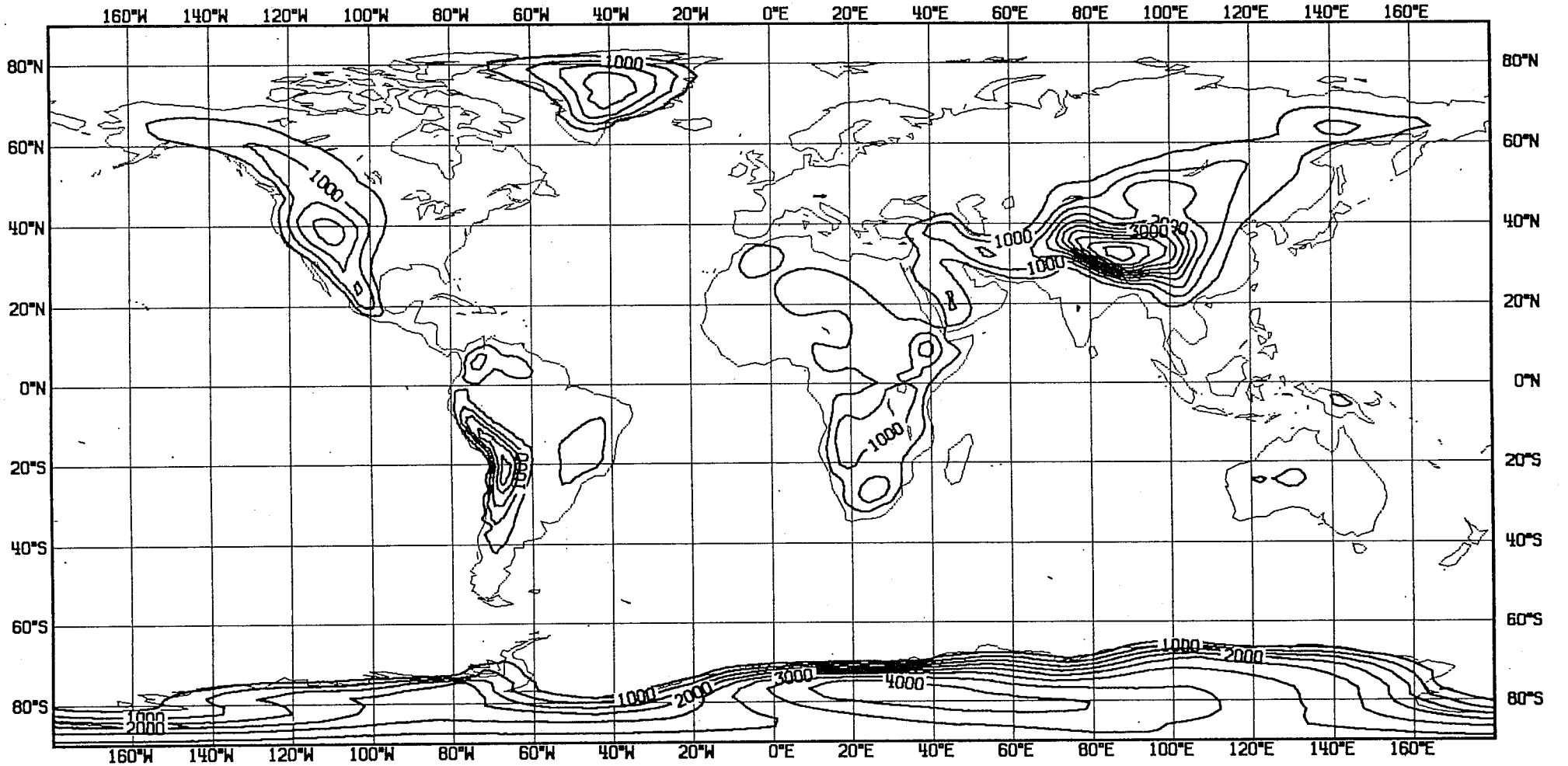
160°W 140°W 120°W 100°W 80°W 60°W 40°W 20°W 0°E 20°E 40°E 60°E 80°E 100°E 120°E 140°E 160°E
80°N 60°N 40°N 20°N 0°N 20°S 40°S 60°S 80°S
1000
2000
3000
4000
OLD OROGRAPHY: 00

Fig. 1

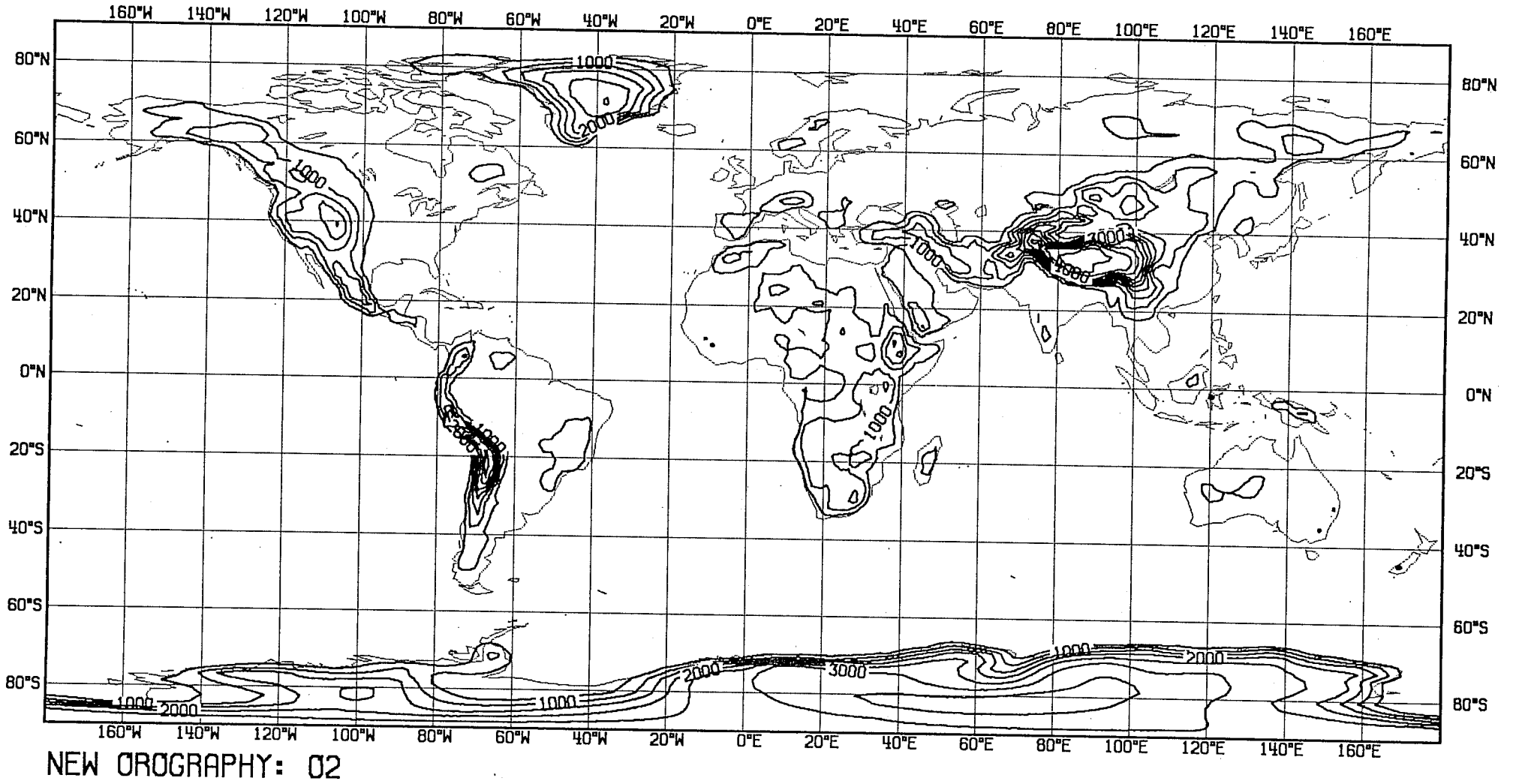
160°W
140°W
120°W
100°W
80°W
60°W
40°W
20°W
0°E
20°E
40°E
60°E
80°E
100°E
120°E
140°E
160°E
80°N
60°N
40°N
20°N
0°N
20°S
40°S
60°S
80°S
1000
2000
3000
NEW OROGRAPHY: 02

Fig. 2

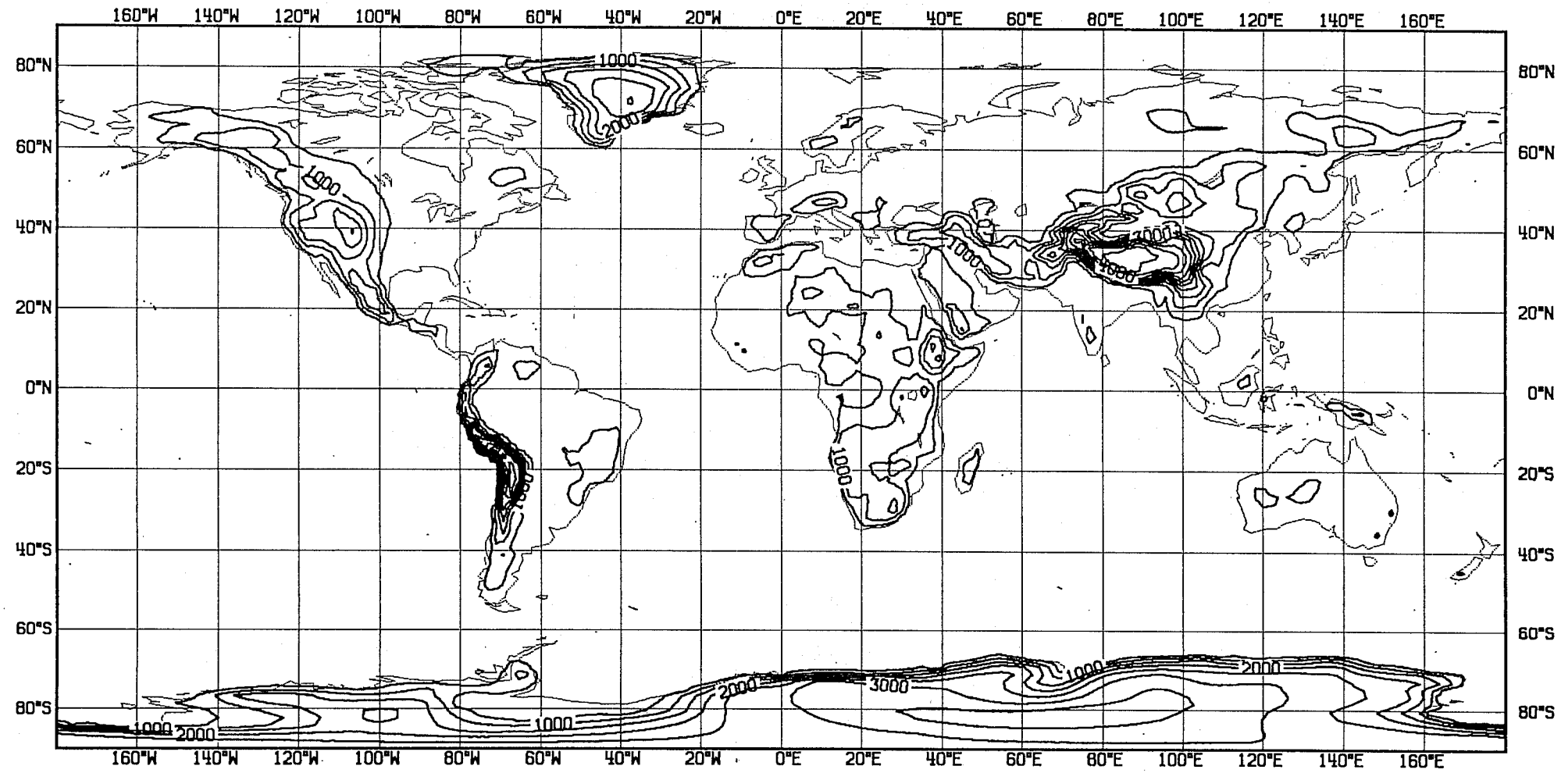
160°W 140°W 120°W 100°W 80°W 60°W 40°W 20°W 0°E 20°E 40°E 60°E 80°E 100°E 120°E 140°E 160°E
80°N 60°N 40°N 20°N 0°N 20°S 40°S 60°S 80°S
1000
2000
3000
NEW OROGRAPHY: 03 (OPERATIONAL)

Fig. 3

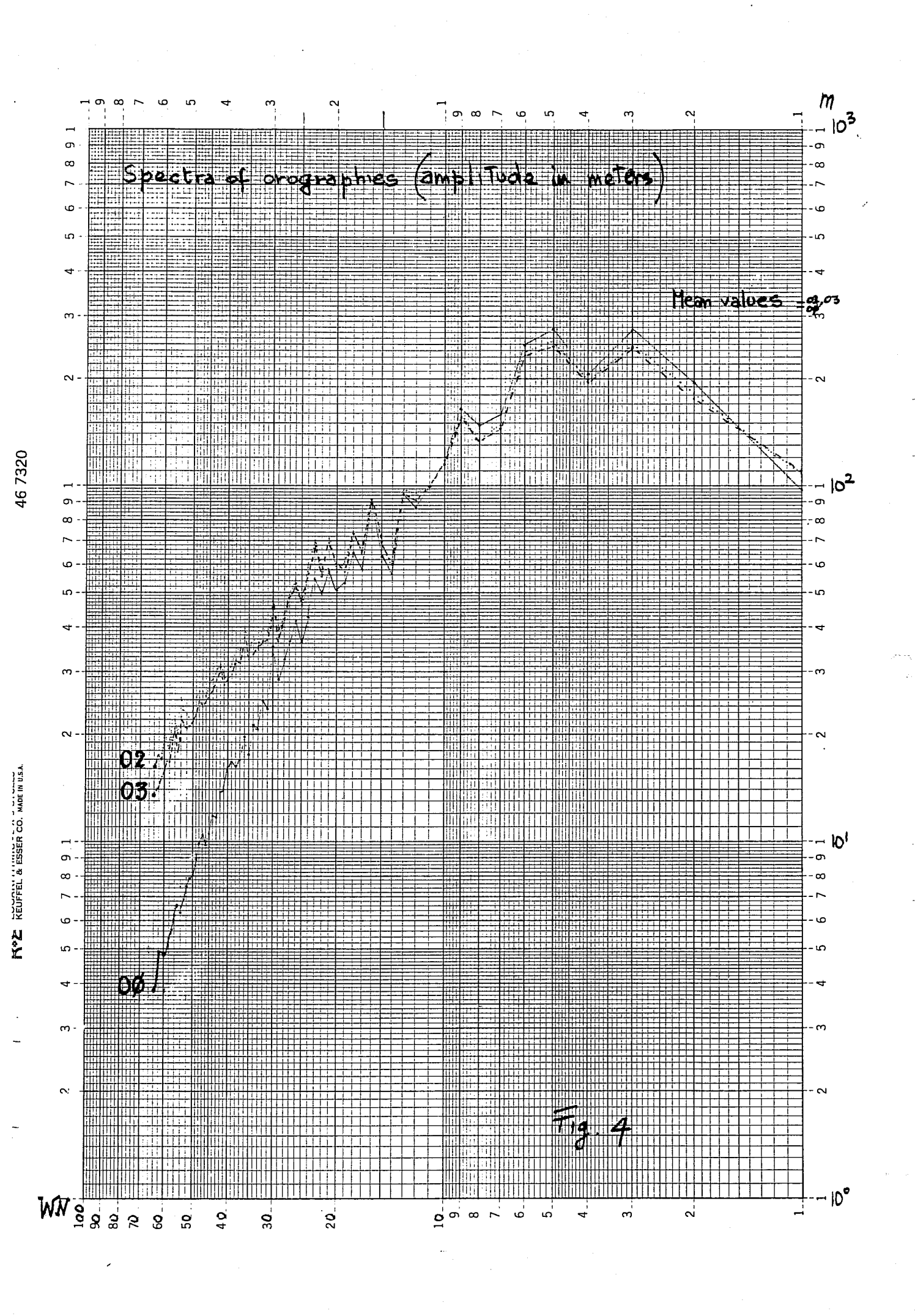
Spectra of orographies (amplitude in meters)
Mean values
02.
03.
00.
m
WN
Fig. 4

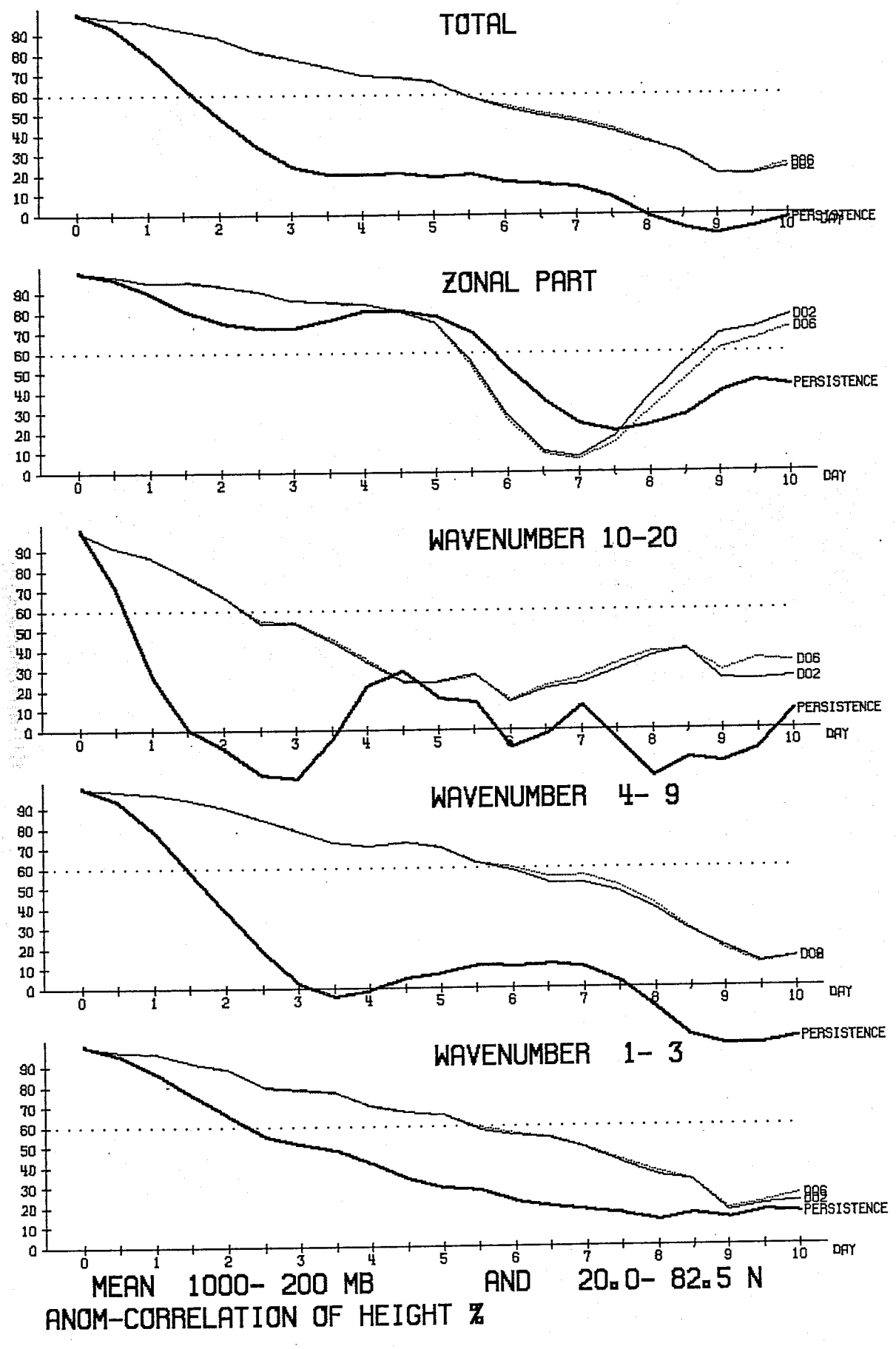
TOTAL
PERSISTENCE
DAY
ZONAL PART
D02
D06
PERSISTENCE
DAY
WAVENUMBER 10-20
D06
D02
PERSISTENCE
DAY
WAVENUMBER 4- 9
D08
PERSISTENCE
DAY
WAVENUMBER 1- 3
D06
D02
PERSISTENCE
DAY
MEAN 1000- 200 MB AND 20.0- 82.5 N
ANOM-CORRELATION OF HEIGHT %

Fig. 5

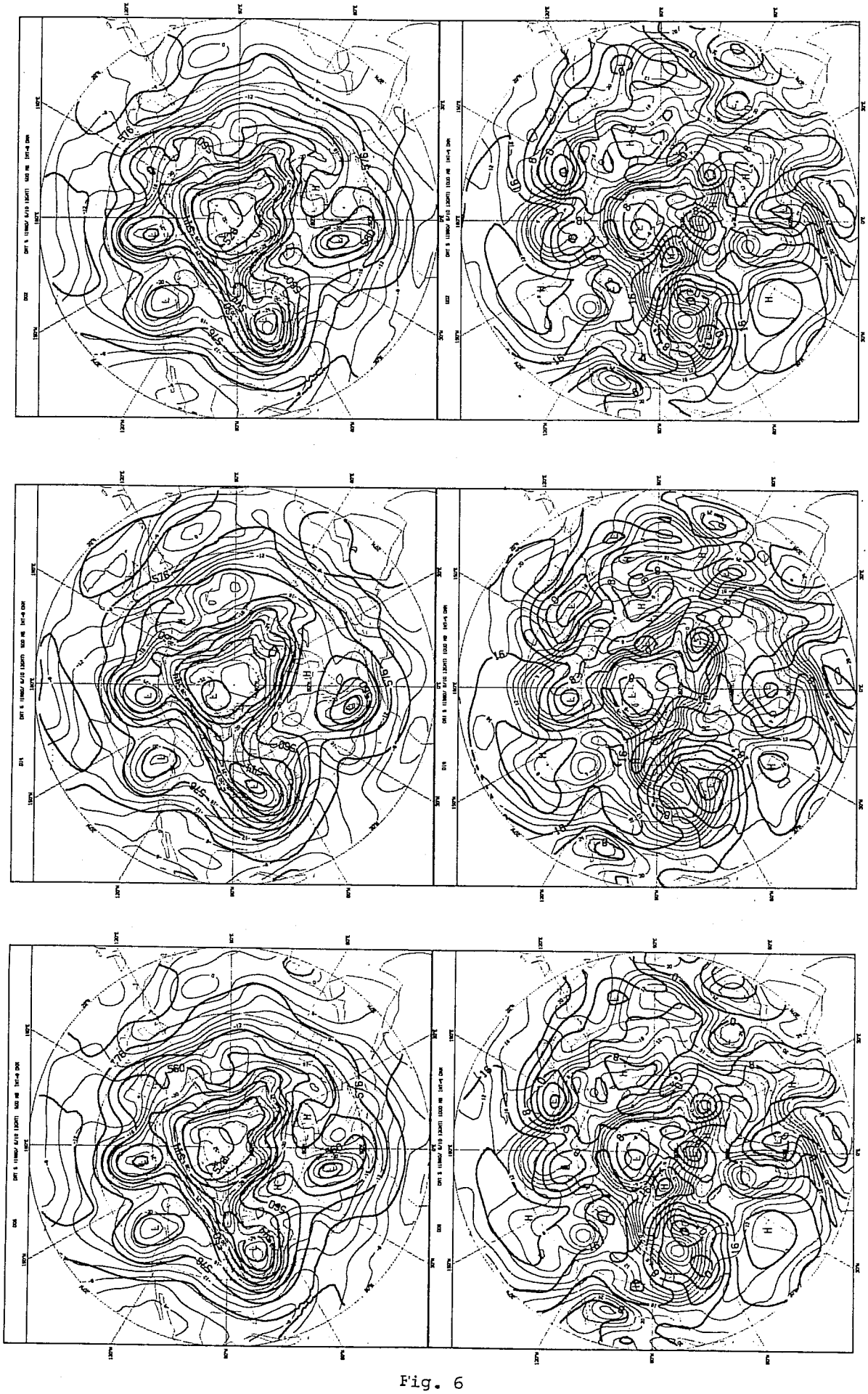

Fig. 6

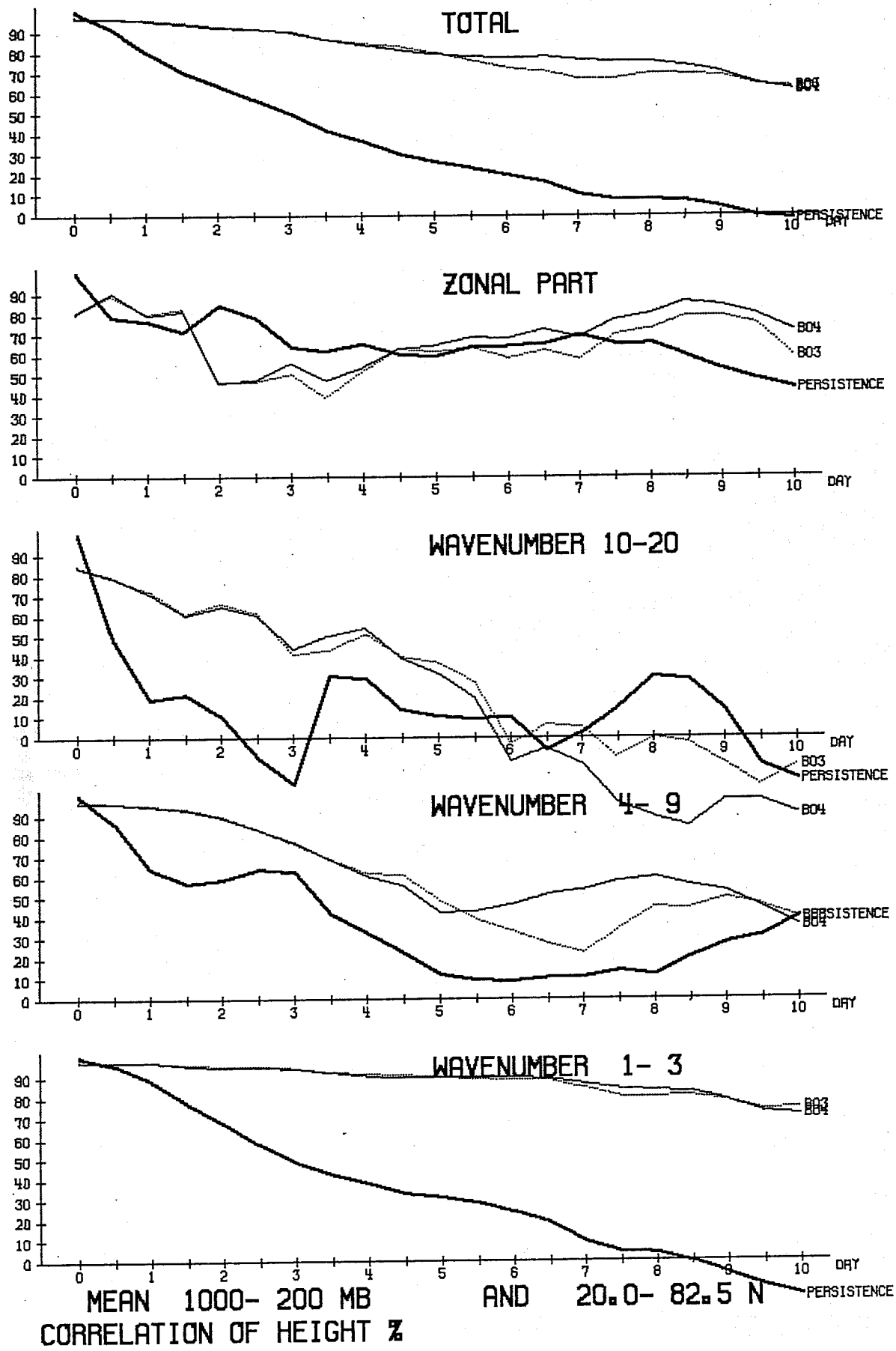
TOTAL
B04
PERSISTENCE
DAY
ZONAL PART
B04
B03
PERSISTENCE
DAY
WAVENUMBER 10-20
DAY
B03
PERSISTENCE
WAVENUMBER 4- 9
B04
PERSISTENCE
B04
DAY
WAVENUMBER 1- 3
B03
B04
DAY
PERSISTENCE
MEAN 1000- 200 MB AND 20.0- 82.5 N
CORRELATION OF HEIGHT %

Fig. 7

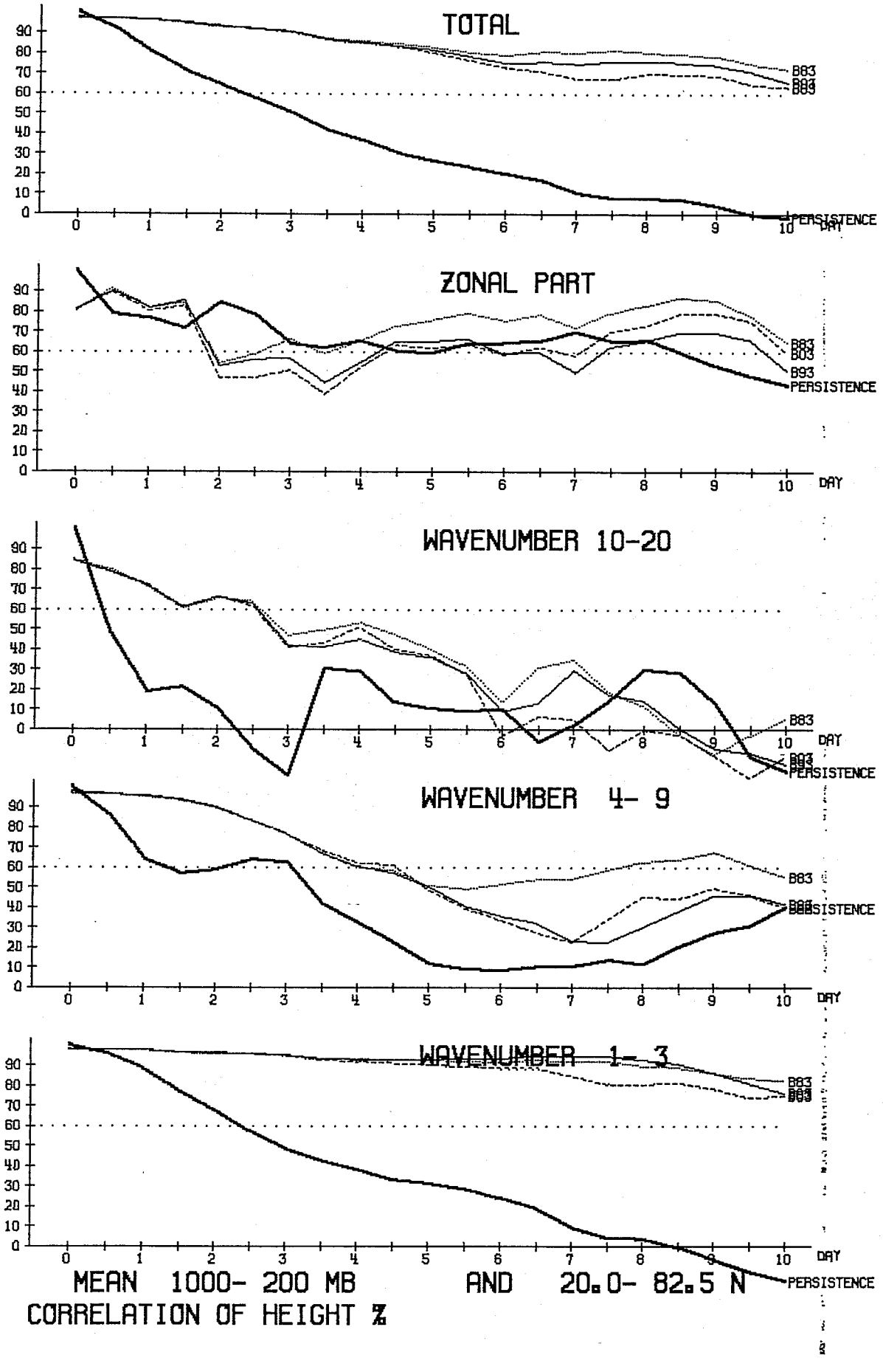
TOTAL
ZONAL PART
WAVENUMBER 10-20
WAVENUMBER 4- 9
WAVENUMBER 1- 3
B83
B93
PERSISTENCE
DAY
MEAN 1000- 200 MB AND 20.0- 82.5 N
CORRELATION OF HEIGHT %

Fig. 8

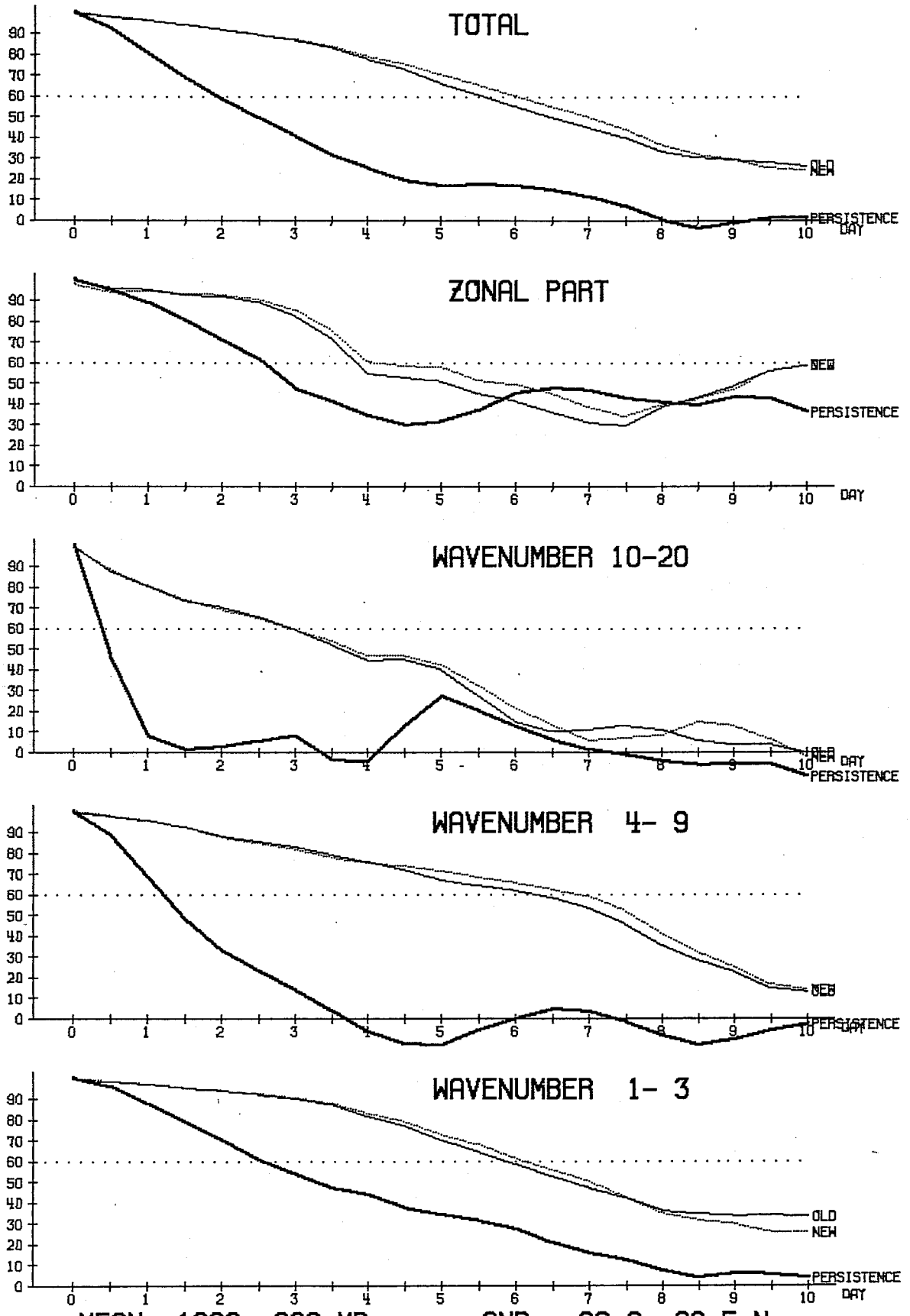
TOTAL
OLD
NEW
PERSISTENCE
DAY
ZONAL PART
NEW
PERSISTENCE
DAY
WAVENUMBER 10-20
OLD
NEW
DAY
PERSISTENCE
WAVENUMBER 4- 9
NEW
PERSISTENCE
DAY
WAVENUMBER 1- 3
OLD
NEW
PERSISTENCE
DAY
MEAN 1000- 200 MB AND 20.0- 82.5 N
ANOM-CORRELATION OF HEIGHT (M) 4 CASES

Fig. 9

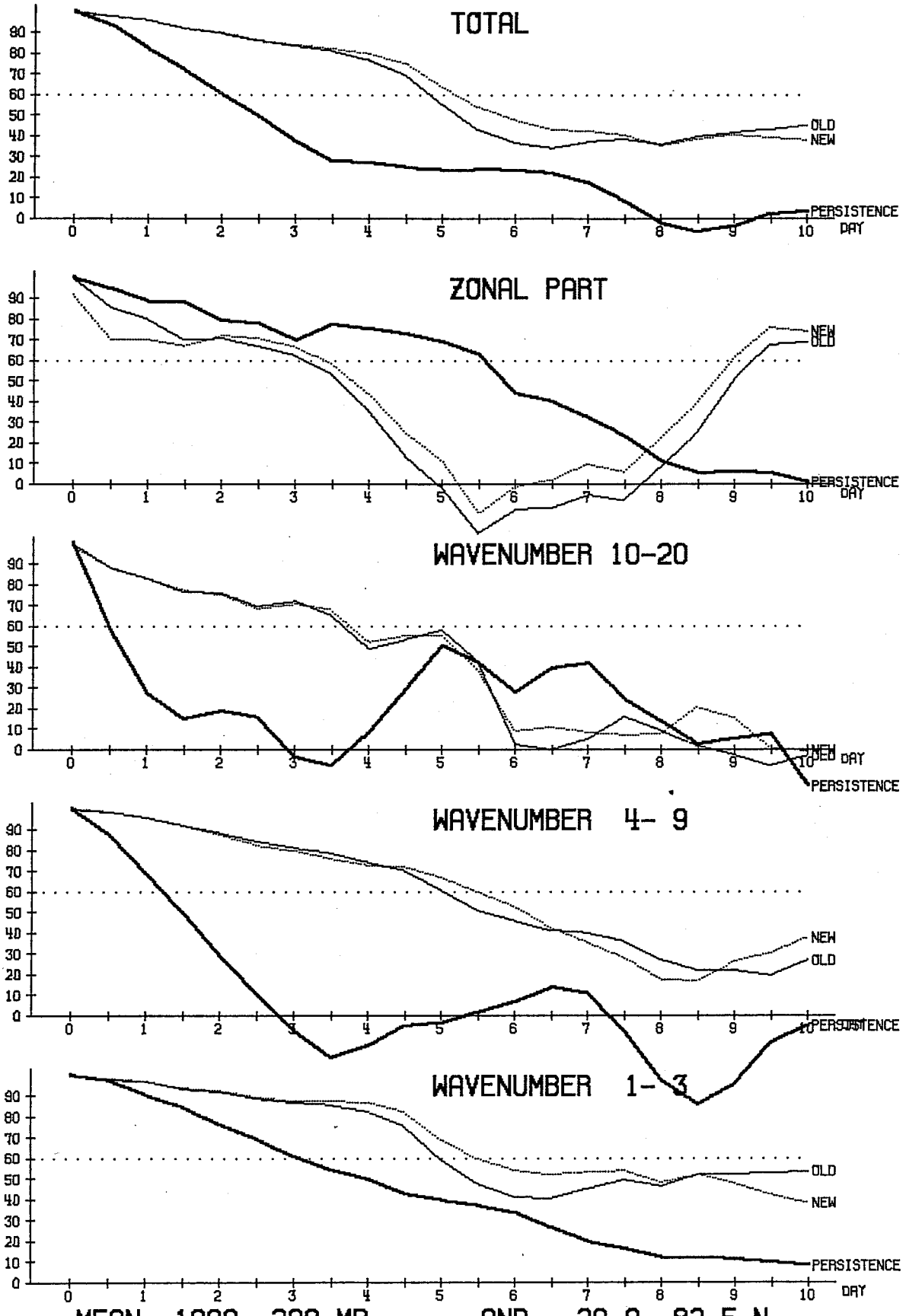
TOTAL
OLD
NEW
PERSISTENCE
DAY
ZONAL PART
NEW
OLD
PERSISTENCE
DAY
WAVENUMBER 10-20
NEW
OLD
DAY
PERSISTENCE
WAVENUMBER 4- 9
NEW
OLD
PERSISTENCE
WAVENUMBER 1- 3
OLD
NEW
PERSISTENCE
DAY
MEAN 1000- 200 MB AND 20.0- 82.5 N
ANOM-CORREL OF HEIGHT STANDING

Fig. 10

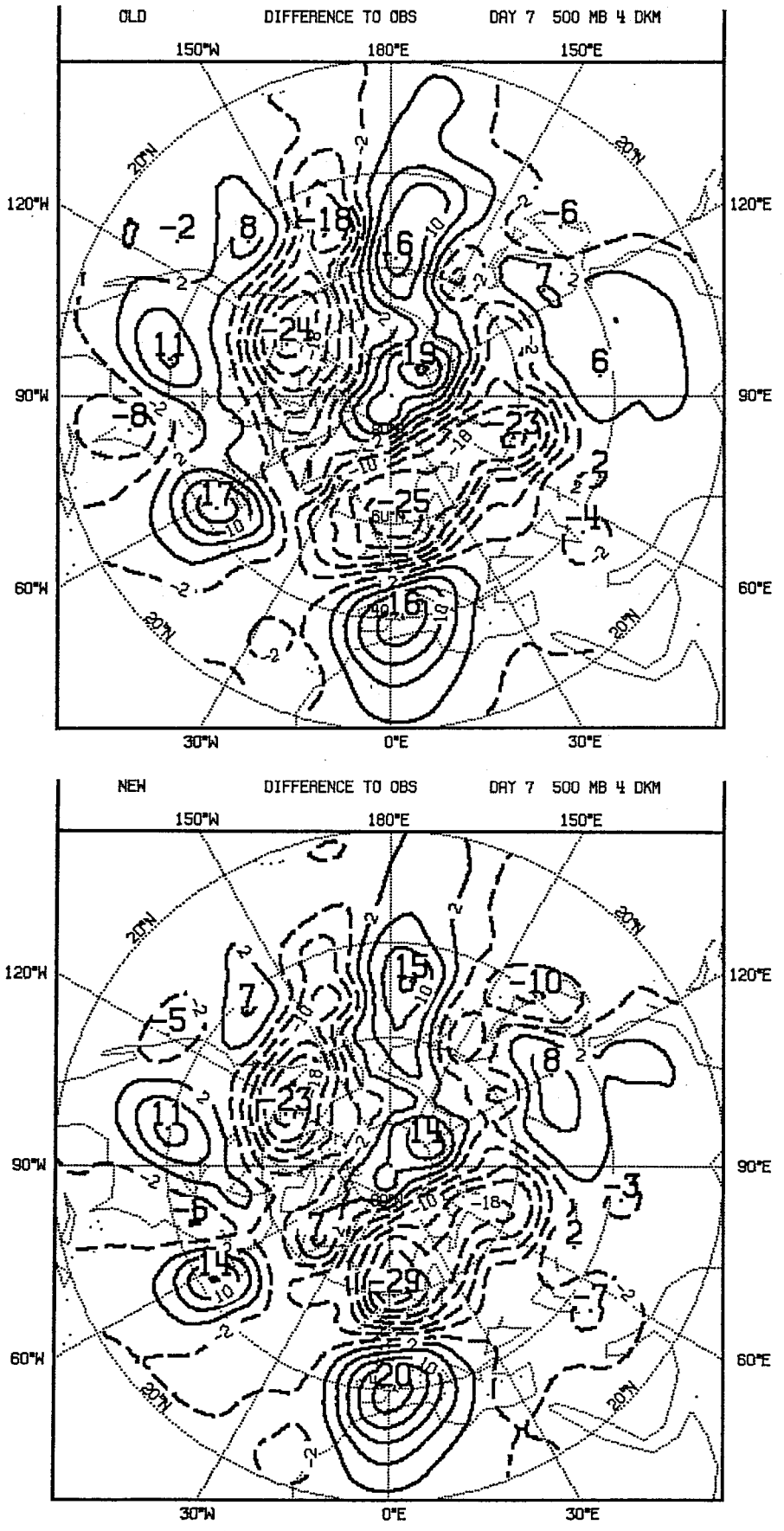
OLD DIFFERENCE TO OBS DAY 7 500 MB 4 DKM
150°W
180°E
150°E
120°W
120°E
90°W
90°E
60°W
60°E
30°W
0°E
30°E
20°N
NEW DIFFERENCE TO OBS DAY 7 500 MB 4 DKM
150°W
180°E
150°E
120°W
120°E
90°W
90°E
60°W
60°E
30°W
0°E
30°E
20°N

Fig. 11

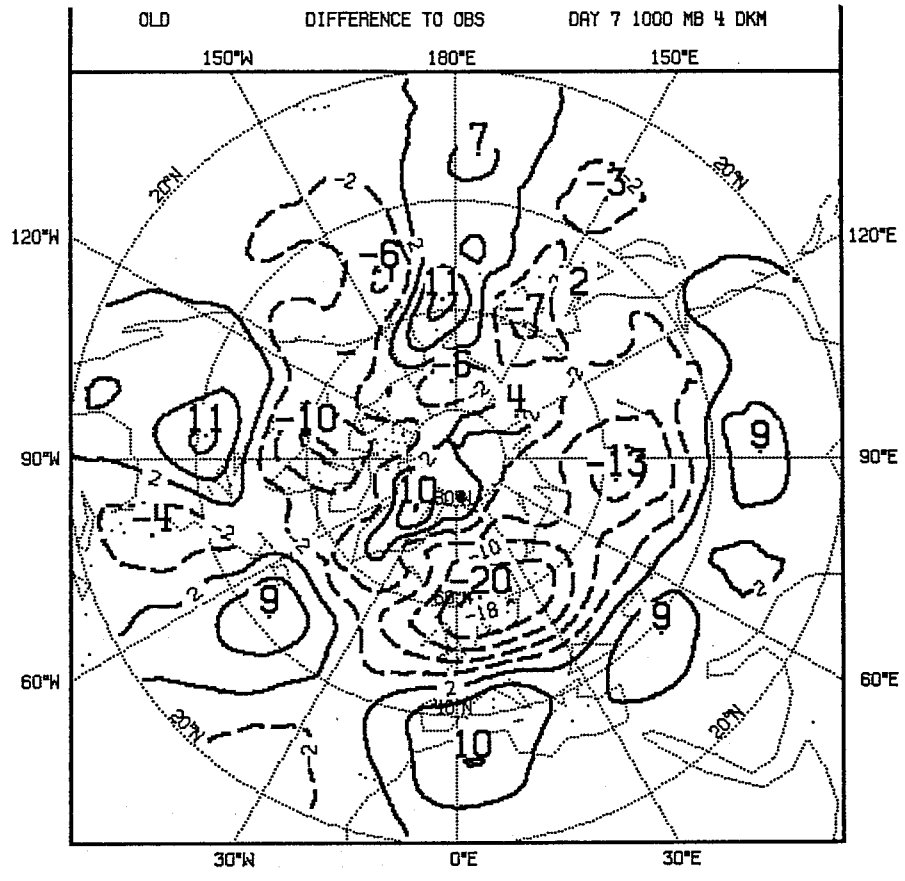
OLD
DIFFERENCE TO OBS
DAY 7 1000 MB 4 DKM
150°W
180°E
150°E
120°W
120°E
90°W
90°E
60°W
60°E
30°W
0°E
30°E
20°N
80°N
70°N
60°N
50°N
40°N

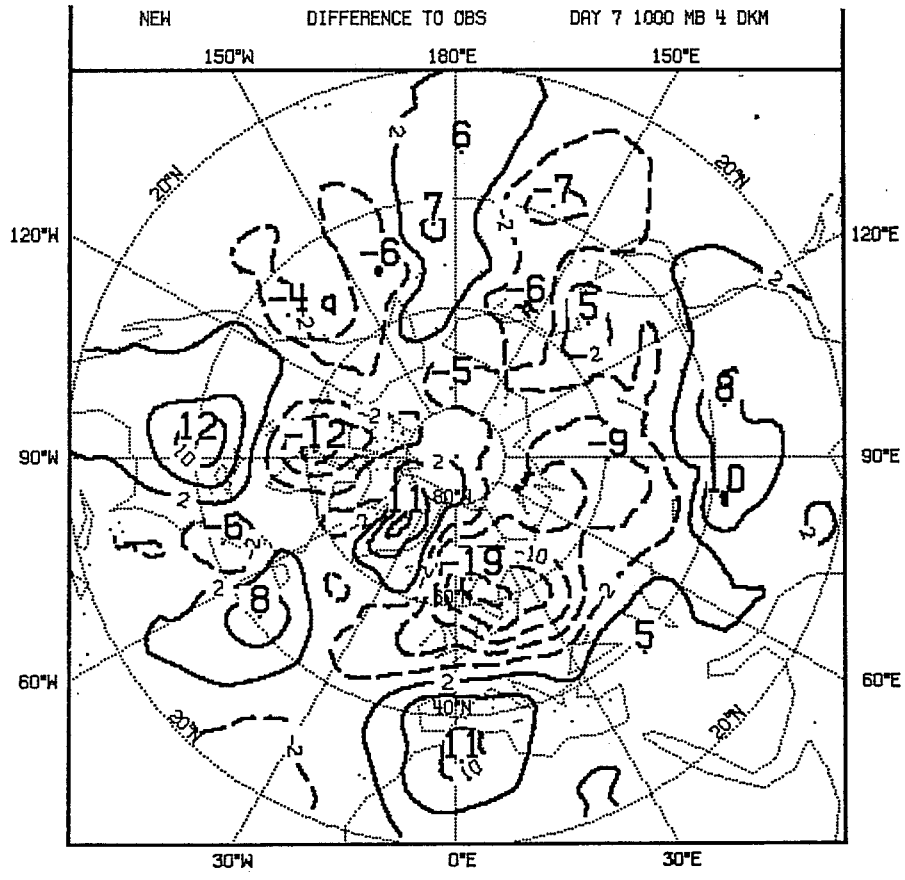
NEW
DIFFERENCE TO OBS
DAY 7 1000 MB 4 DKM
150°W
180°E
150°E
120°W
120°E
90°W
90°E
60°W
60°E
30°W
0°E
30°E
20°N
80°N
70°N
60°N
50°N
40°N

Fig. 12

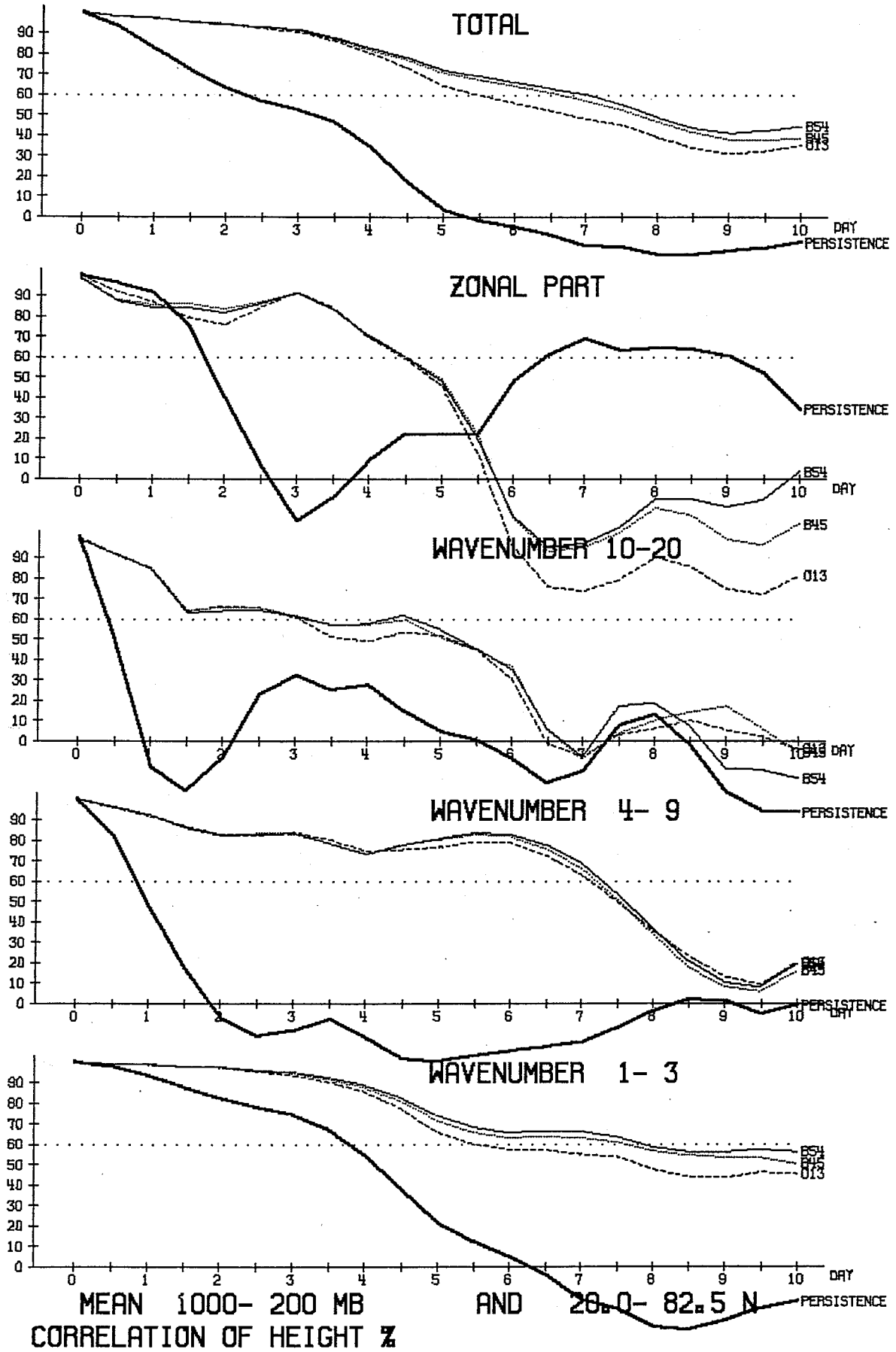
TOTAL
DAY
B54
B45
013
PERSISTENCE
ZONAL PART
PERSISTENCE
B54
DAY
B45
013
WAVENUMBER 10-20
DAY
B54
PERSISTENCE
WAVENUMBER 4- 9
PERSISTENCE
DAY
WAVENUMBER 1- 3
B54
B45
013
DAY
PERSISTENCE
MEAN 1000- 200 MB AND 28.0- 82.5 N
CORRELATION OF HEIGHT %

Fig. 13

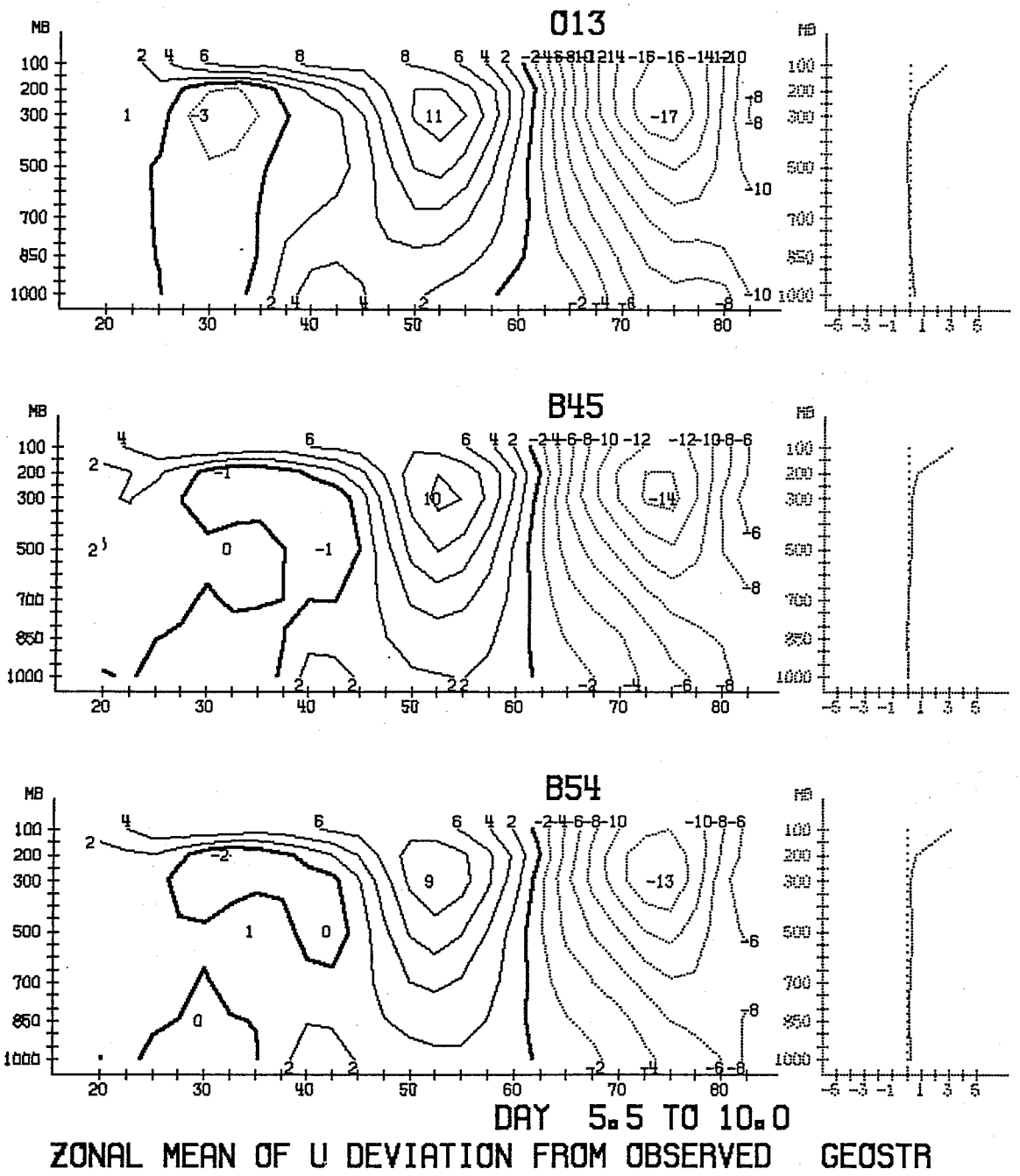
013
B45
B54
MB
100
200
300
500
700
850
1000
20
30
40
50
60
70
80
-5 -3 -1 1 3 5
DAY 5.5 TO 10.0
ZONAL MEAN OF U DEVIATION FROM OBSERVED GEOSTR

Fig. 14

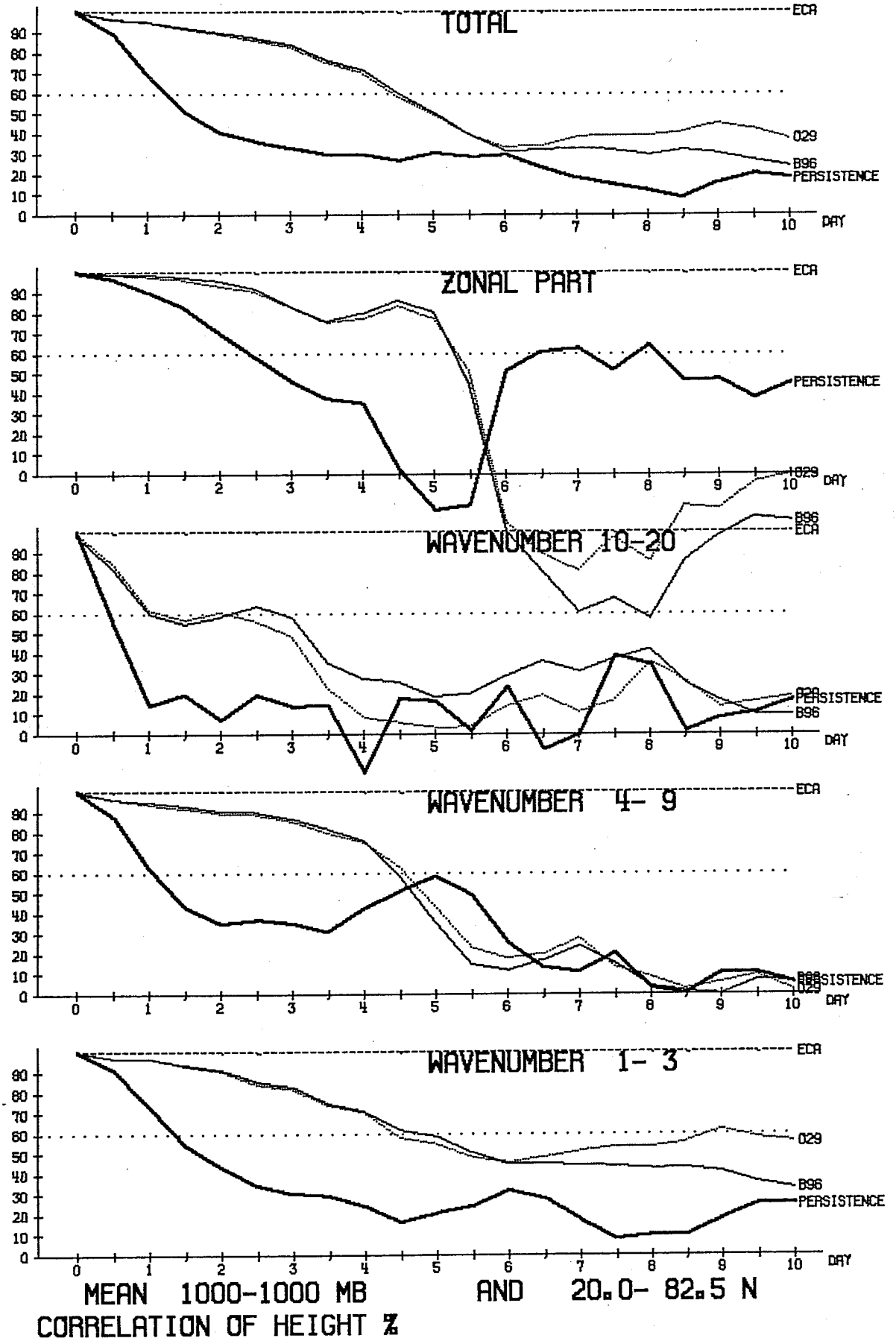
TOTAL
ECA
029
B96
PERSISTENCE
DAY
ZONAL PART
ECA
PERSISTENCE
B96
DAY
WAVENUMBER 10-20
ECA
B96
PERSISTENCE
DAY
WAVENUMBER 4- 9
ECA
PERSISTENCE
DAY
WAVENUMBER 1- 3
ECA
029
B96
PERSISTENCE
DAY
MEAN 1000-1000 MB AND 20.0- 82.5 N
CORRELATION OF HEIGHT %

Fig. 15

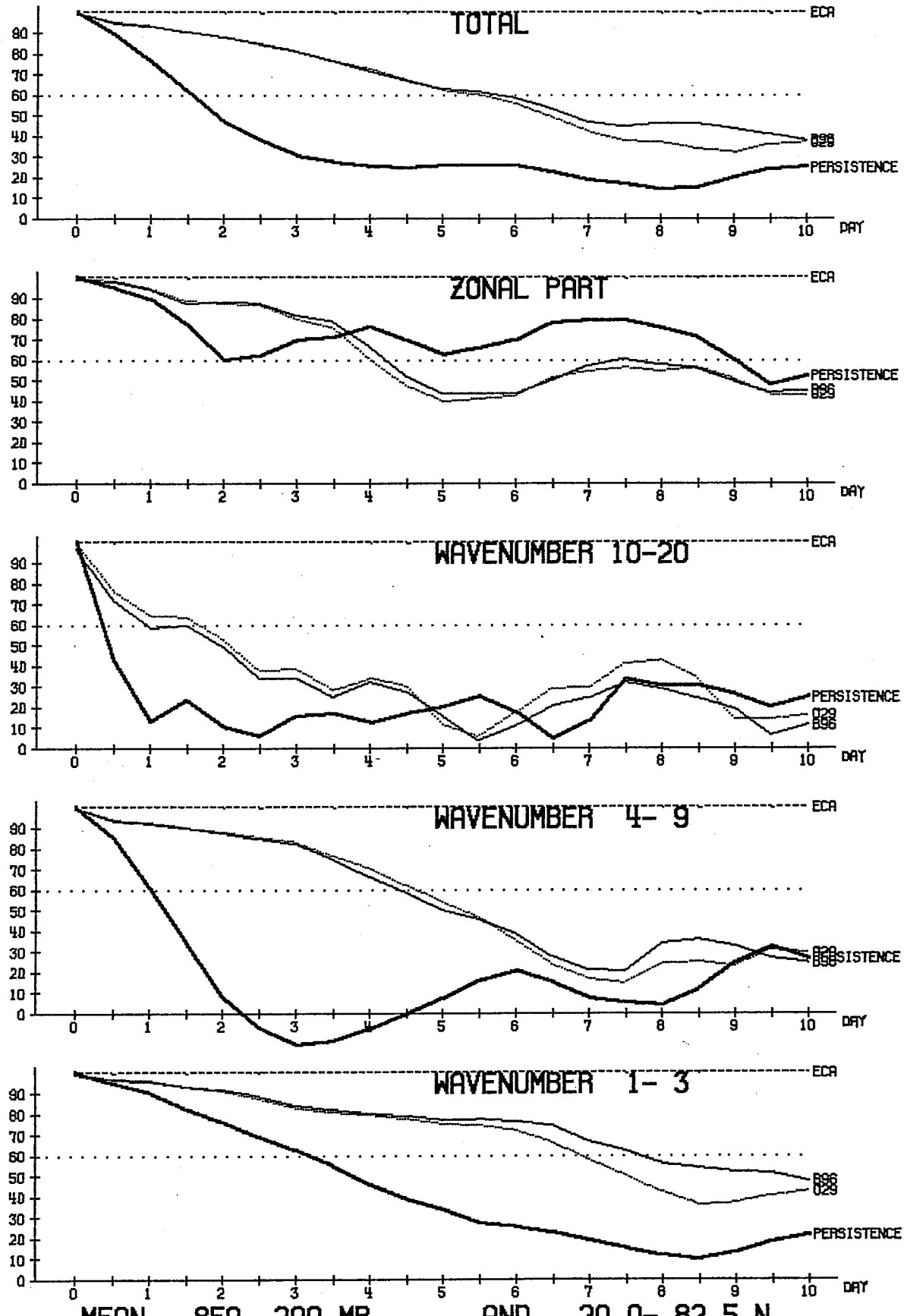
TOTAL
ECA
PERSISTENCE
DAY
ZONAL PART
ECA
PERSISTENCE
DAY
WAVENUMBER 10-20
ECA
PERSISTENCE
DAY
WAVENUMBER 4- 9
ECA
DAY
WAVENUMBER 1- 3
ECA
DAY
MEAN 850- 200 MB AND 20.0- 82.5 N
CORRELATION OF TEMPERATURE %

Fig. 16

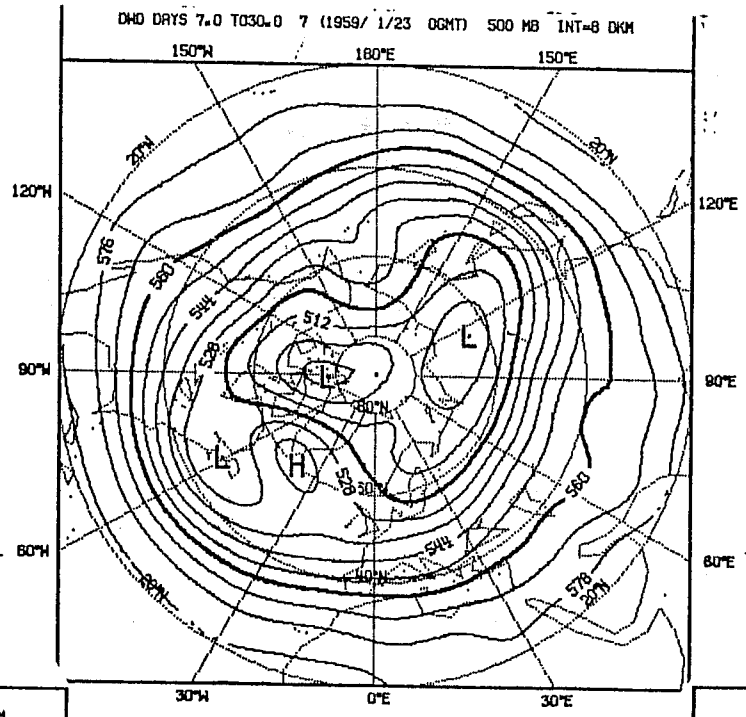

B52 (OM)

B53 (NM)

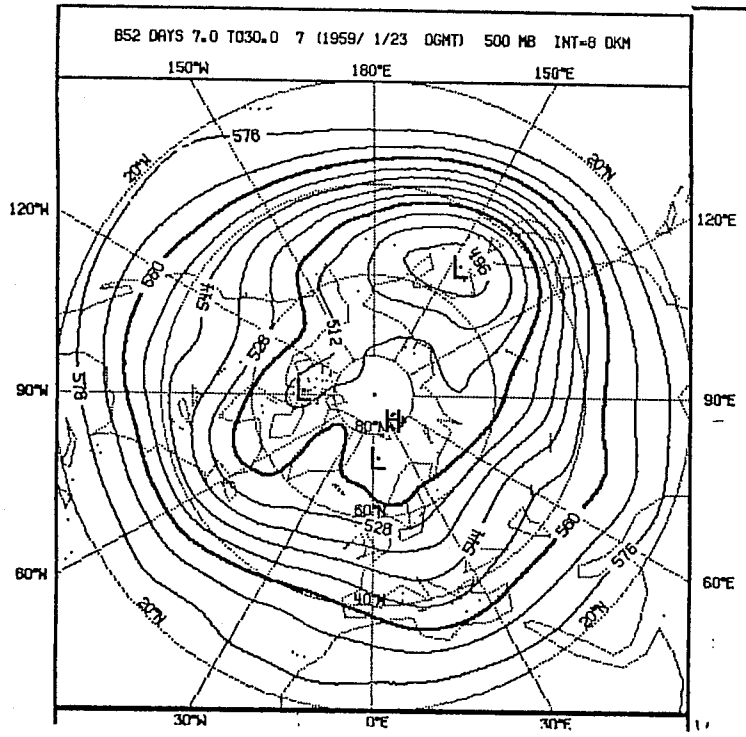

DWD

DAYS 7 to 30

500 mb

mean height

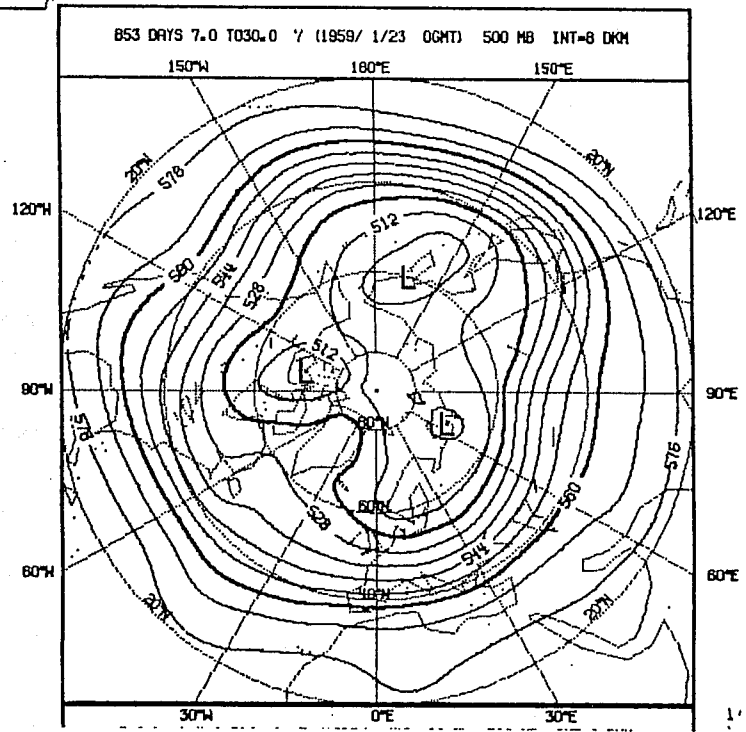

Fig. 17

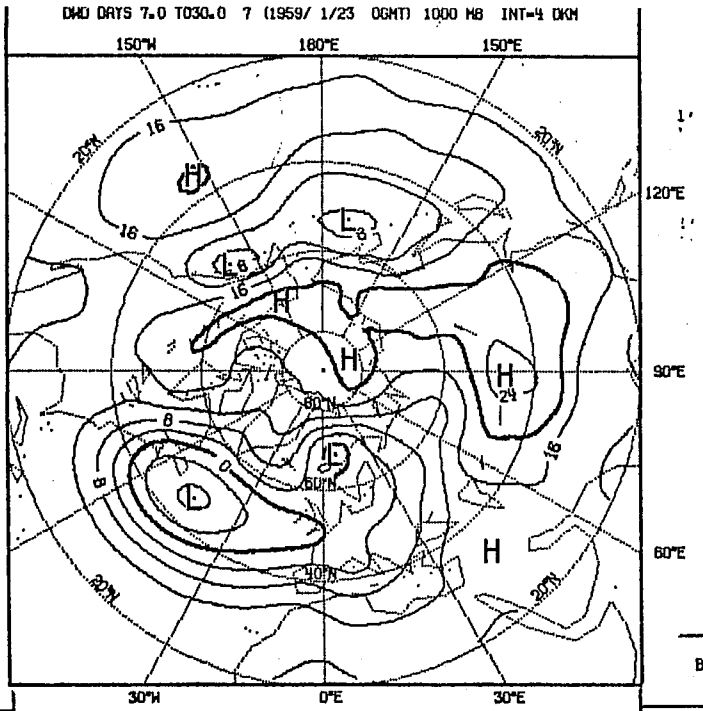

DWD

B52 (OM)

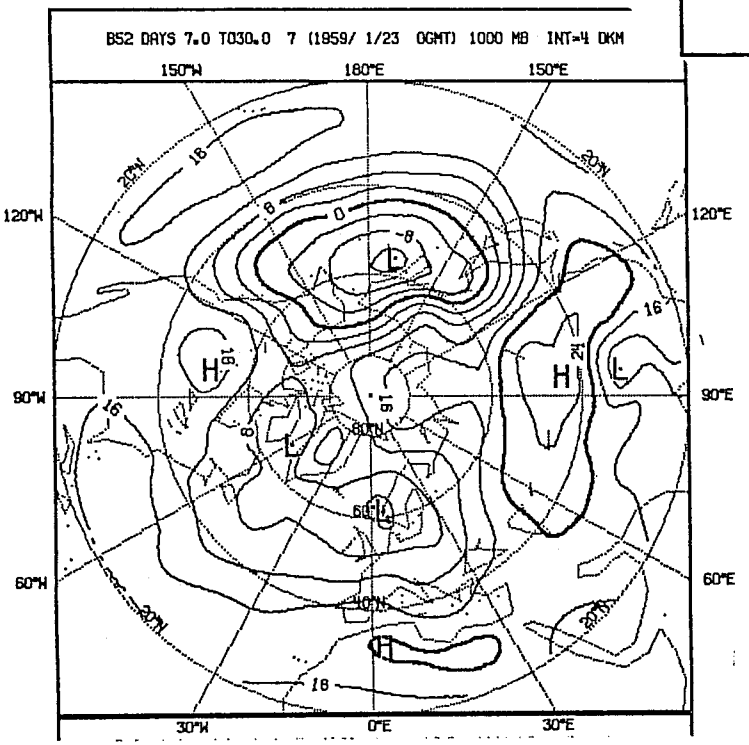

B53 (NM)

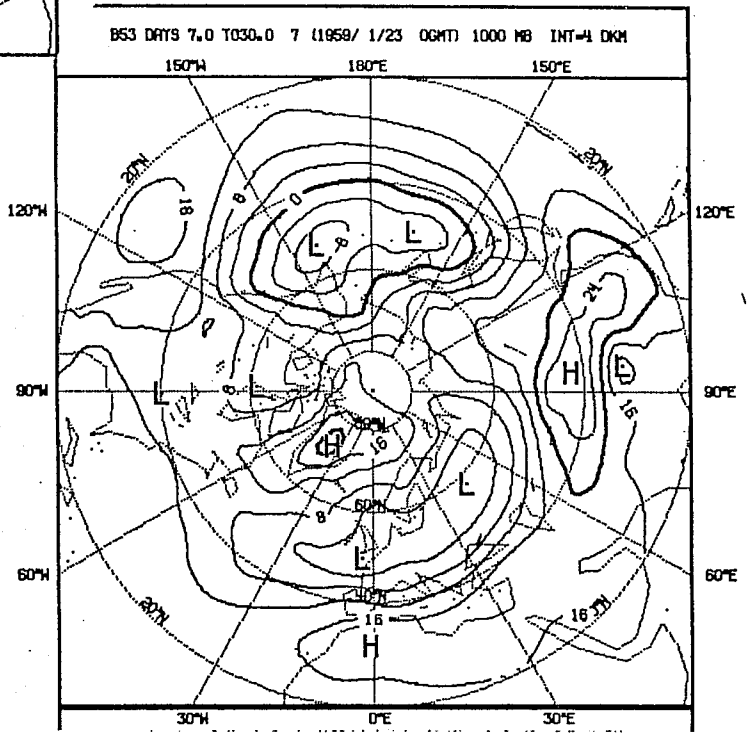

DAYS 7 to 30

1000 mb

mean height

Fig. 18

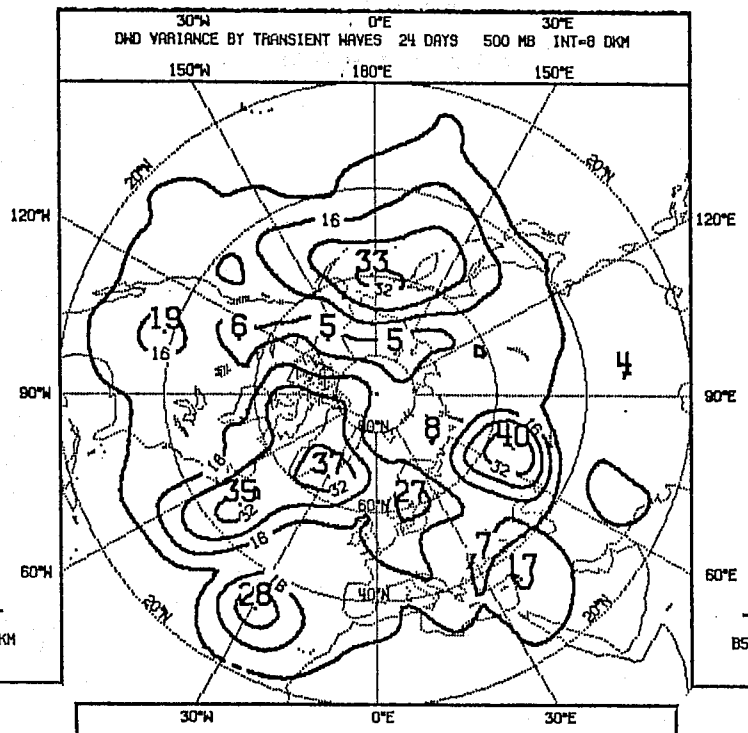

B52 (OM)

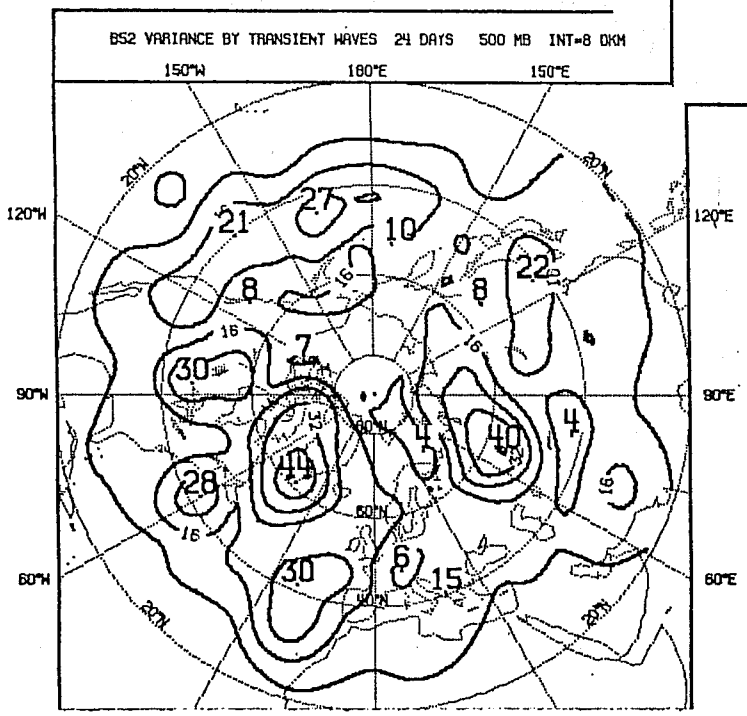

B53 (NM)

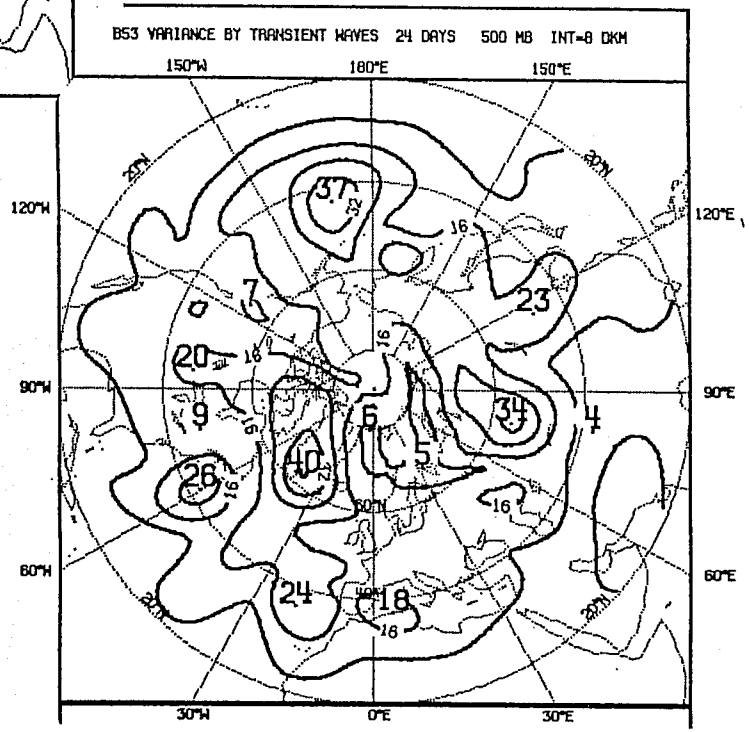

DWD

TRANSIENT

WAVES

VARIANCE

(24 DAYS)

500 mb

Fig. 19

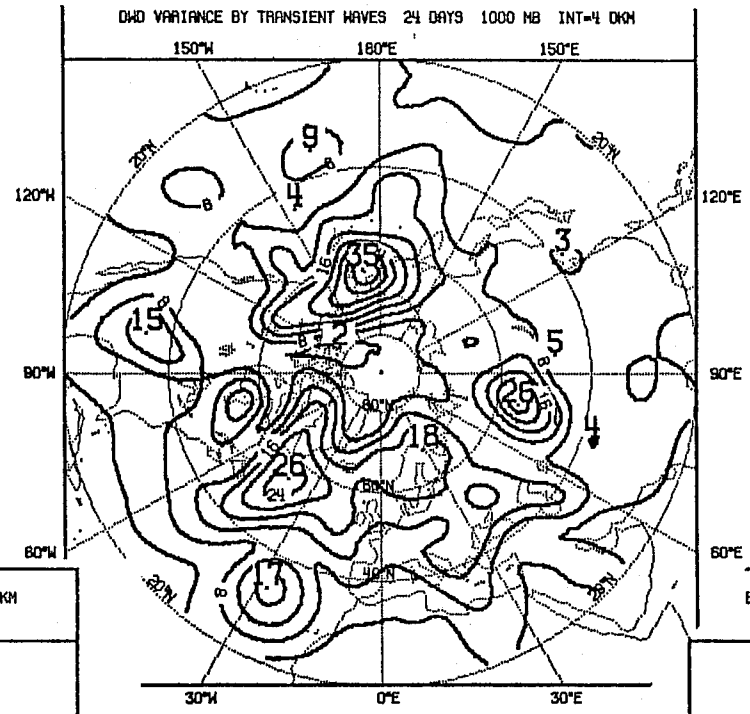

B52 (OM)

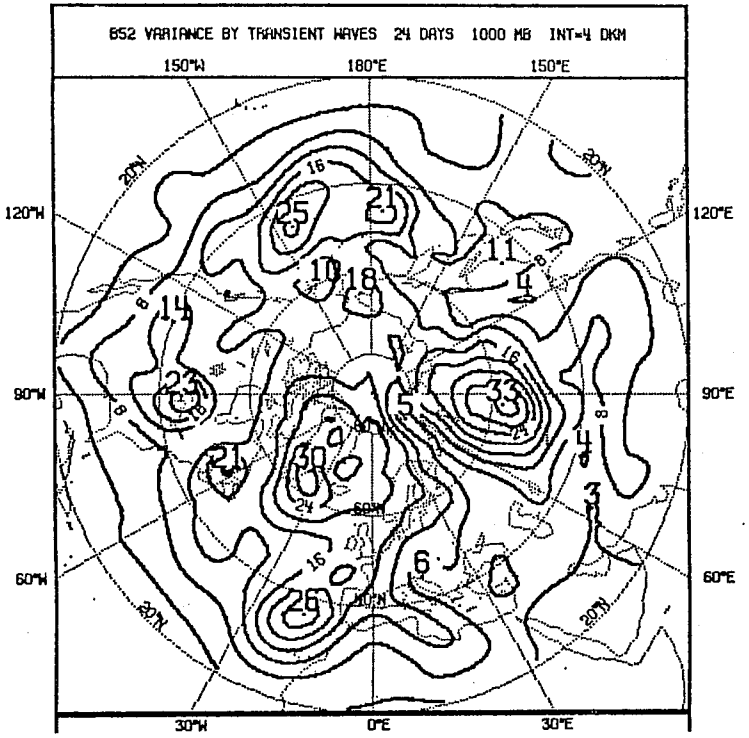

B53 (NM)

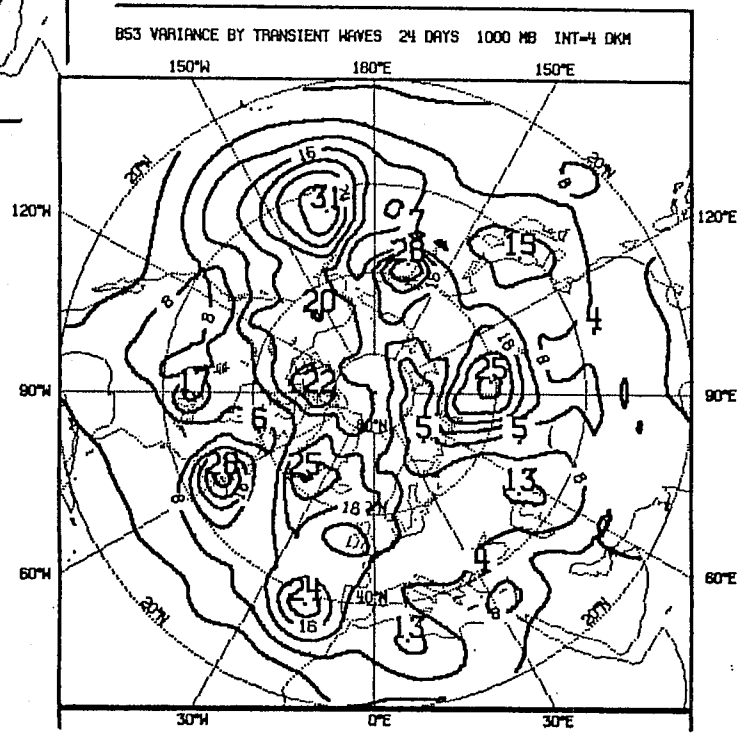

DWD

TRANSIENT WAVES VARIANCE (24 DAYS)

1000 mb

Fig. 20

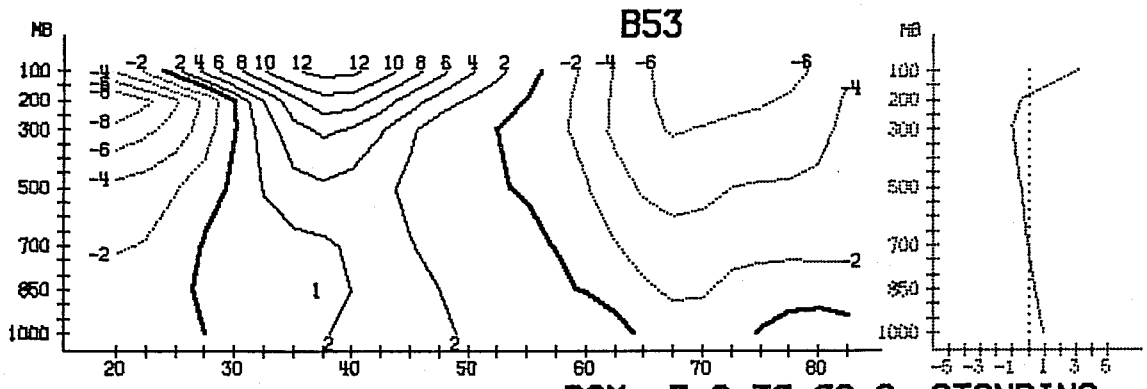
B53
MB
DAY 7.0 TO 30.0 STANDING
ZONAL MEAN OF U DEVIATION FROM OBSERVED GEOSTR

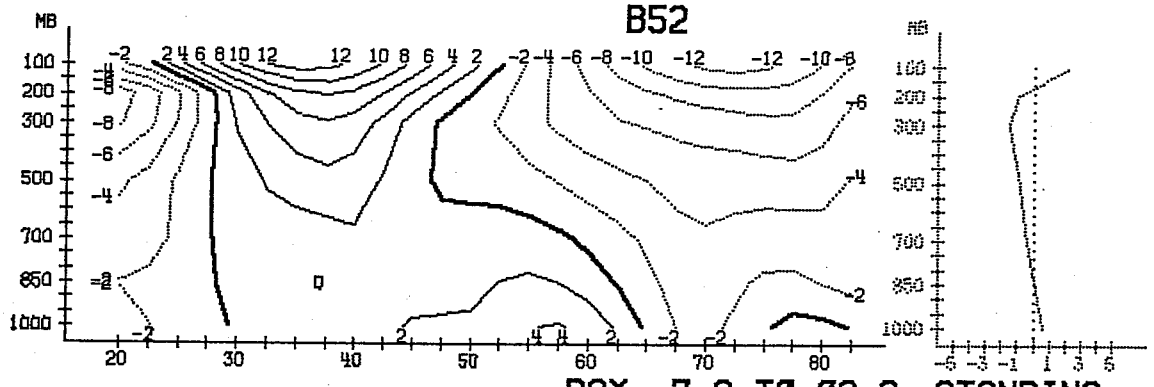
B52
MB
DAY 7.0 TO 30.0 STANDING
ZONAL MEAN OF U DEVIATION FROM OBSERVED GEOSTR

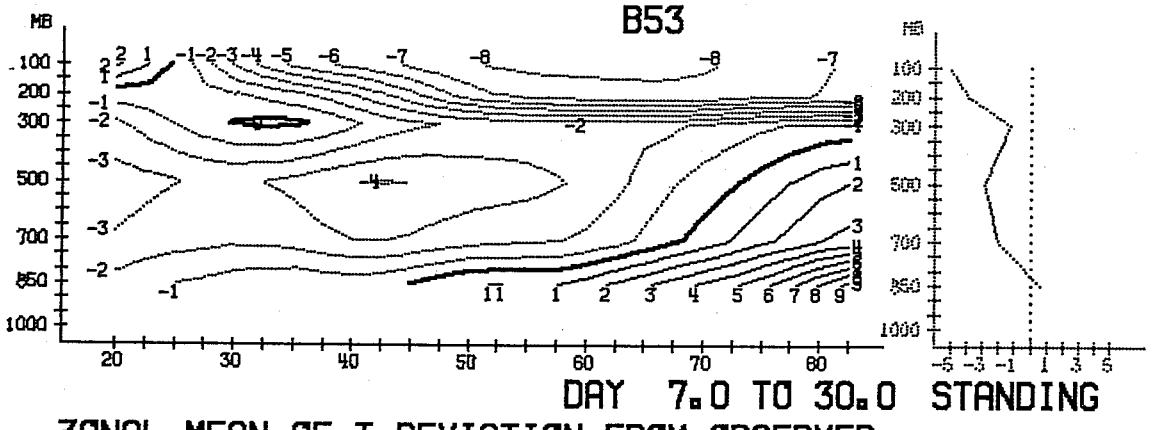
B53
MB
DAY 7.0 TO 30.0 STANDING
ZONAL MEAN OF T DEVIATION FROM OBSERVED

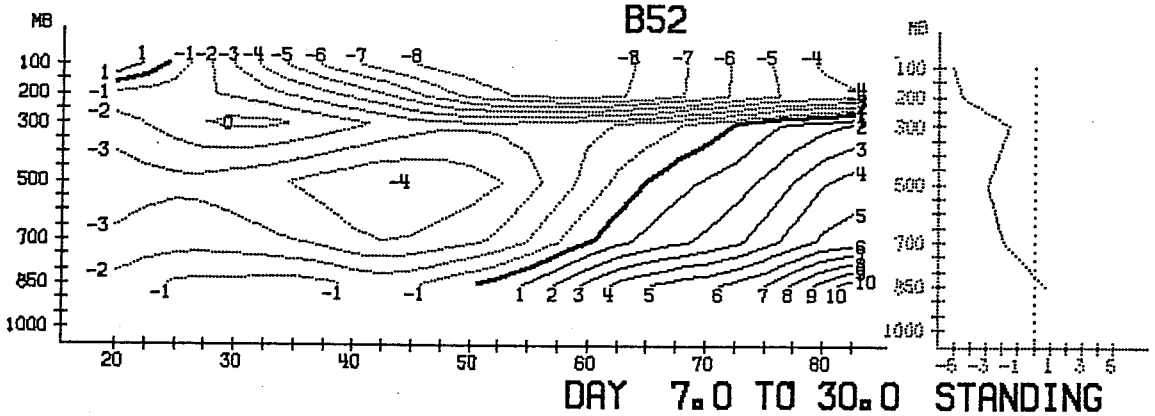
B52
MB
DAY 7.0 TO 30.0 STANDING
ZONAL MEAN OF T DEVIATION FROM OBSERVED

Fig. 21

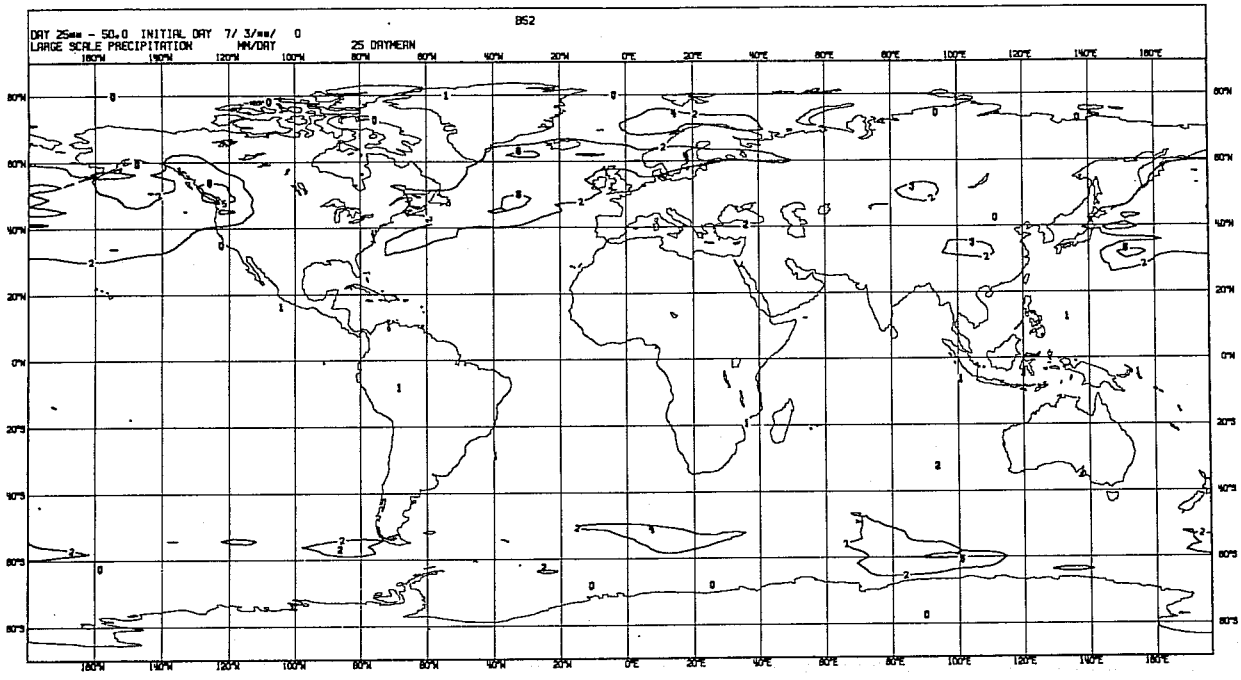
BS2
DAY 25ᵐᵐ - 50.0 INITIAL DAY 7/ 3/ᵐᵐ/ 0
LARGE SCALE PRECIPITATION MM/DAY
25 DAYMEAN

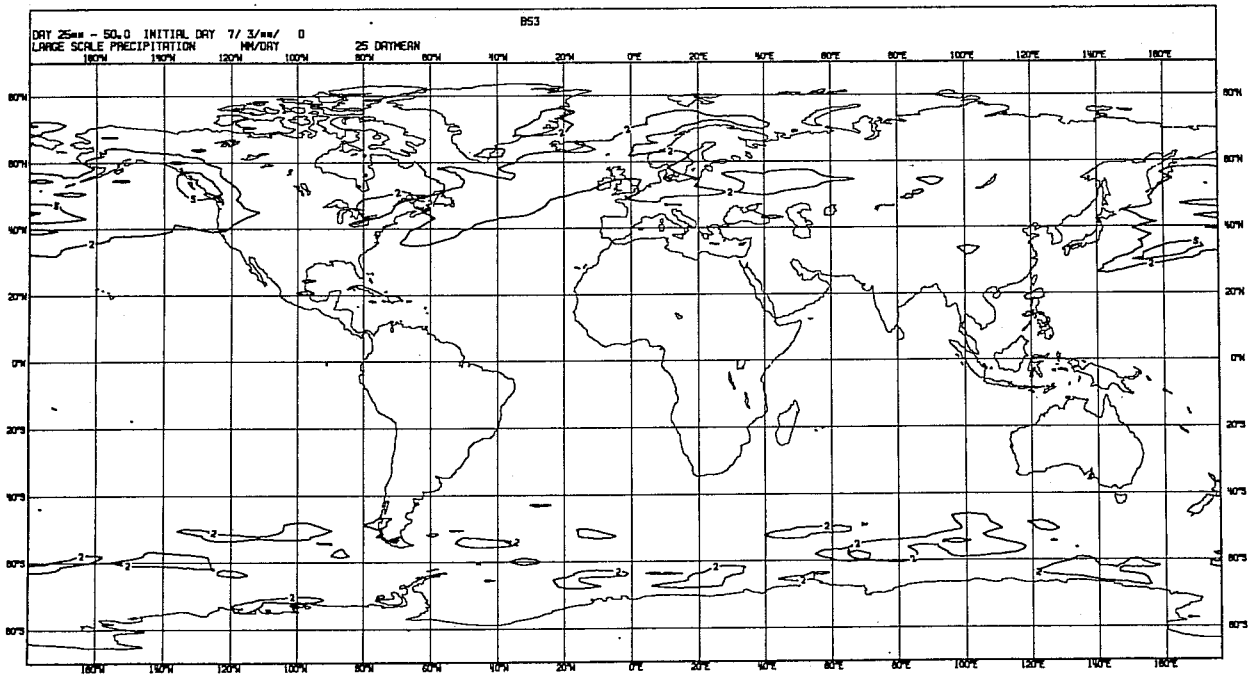
BS3
DAY 25ᵐᵐ - 50.0 INITIAL DAY 7/ 3/ᵐᵐ/ 0
LARGE SCALE PRECIPITATION MM/DAY
25 DAYMEAN

Fig. 22

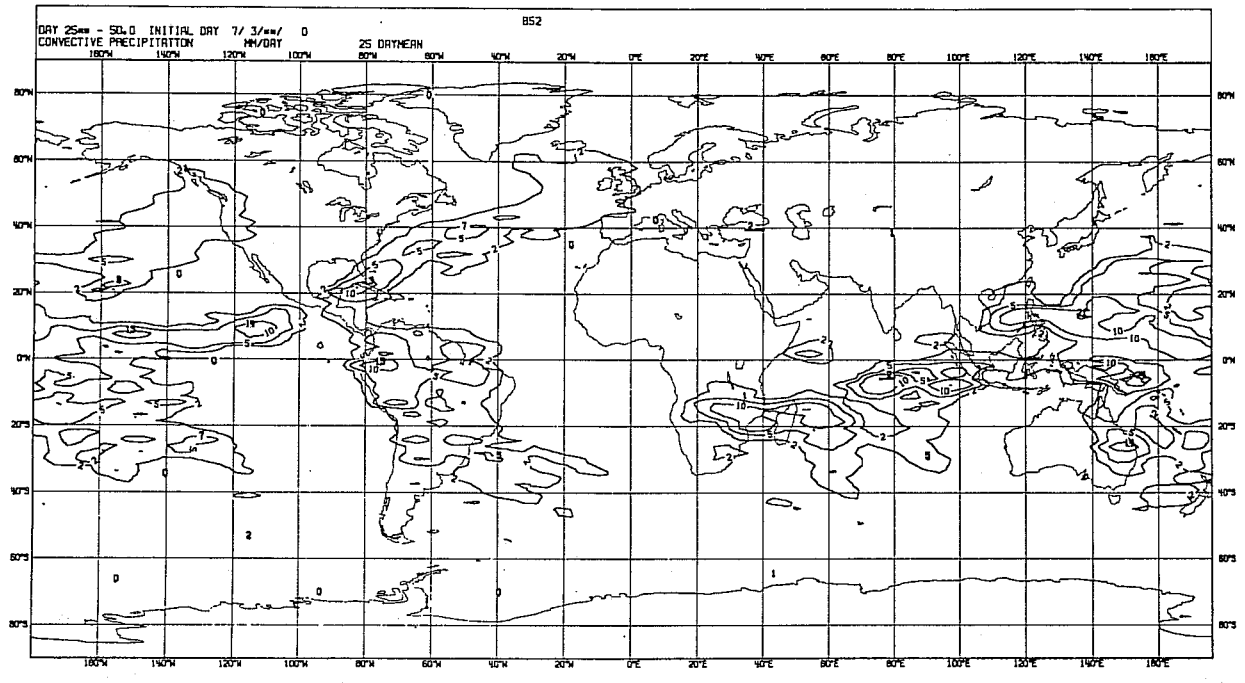
852
DAY 25₀₀ - 50.0 INITIAL DAY 7/ 3/₀₀/ 0
CONVECTIVE PRECIPITATION MM/DAY
25 DAYMEAN

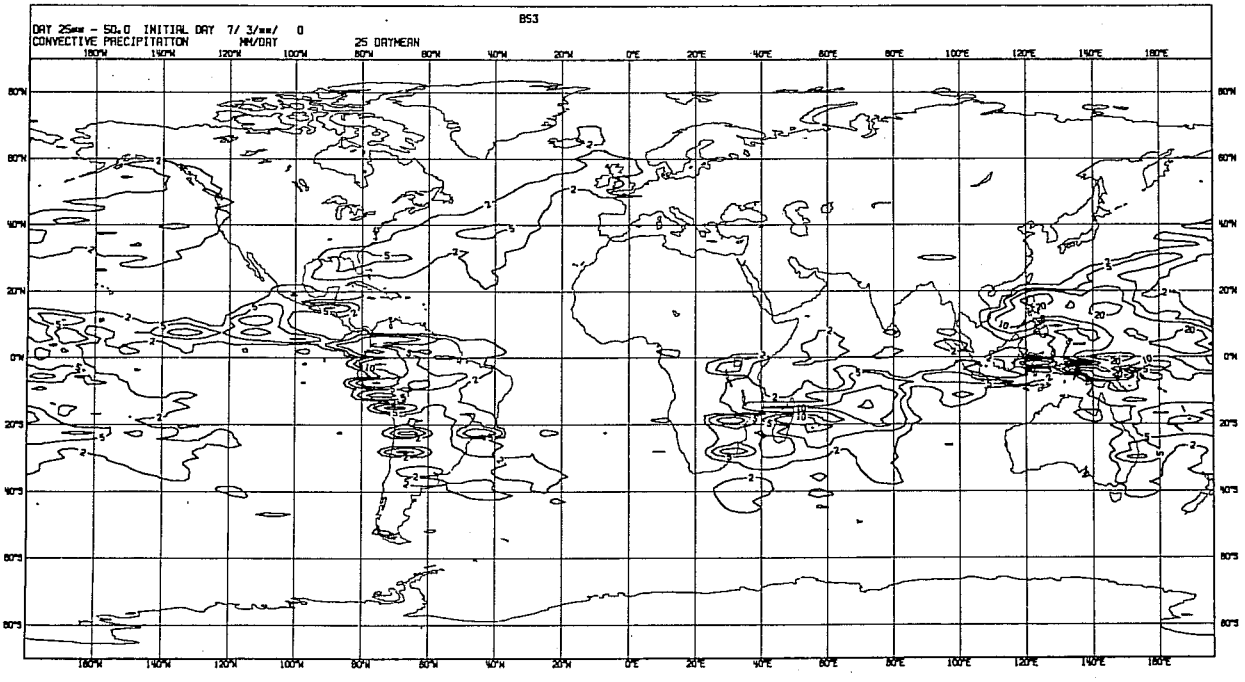
853
DAY 25₀₀ - 50.0 INITIAL DAY 7/ 3/₀₀/ 0
CONVECTIVE PRECIPITATION MM/DAY
25 DAYMEAN

Fig. 23

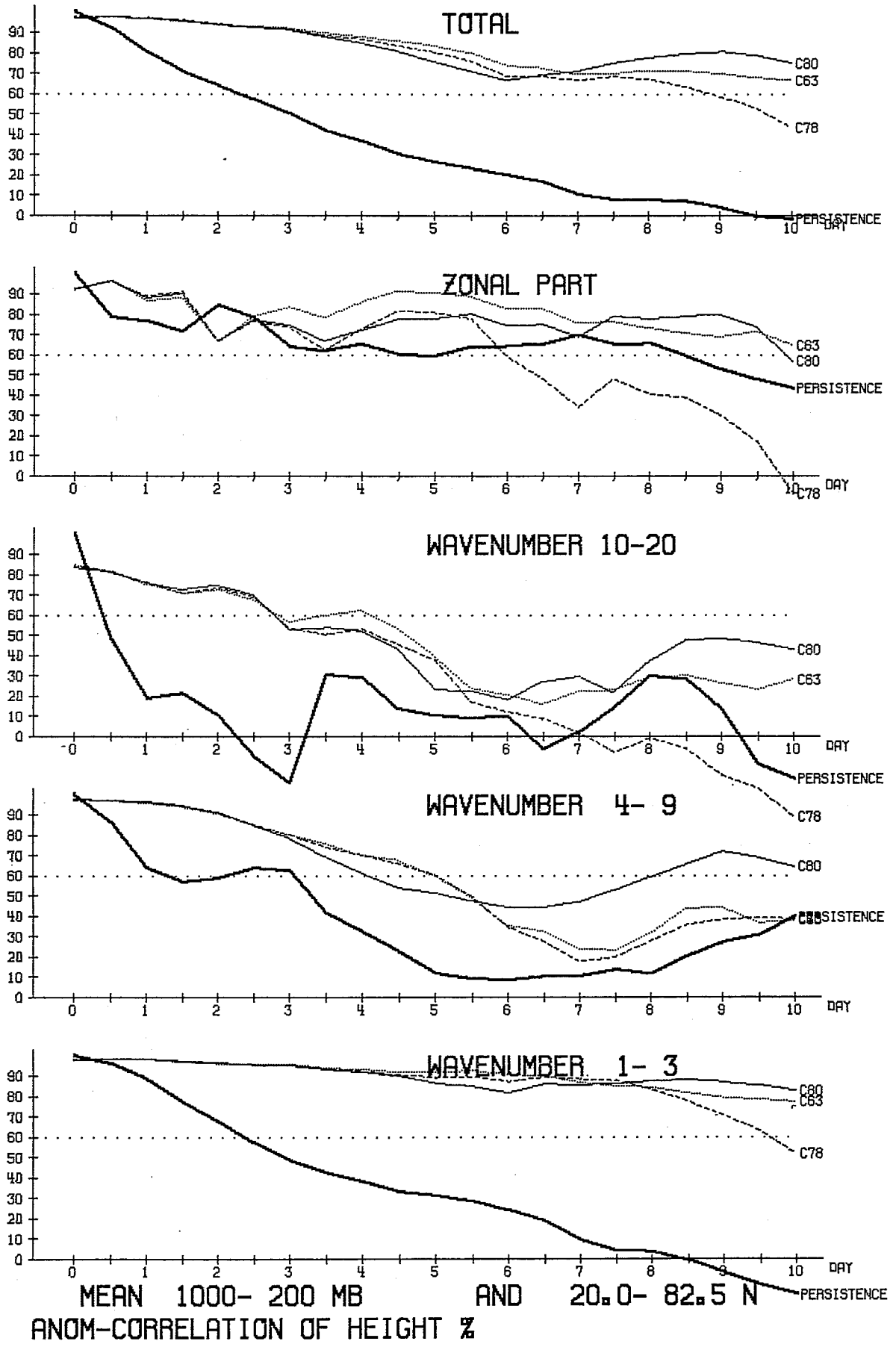
TOTAL
C80
C63
C78
PERSISTENCE
DAY
ZONAL PART
C63
C80
PERSISTENCE
C78
DAY
WAVENUMBER 10-20
C80
C63
DAY
PERSISTENCE
C78
WAVENUMBER 4- 9
C80
PERSISTENCE
DAY
WAVENUMBER 1- 3
C80
C63
C78
DAY
PERSISTENCE
MEAN 1000- 200 MB AND 20.0- 82.5 N
ANOM-CORRELATION OF HEIGHT %

Fig. 24

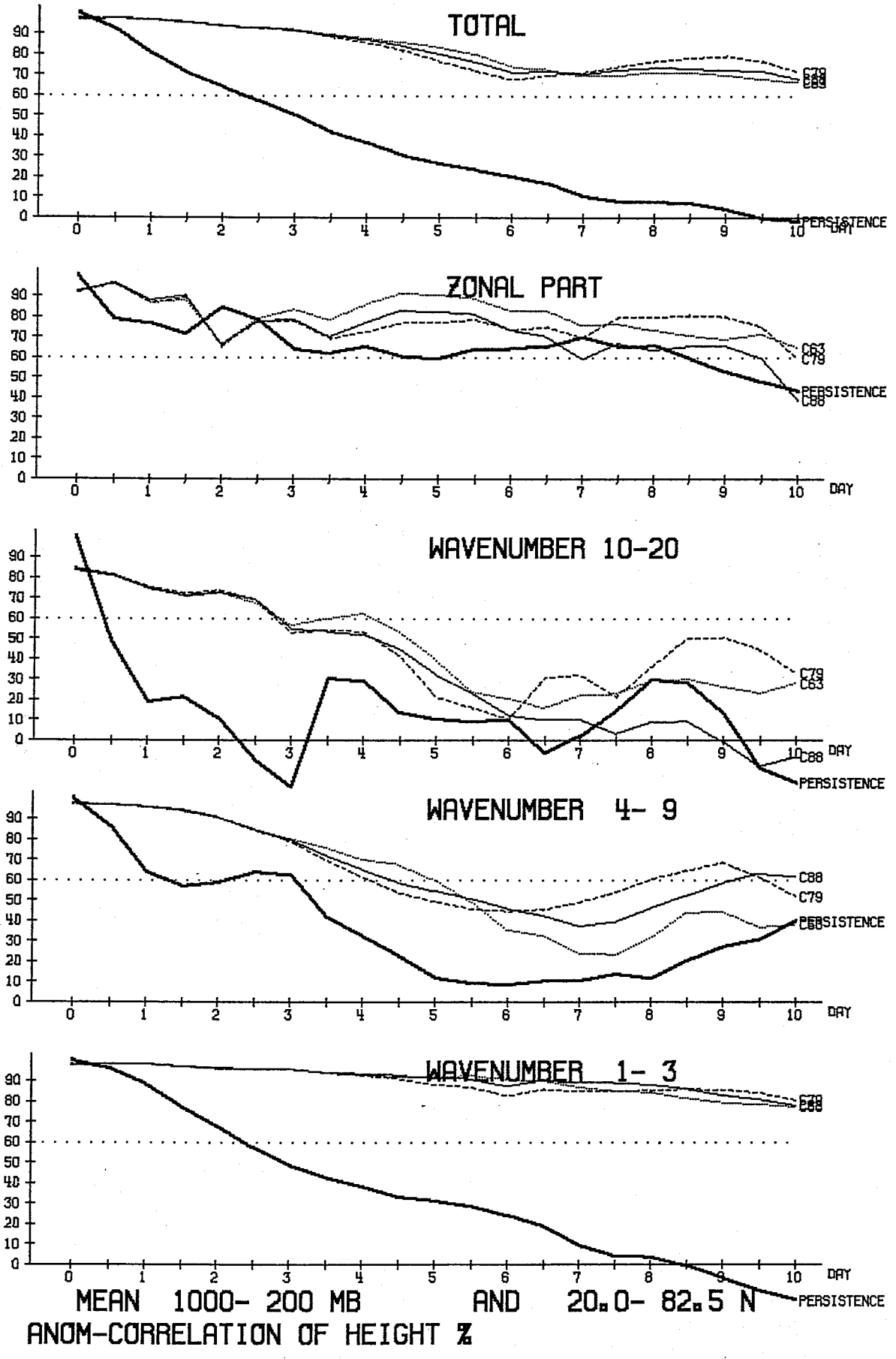
TOTAL
C79
C88
PERSISTENCE
DAY
ZONAL PART
C63
C79
C88
PERSISTENCE
DAY
WAVENUMBER 10-20
C79
C63
C88
PERSISTENCE
DAY
WAVENUMBER 4- 9
C88
C79
C88
PERSISTENCE
DAY
WAVENUMBER 1- 3
C79
C88
PERSISTENCE
DAY
MEAN 1000- 200 MB AND 20.0- 82.5 N
ANOM-CORRELATION OF HEIGHT %

Fig. 25

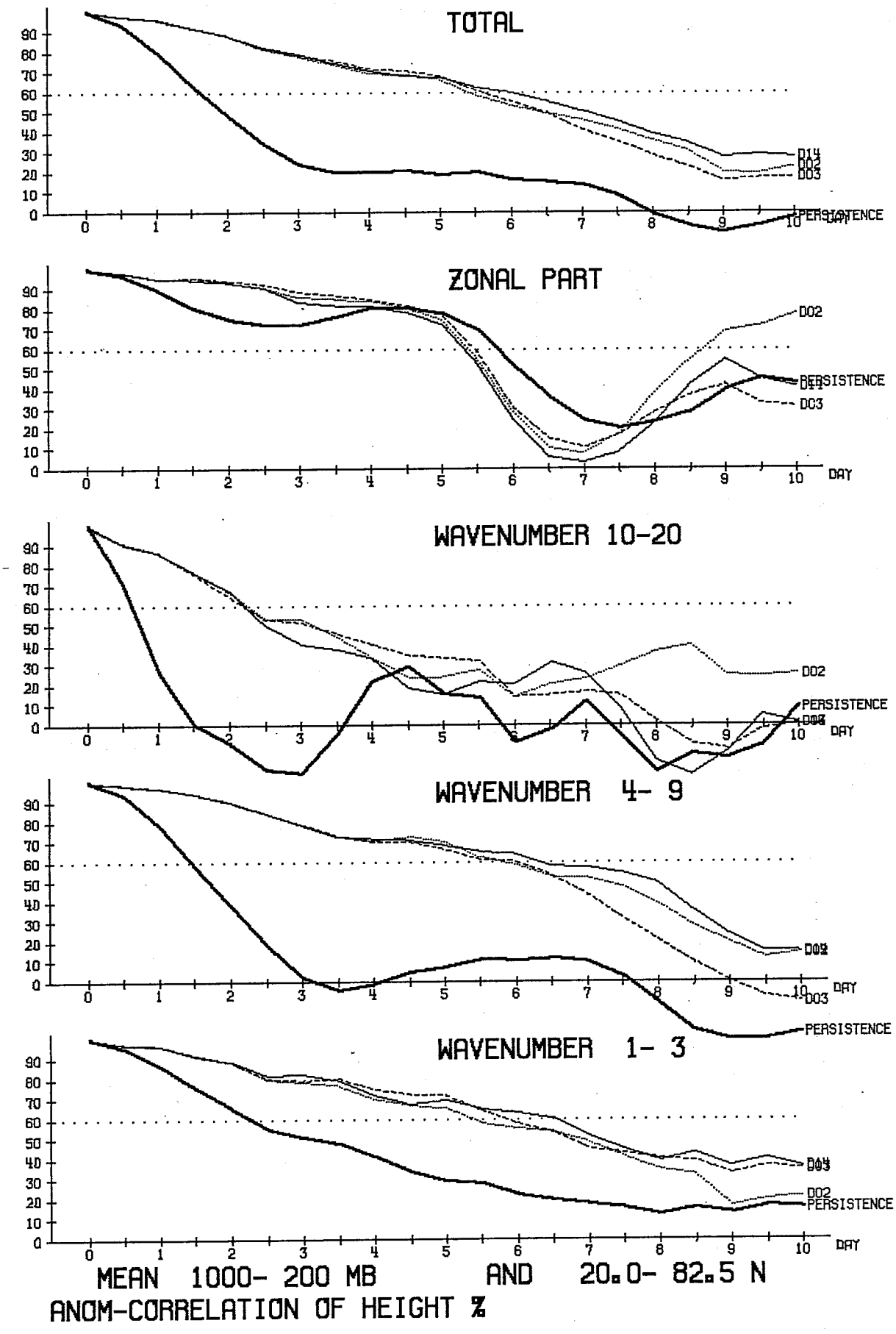
TOTAL
D14
D02
D03
PERSISTENCE
DAY
ZONAL PART
D02
PERSISTENCE
D03
DAY
WAVENUMBER 10-20
D02
PERSISTENCE
DAY
WAVENUMBER 4- 9
D03
PERSISTENCE
DAY
WAVENUMBER 1- 3
D02
PERSISTENCE
DAY
MEAN 1000- 200 MB AND 20.0- 82.5 N
ANOM-CORRELATION OF HEIGHT %

Fig. 26

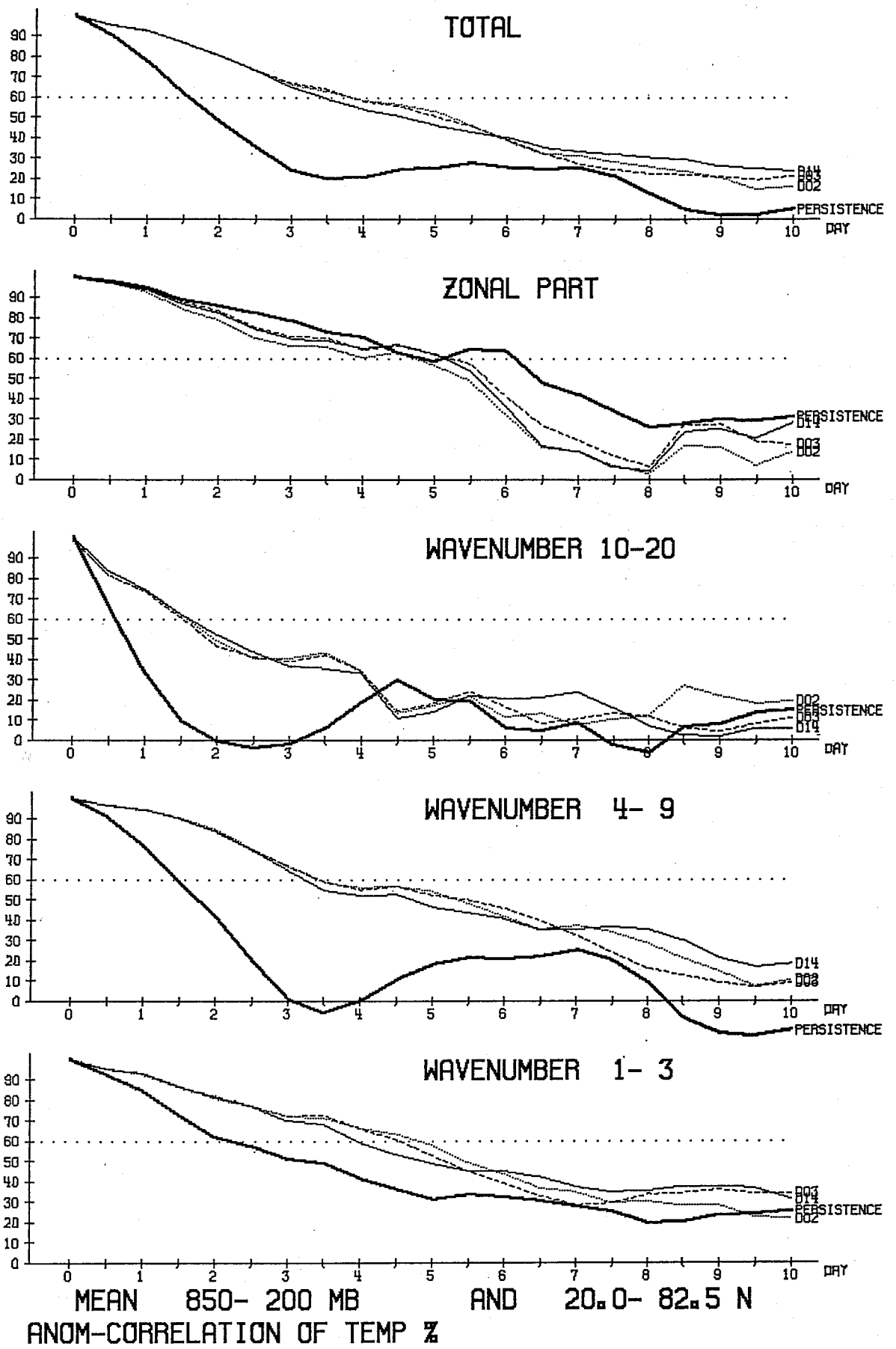
TOTAL
ZONAL PART
WAVENUMBER 10-20
WAVENUMBER 4- 9
WAVENUMBER 1- 3
PERSISTENCE
D14
D03
D02
DAY
MEAN 850- 200 MB AND 20.0- 82.5 N
ANOM-CORRELATION OF TEMP %

Fig. 27

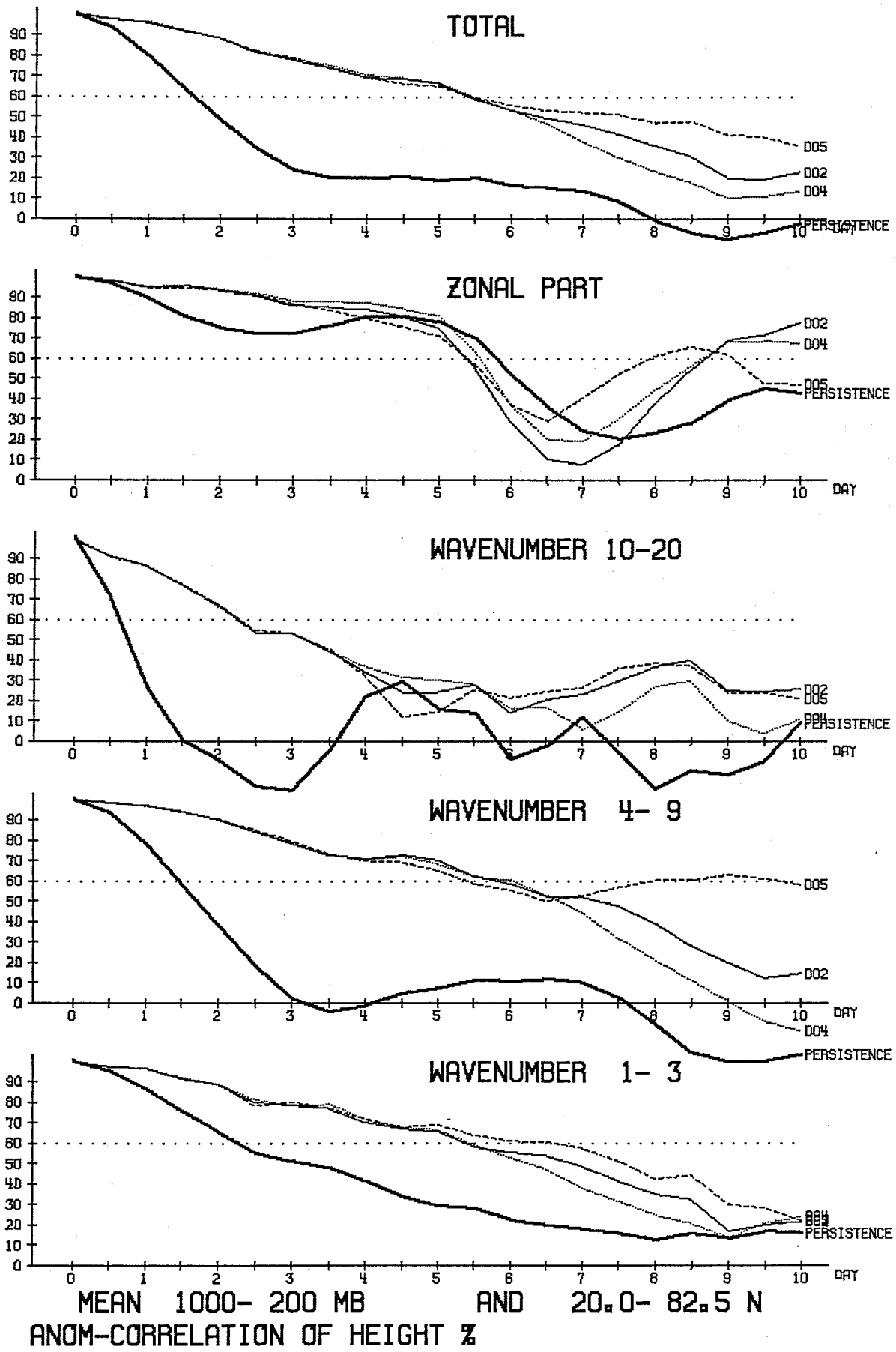
TOTAL
D05
D02
D04
PERSISTENCE
DAY
ZONAL PART
D02
D04
D05
PERSISTENCE
DAY
WAVENUMBER 10-20
D02
D05
D04
PERSISTENCE
DAY
WAVENUMBER 4- 9
D05
D02
DAY
D04
PERSISTENCE
WAVENUMBER 1- 3
D04
D02
PERSISTENCE
DAY
MEAN 1000- 200 MB AND 20.0- 82.5 N
ANOM-CORRELATION OF HEIGHT %

Fig. 28

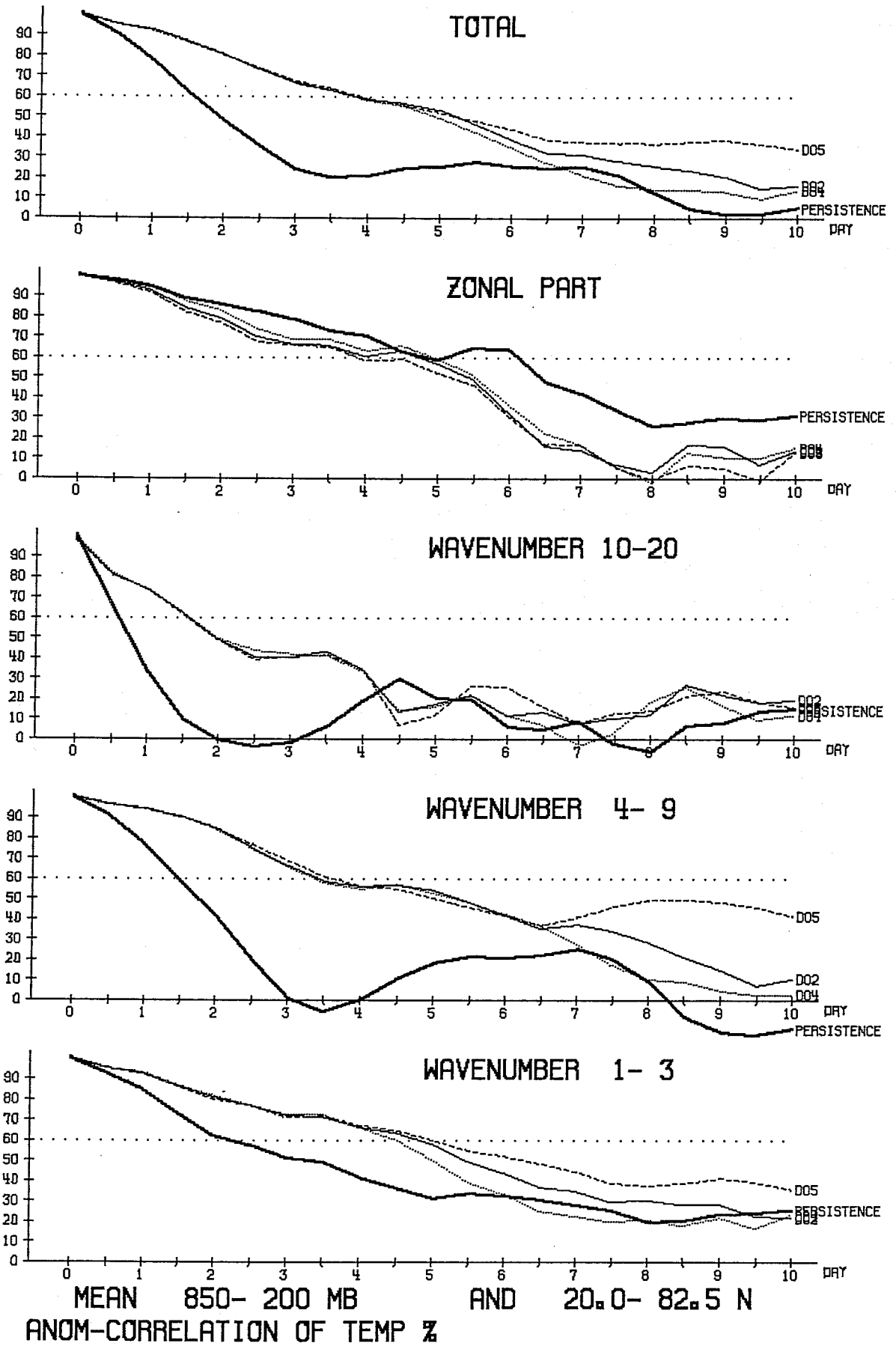
TOTAL
ZONAL PART
WAVENUMBER 10-20
WAVENUMBER 4- 9
WAVENUMBER 1- 3
DAY
PERSISTENCE
MEAN 850- 200 MB AND 20.0- 82.5 N
ANOM-CORRELATION OF TEMP %

Fig. 29

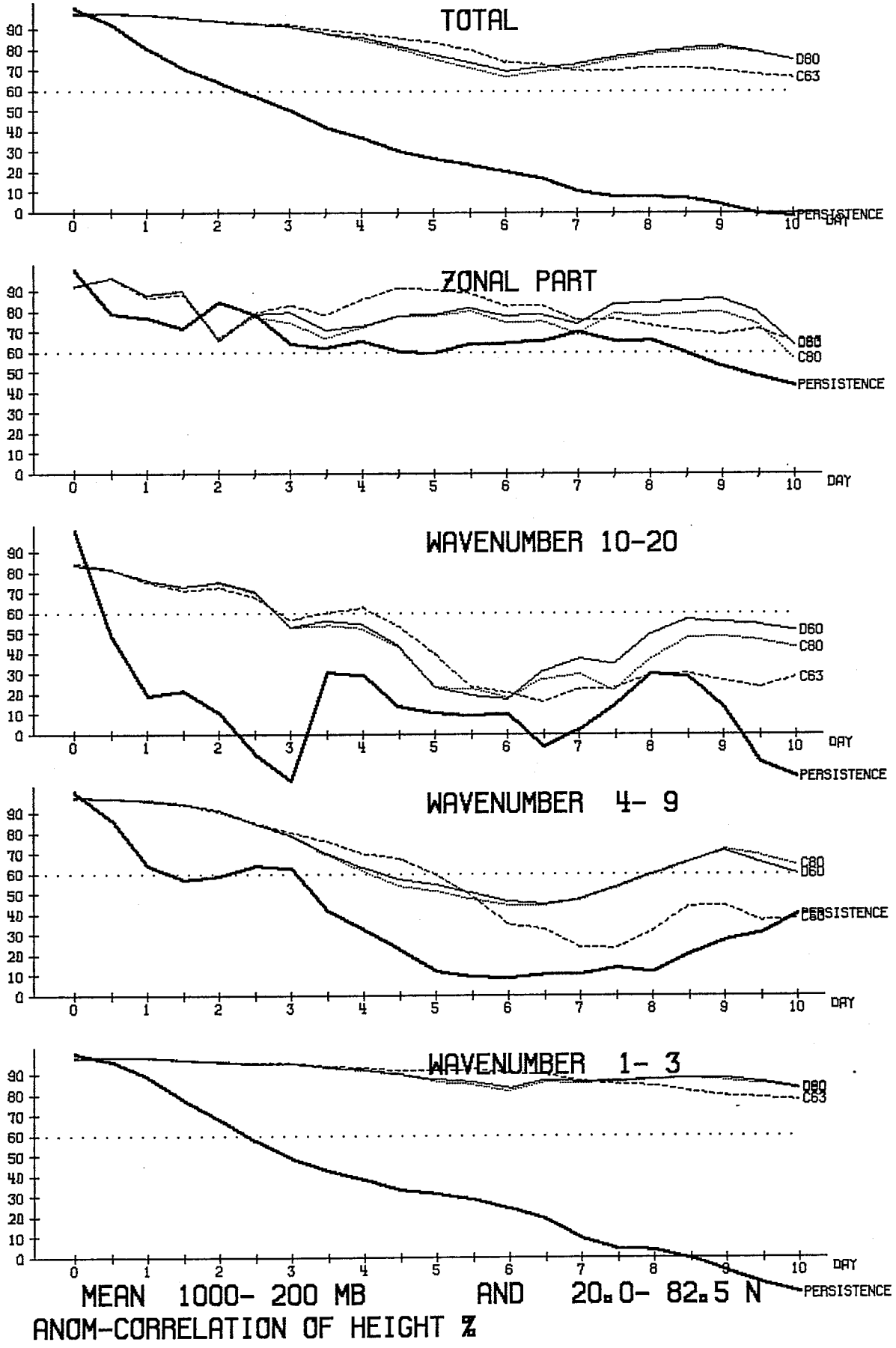
TOTAL
D80
C63
PERSISTENCE
DAY
ZONAL PART
D80
C80
PERSISTENCE
DAY
WAVENUMBER 10-20
D80
C80
C63
PERSISTENCE
DAY
WAVENUMBER 4- 9
C80
D80
PERSISTENCE
DAY
WAVENUMBER 1- 3
D80
C63
PERSISTENCE
DAY
MEAN 1000- 200 MB AND 20.0- 82.5 N
ANOM-CORRELATION OF HEIGHT %

Fig. 30

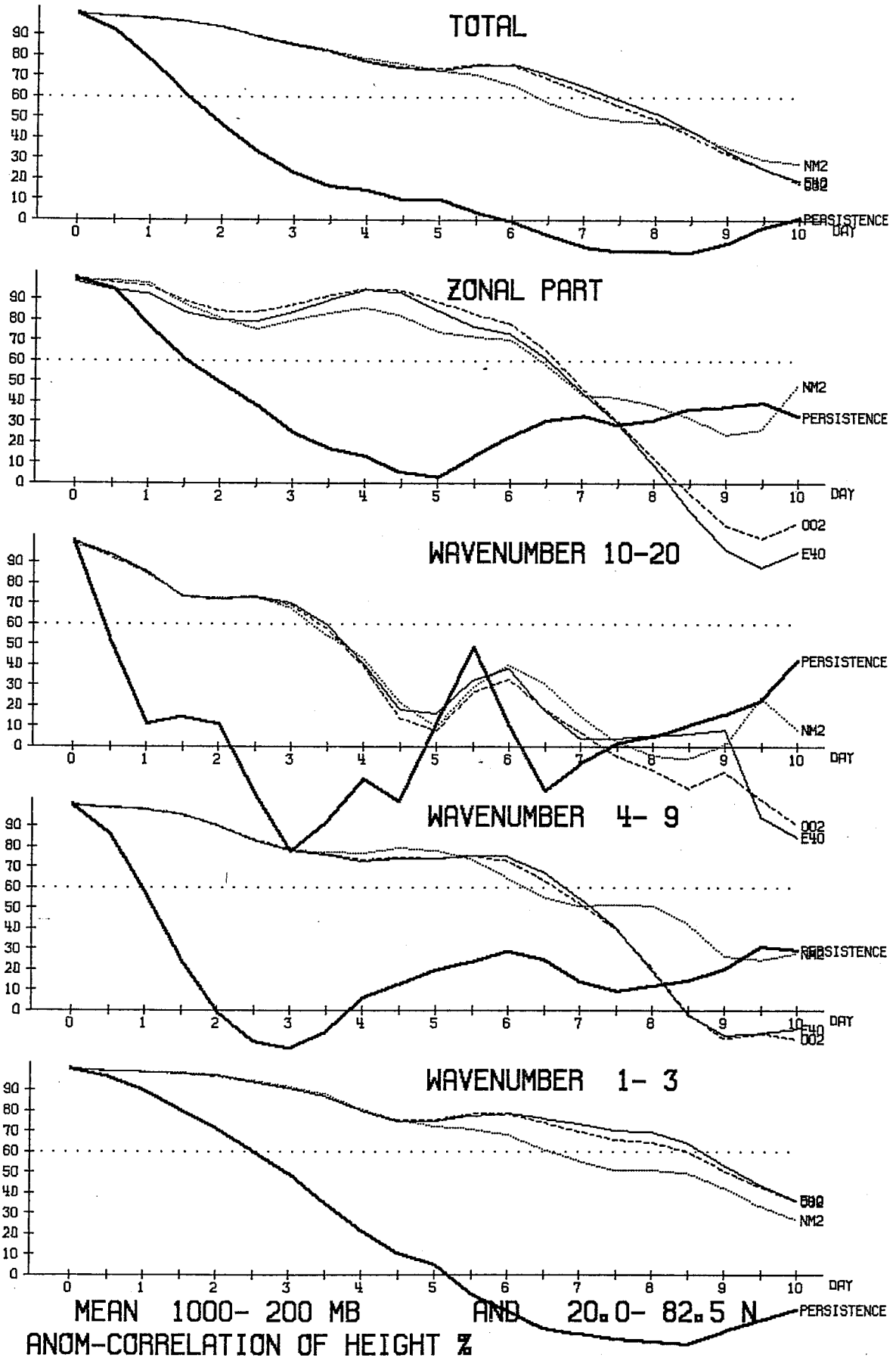
TOTAL
NM2
002
E40
PERSISTENCE
DAY
ZONAL PART
NM2
PERSISTENCE
DAY
002
E40
WAVENUMBER 10-20
PERSISTENCE
NM2
DAY
002
E40
WAVENUMBER 4- 9
PERSISTENCE
NM2
DAY
E40
002
WAVENUMBER 1- 3
002
NM2
DAY
PERSISTENCE
MEAN 1000- 200 MB AND 20.0- 82.5 N
ANOM-CORRELATION OF HEIGHT %

Fig. 31

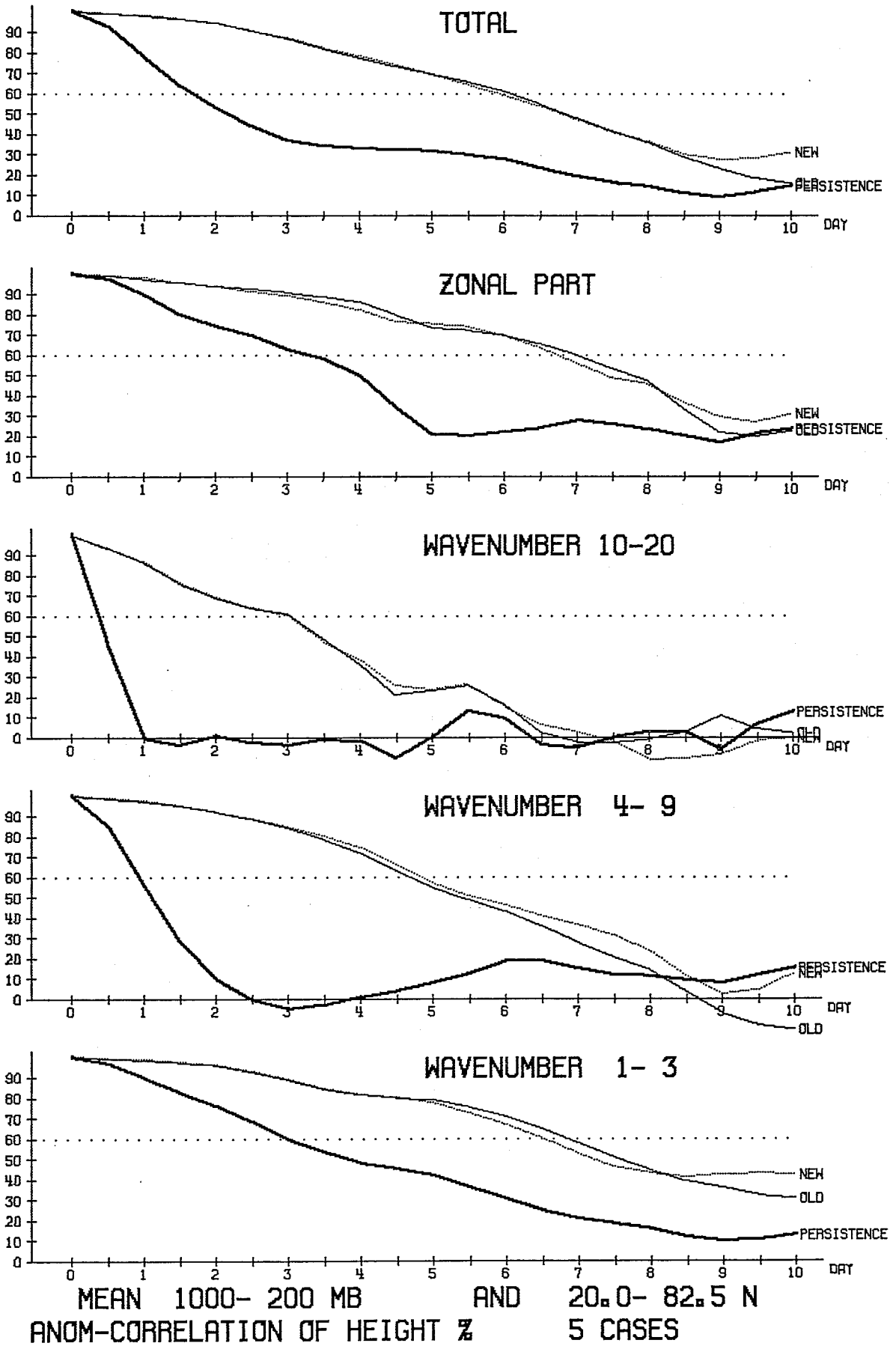
TOTAL
NEW
PERSISTENCE
DAY
ZONAL PART
NEW
PERSISTENCE
DAY
WAVENUMBER 10-20
PERSISTENCE
NEW
DAY
WAVENUMBER 4- 9
PERSISTENCE
NEW
OLD
DAY
WAVENUMBER 1- 3
NEW
OLD
PERSISTENCE
DAY
MEAN 1000- 200 MB AND 20.0- 82.5 N
ANOM-CORRELATION OF HEIGHT % 5 CASES

Fig. 32

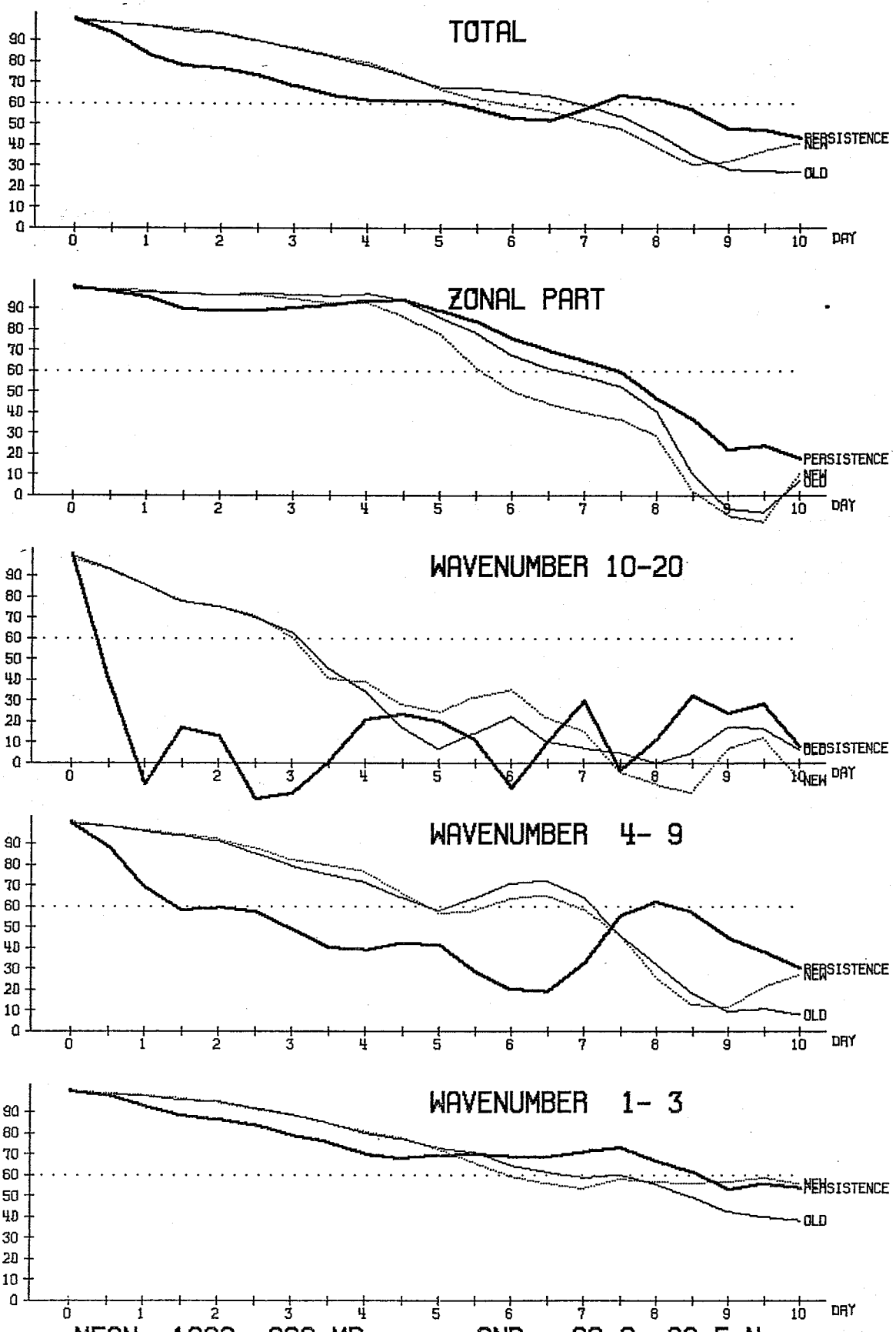
TOTAL
PERSISTENCE
NEW
OLD
DAY
ZONAL PART
PERSISTENCE
NEW
OLD
DAY
WAVENUMBER 10-20
PERSISTENCE
NEW
DAY
WAVENUMBER 4- 9
PERSISTENCE
NEW
OLD
DAY
WAVENUMBER 1- 3
PERSISTENCE
NEW
OLD
DAY
MEAN 1000- 200 MB AND 20.0- 82.5 N
ANOM-CORREL OF HEIGHT STANDING

Fig. 33

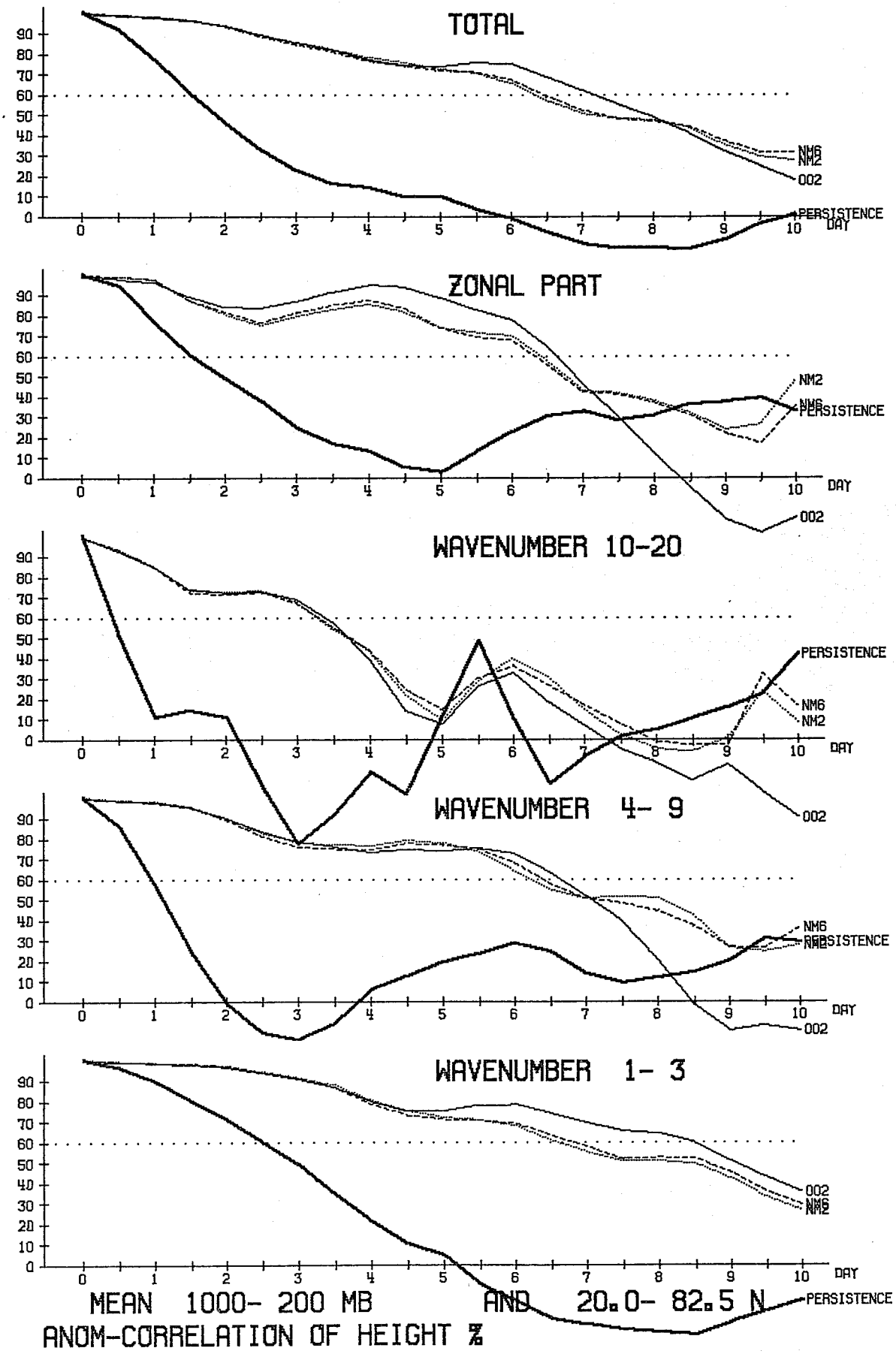
TOTAL
NM6
NM2
002
PERSISTENCE
DAY
ZONAL PART
NM2
NM6
PERSISTENCE
DAY
002
WAVENUMBER 10-20
PERSISTENCE
NM6
NM2
DAY
002
WAVENUMBER 4- 9
NM6
PERSISTENCE
DAY
002
WAVENUMBER 1- 3
002
NM6
NM2
DAY
PERSISTENCE
MEAN 1000- 200 MB AND 20.0- 82.5 N
ANOM-CORRELATION OF HEIGHT %

Fig. 34

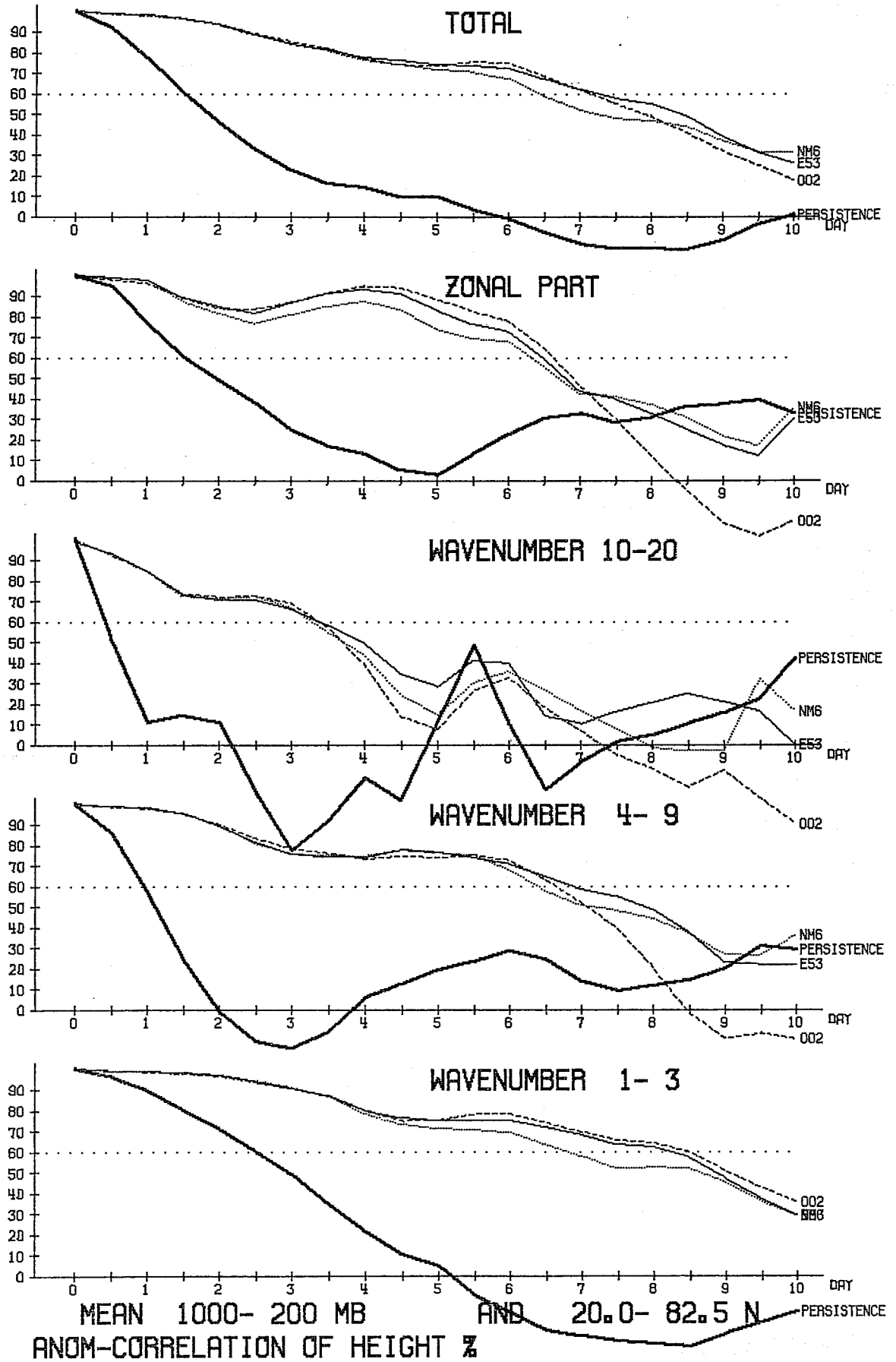
TOTAL
NM6
E53
002
PERSISTENCE
DAY
ZONAL PART
NM6
E53
PERSISTENCE
DAY
002
WAVENUMBER 10-20
PERSISTENCE
NM6
E53
DAY
002
WAVENUMBER 4- 9
NM6
PERSISTENCE
E53
DAY
002
WAVENUMBER 1- 3
002
NM6
DAY
PERSISTENCE
MEAN 1000- 200 MB AND 20.0- 82.5 N
ANOM-CORRELATION OF HEIGHT %

Fig. 35

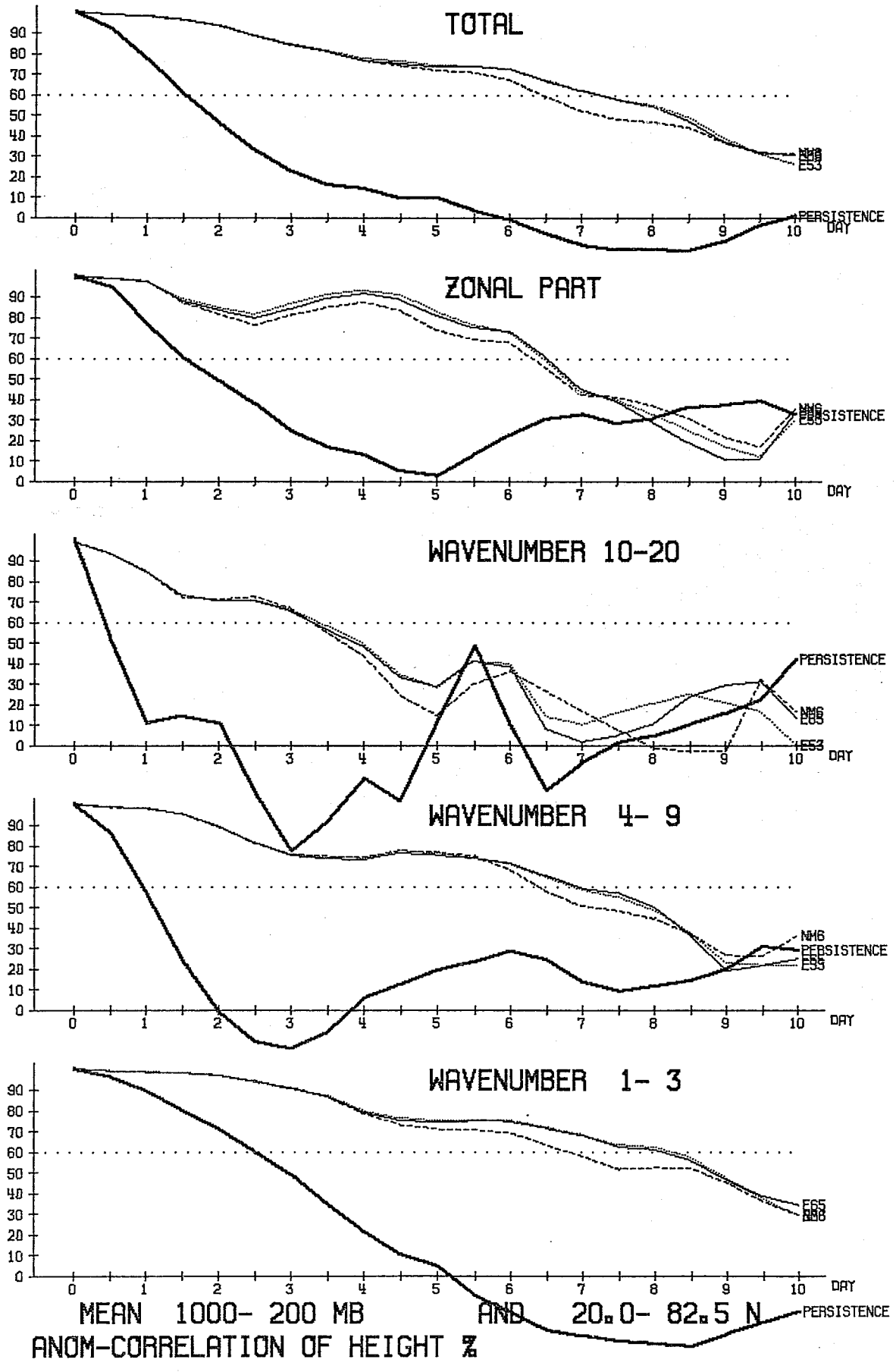
TOTAL
ZONAL PART
WAVENUMBER 10-20
WAVENUMBER 4- 9
WAVENUMBER 1- 3
PERSISTENCE
DAY
MEAN 1000- 200 MB AND 20.0- 82.5 N
ANOM-CORRELATION OF HEIGHT %

Fig. 36

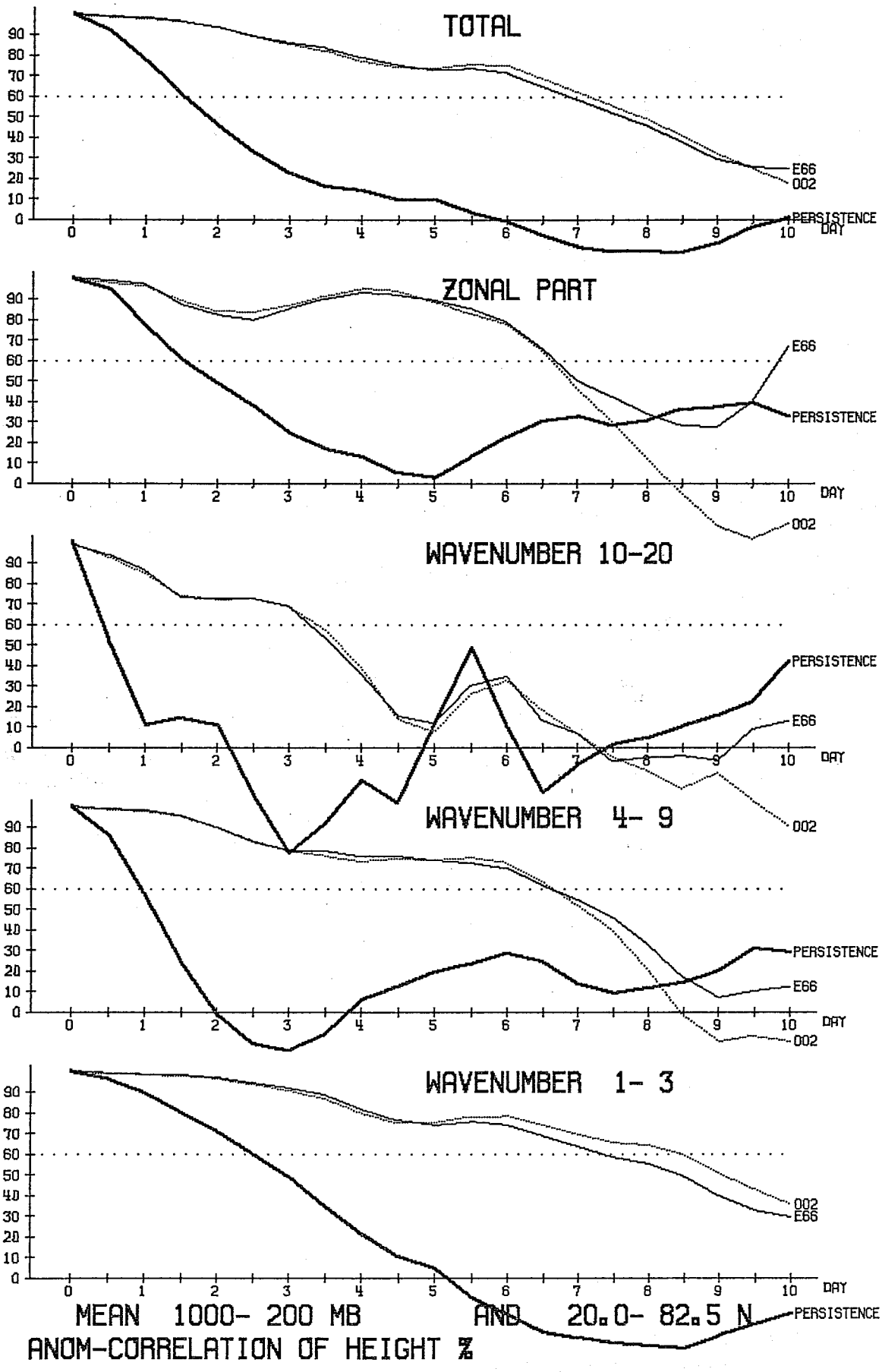
TOTAL
E66
002
PERSISTENCE
DAY
ZONAL PART
E66
PERSISTENCE
002
DAY
WAVENUMBER 10-20
PERSISTENCE
E66
002
DAY
WAVENUMBER 4- 9
PERSISTENCE
E66
002
DAY
WAVENUMBER 1- 3
002
E66
PERSISTENCE
DAY
MEAN 1000- 200 MB AND 20.0- 82.5 N
ANOM-CORRELATION OF HEIGHT %

Fig. 37

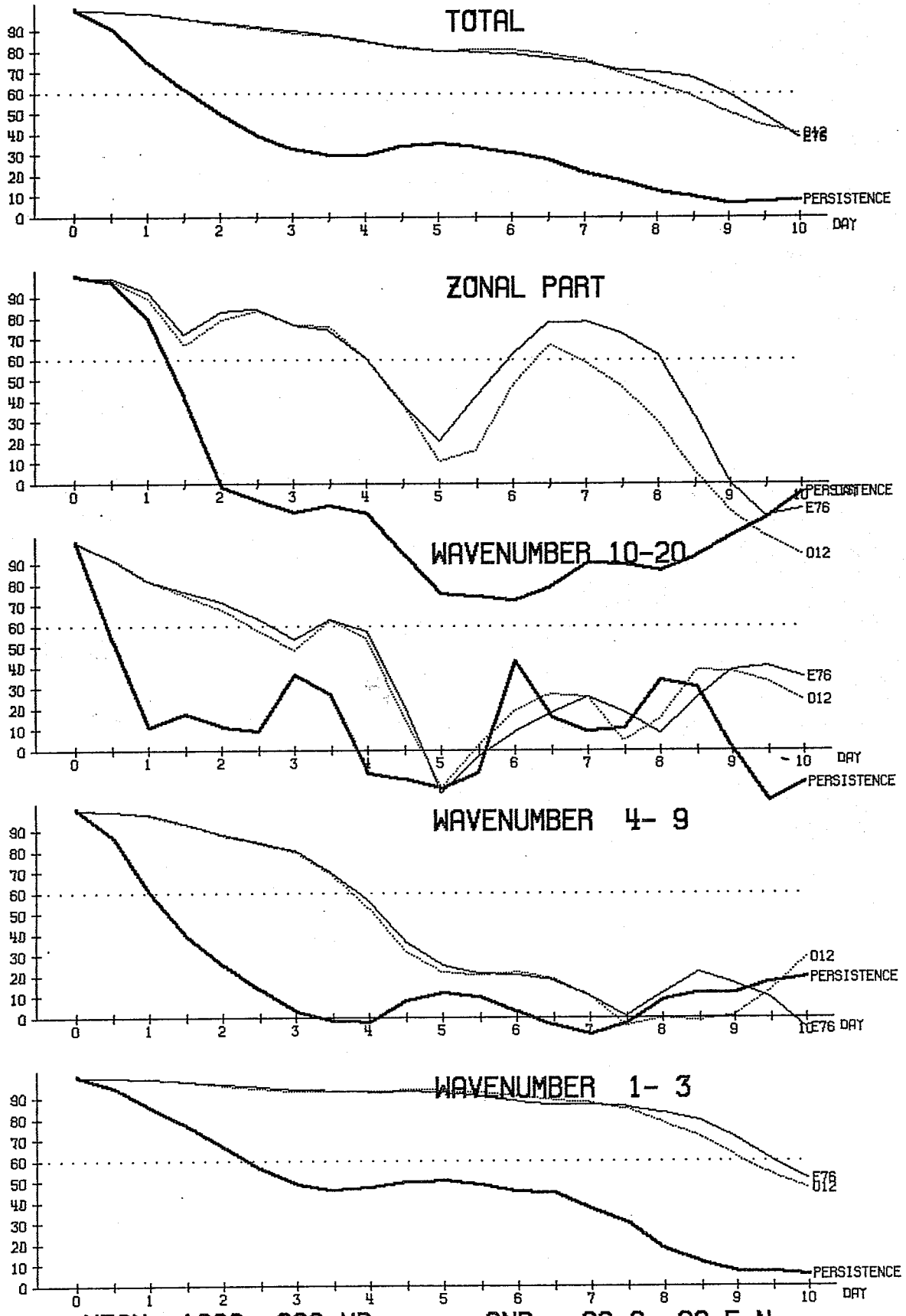
TOTAL
E76
PERSISTENCE
DAY
ZONAL PART
PERSISTENCE
E76
012
WAVENUMBER 10-20
E76
012
DAY
PERSISTENCE
WAVENUMBER 4- 9
012
PERSISTENCE
E76
DAY
WAVENUMBER 1- 3
E76
012
PERSISTENCE
DAY
MEAN 1000- 200 MB AND 20.0- 82.5 N
ANOM-CORRELATION OF HEIGHT %

Fig. 38

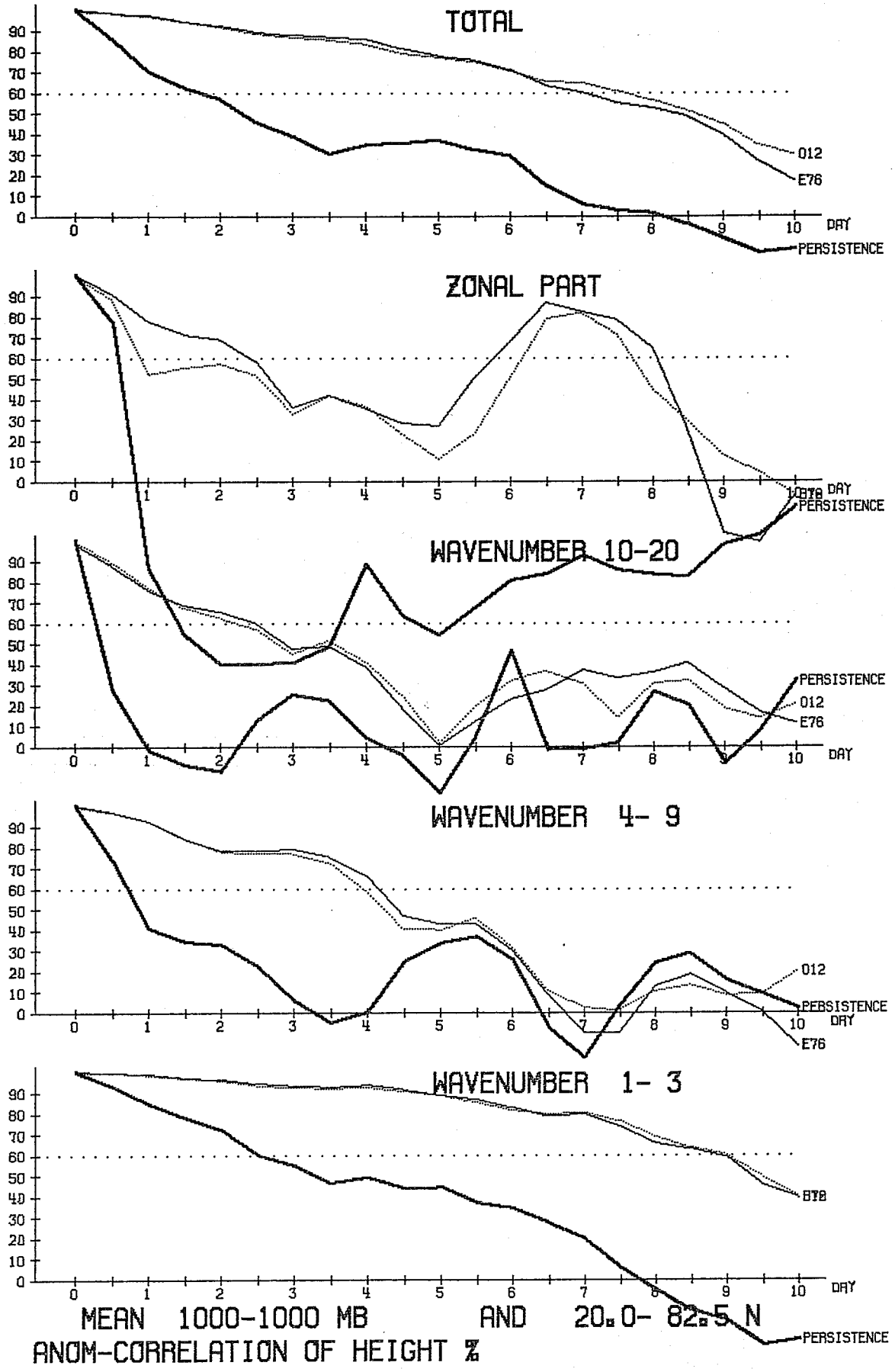
TOTAL
012
E76
DAY
PERSISTENCE
ZONAL PART
DAY
PERSISTENCE
WAVENUMBER 10-20
PERSISTENCE
012
E76
DAY
WAVENUMBER 4- 9
012
PERSISTENCE
DAY
E76
WAVENUMBER 1- 3
DAY
PERSISTENCE
MEAN 1000-1000 MB AND 20.0- 82.5 N
ANOM-CORRELATION OF HEIGHT %

Fig. 39

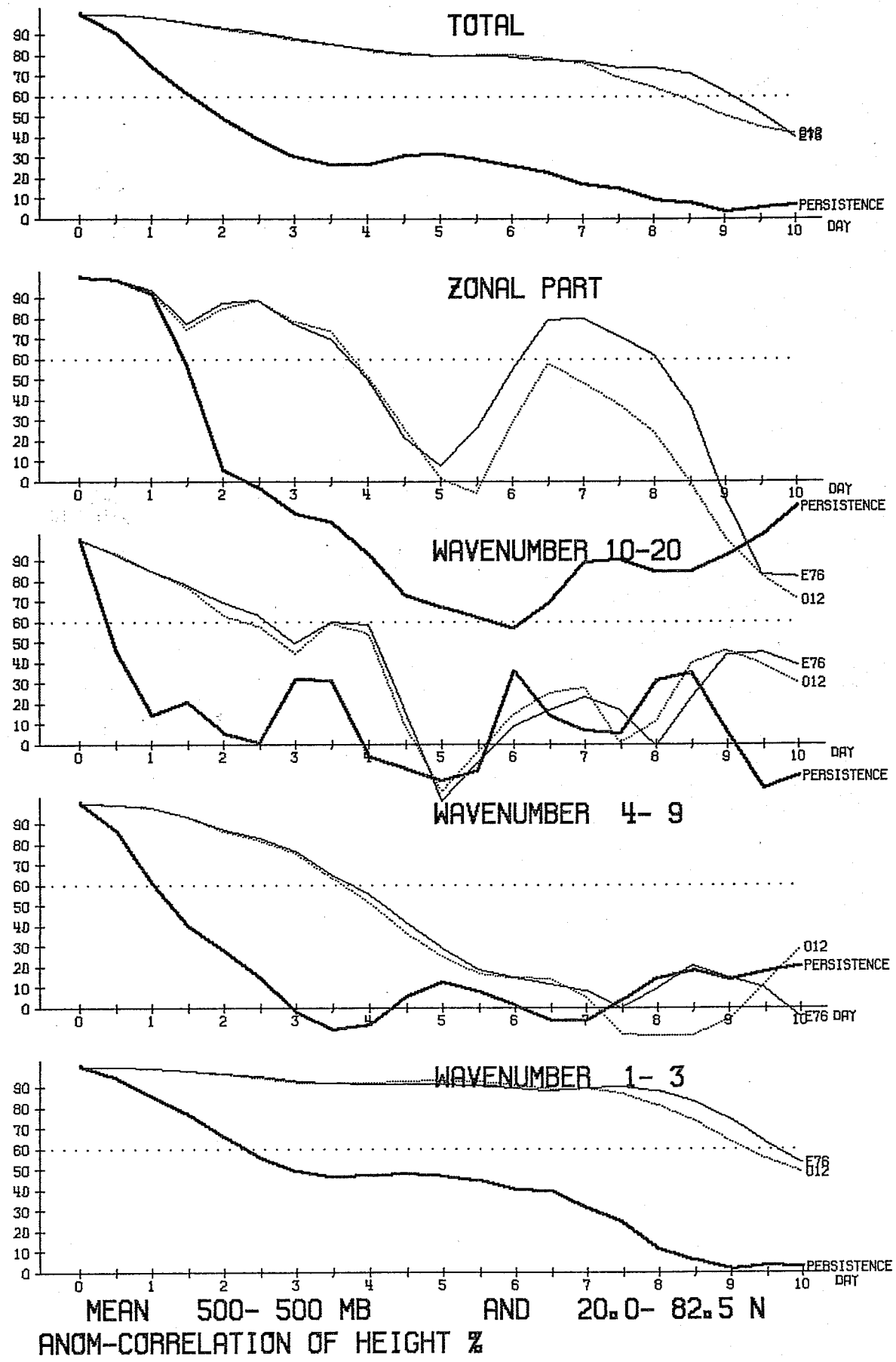
TOTAL
PERSISTENCE
DAY
ZONAL PART
DAY
PERSISTENCE
WAVENUMBER 10-20
E76
012
E76
012
DAY
PERSISTENCE
WAVENUMBER 4- 9
012
PERSISTENCE
E76 DAY
WAVENUMBER 1- 3
E76
012
PERSISTENCE
DAY
MEAN 500- 500 MB AND 20.0- 82.5 N
ANOM-CORRELATION OF HEIGHT %

Fig. 40

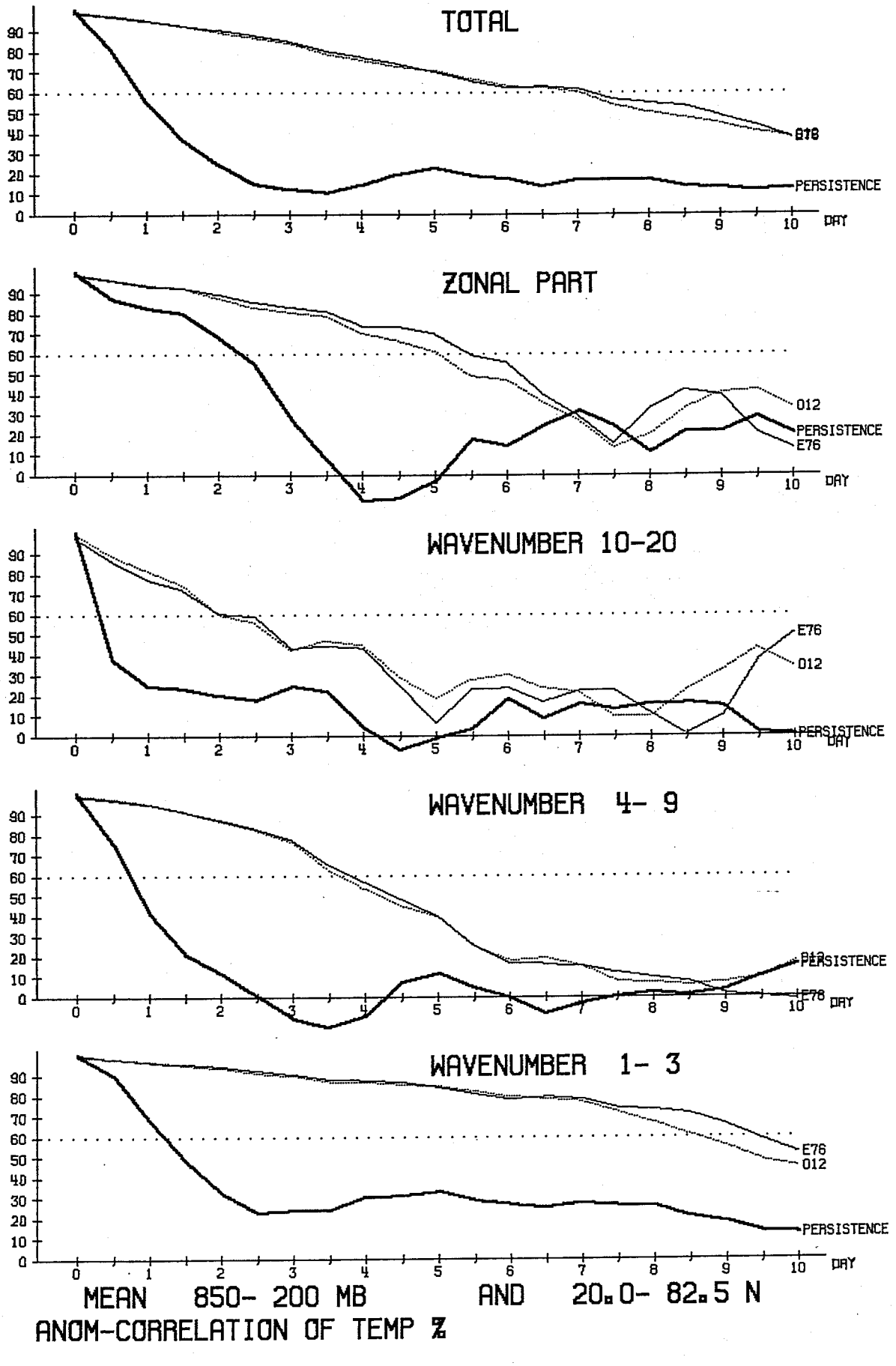
TOTAL
E76
PERSISTENCE
DAY
ZONAL PART
012
PERSISTENCE
E76
DAY
WAVENUMBER 10-20
E76
012
PERSISTENCE
DAY
WAVENUMBER 4- 9
PERSISTENCE
E76
DAY
WAVENUMBER 1- 3
E76
012
PERSISTENCE
DAY
MEAN 850- 200 MB AND 20.0- 82.5 N
ANOM-CORRELATION OF TEMP %

Fig. 41

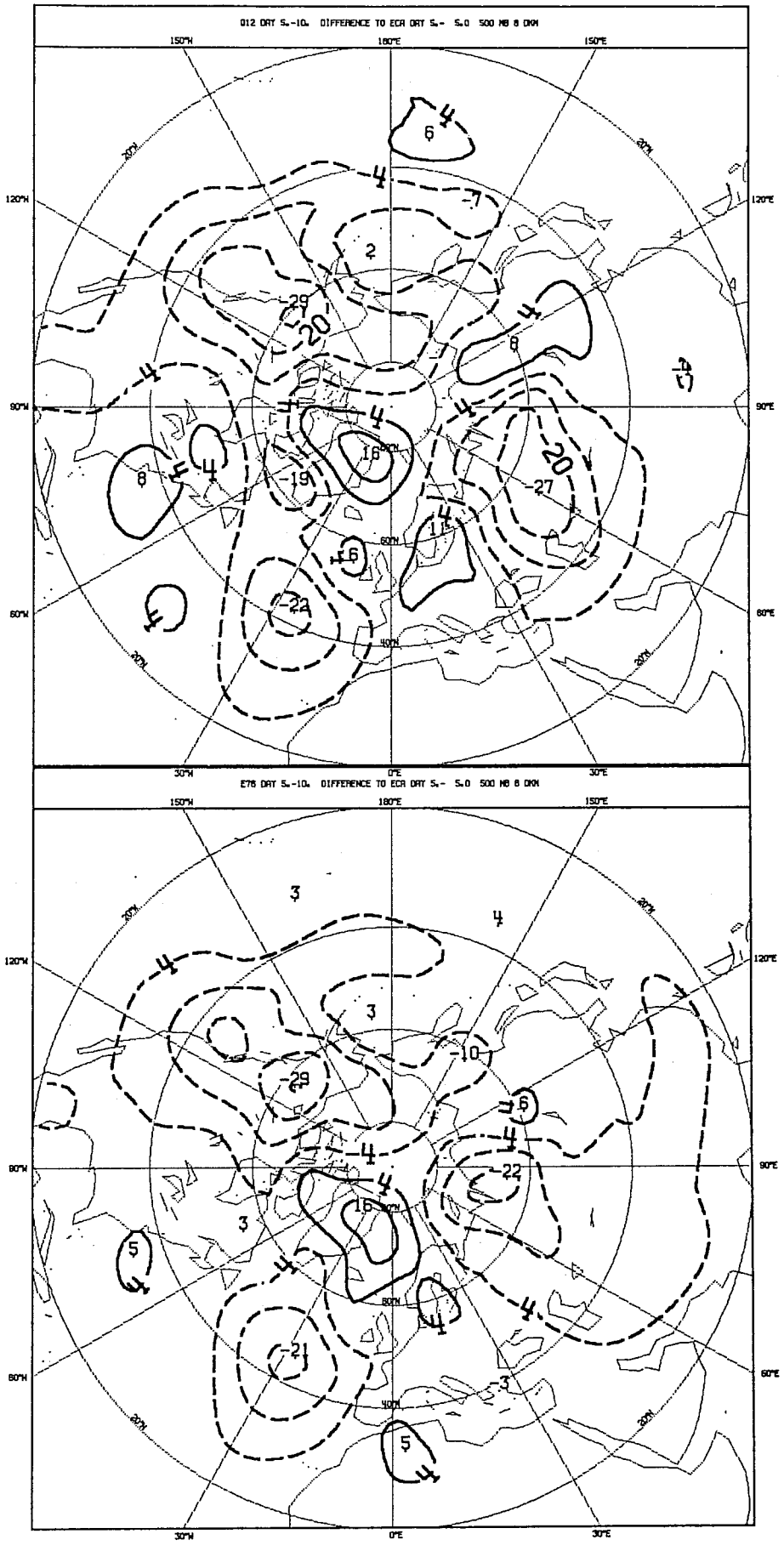
012 DAT 5.-10. DIFFERENCE TO ECA DAT 5.- 5.0 500 MB 8 DKM
150°W
180°E
150°E
120°W
120°E
90°W
90°E
60°W
60°E
30°W
0°E
30°E
20°N
40°N
60°N
E76 DAT 5.-10. DIFFERENCE TO ECA DAT 5.- 5.0 500 MB 8 DKM

Fig. 42

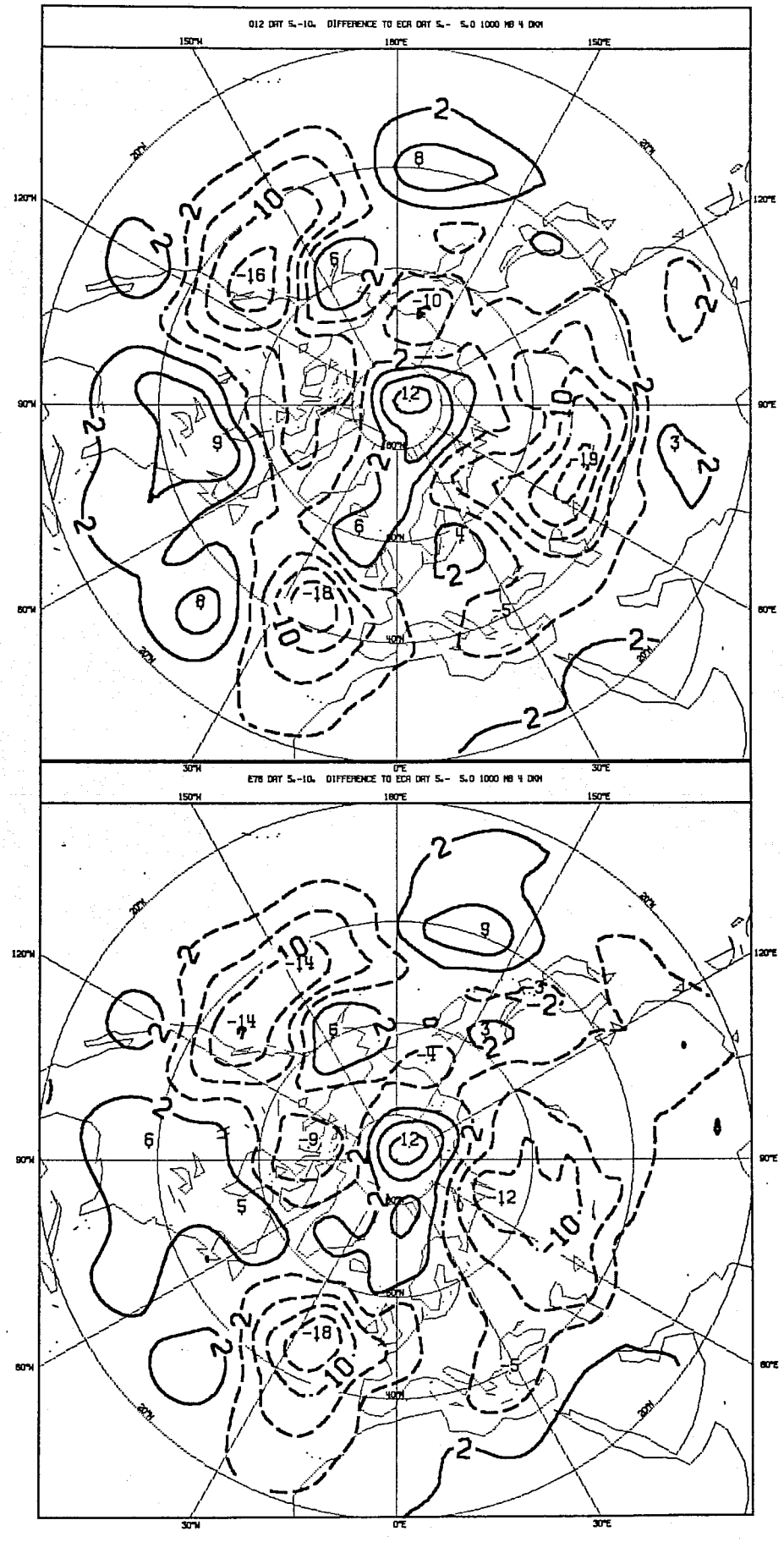
012 DAT 5.-10. DIFFERENCE TO ECA DAT 5.- 5.0 1000 MB 4 DKM
E78 DAT 5.-10. DIFFERENCE TO ECA DAT 5.- 5.0 1000 MB 4 DKM
150°W
180°E
150°E
120°W
120°E
90°W
90°E
60°W
60°E
30°W
0°E
30°E
20N
40N
60N
80N

Fig. 43

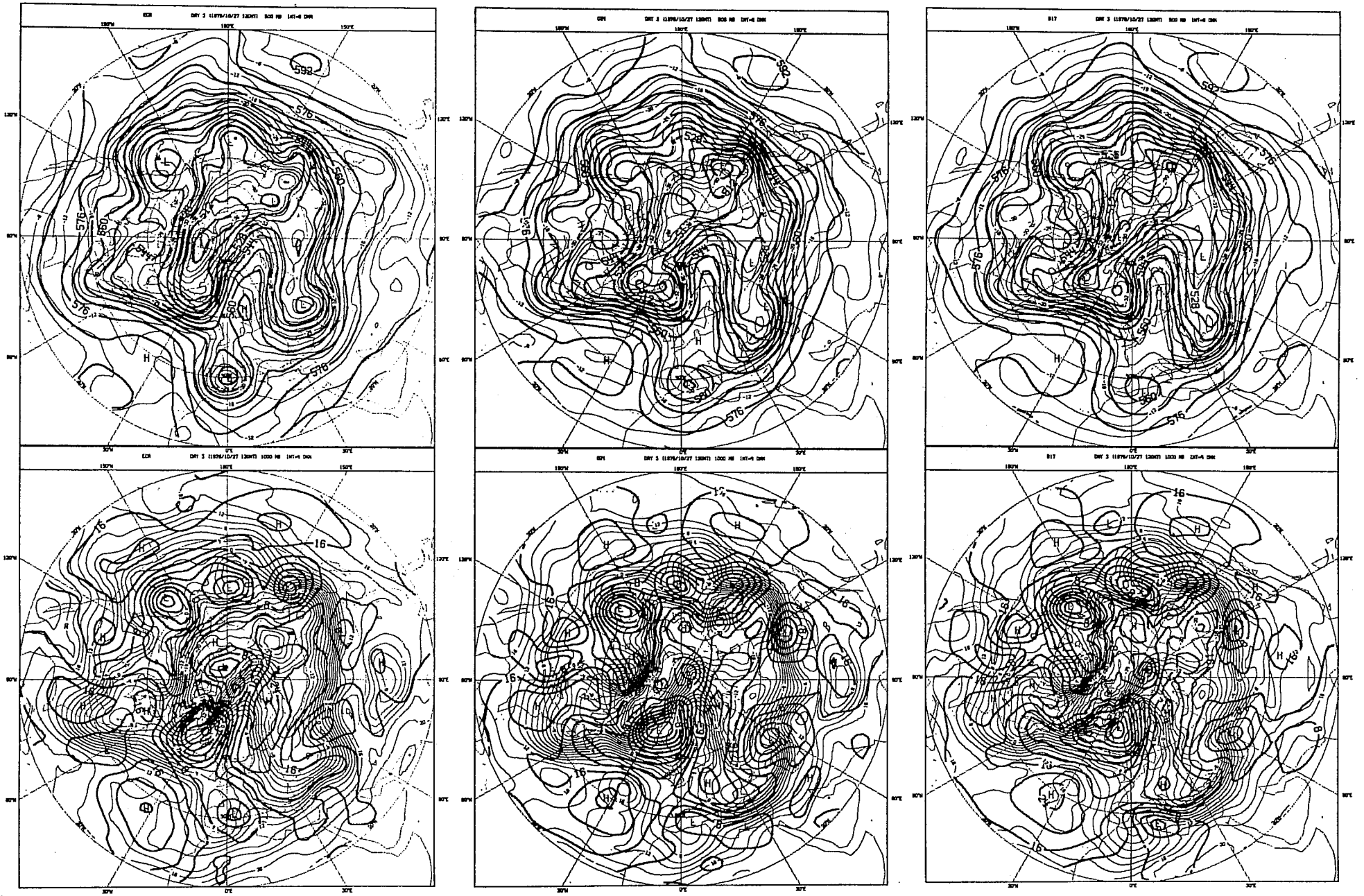

Fig. A1

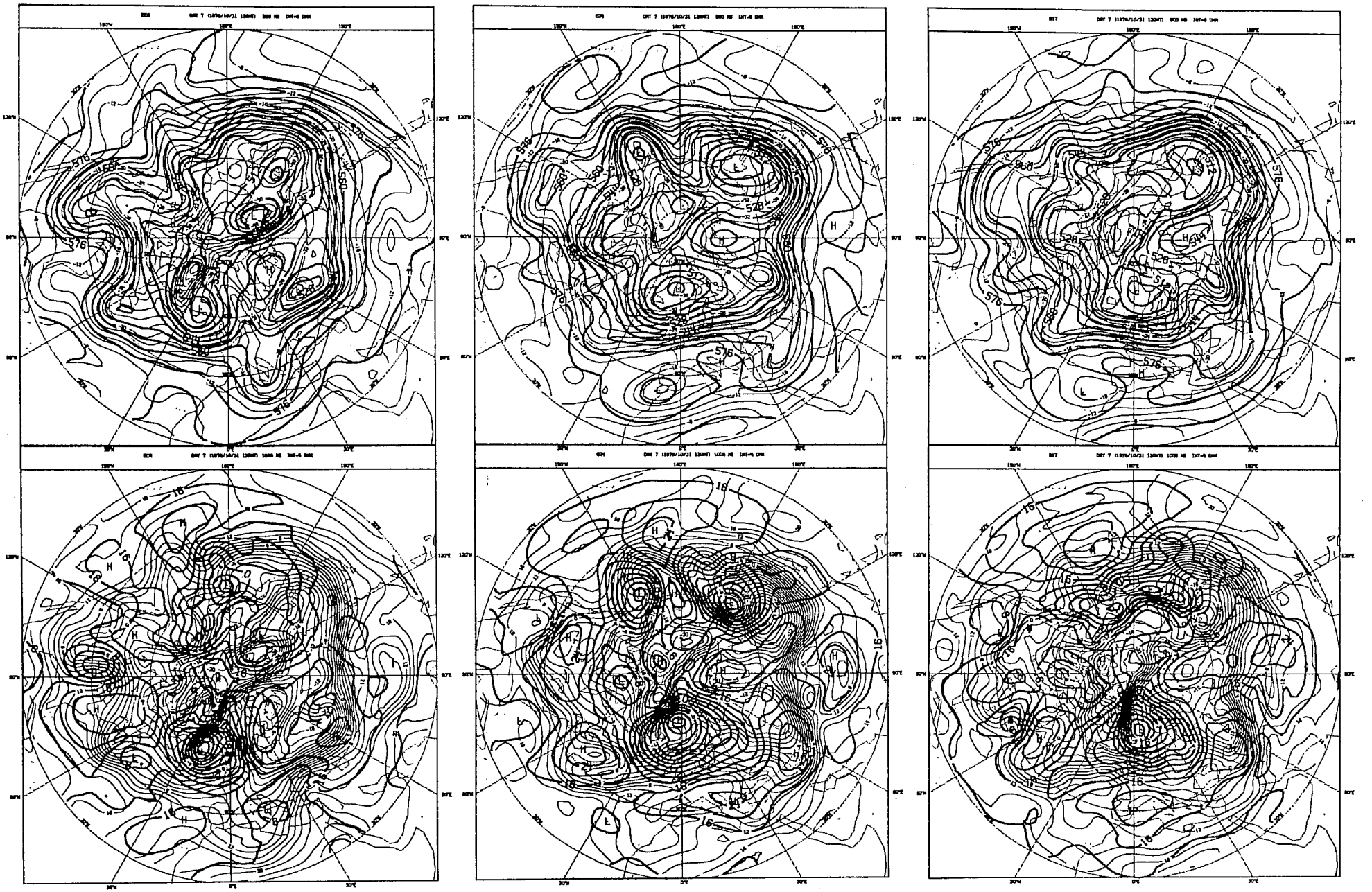

Fig. A2

Variance by Transient waves

500 MB

1000 MB

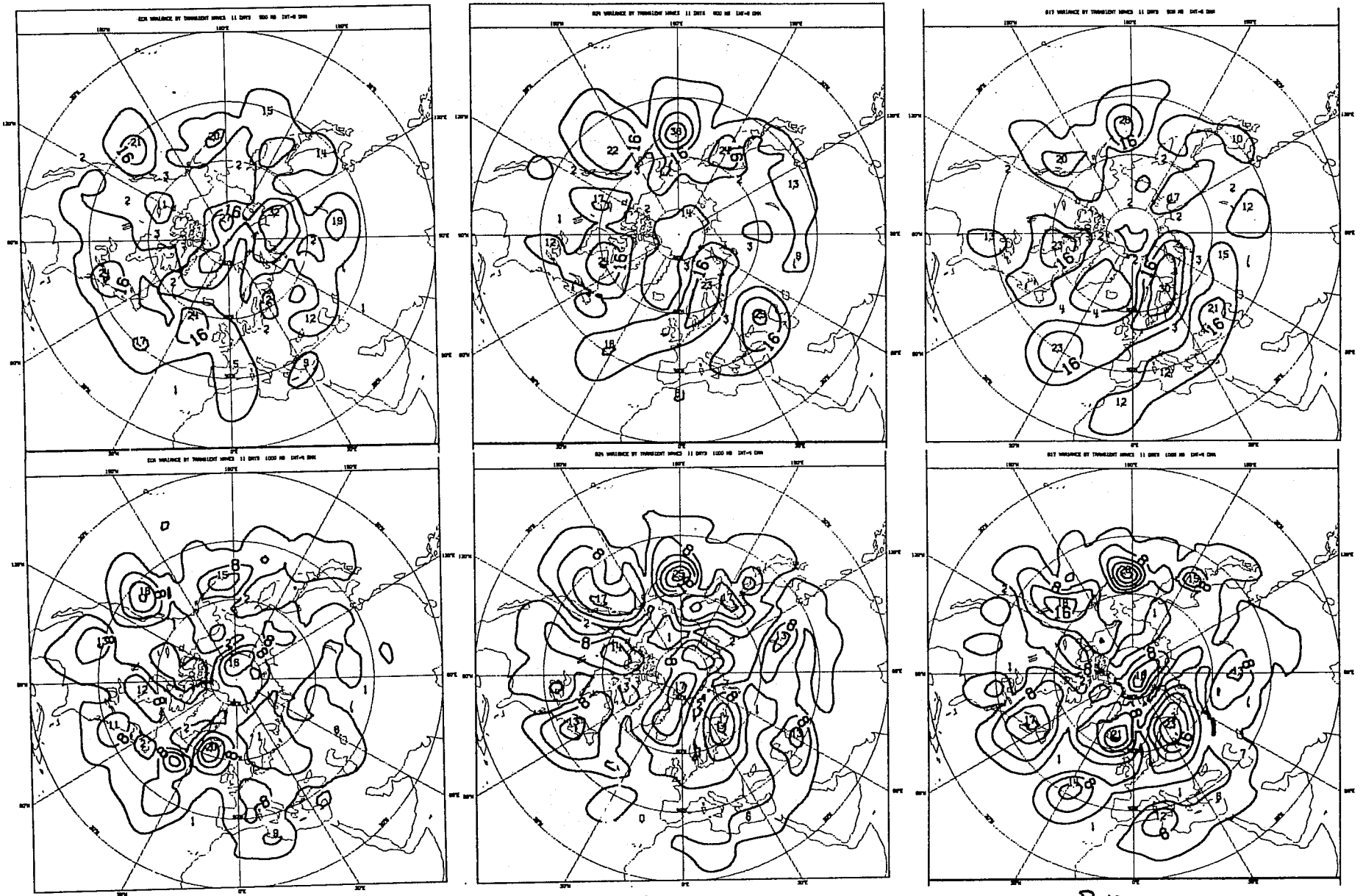

ECA

Fig. A3

Φ24

B17

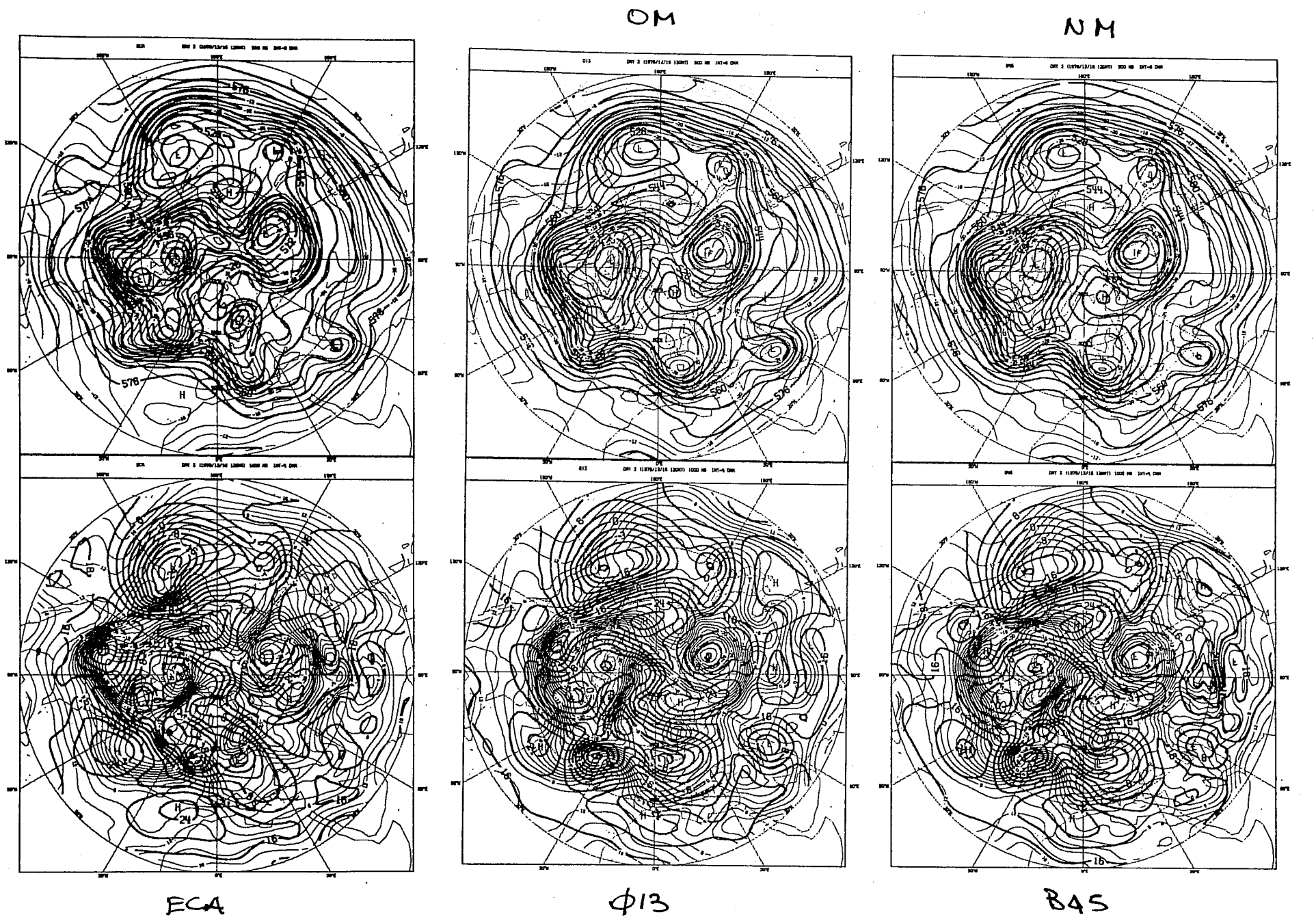

Fig. B1

DAY 3

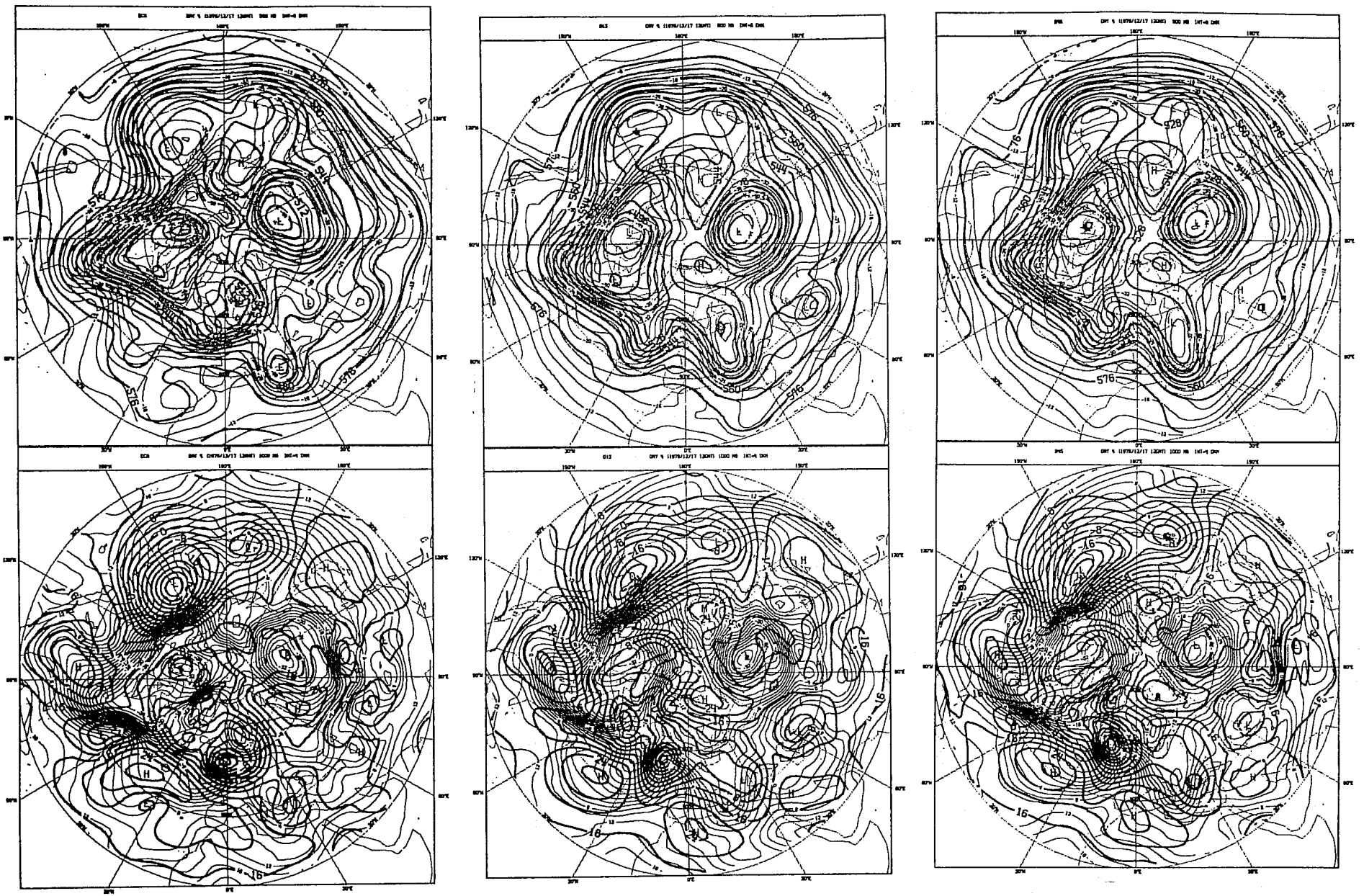

Fig. B2

OM

NM

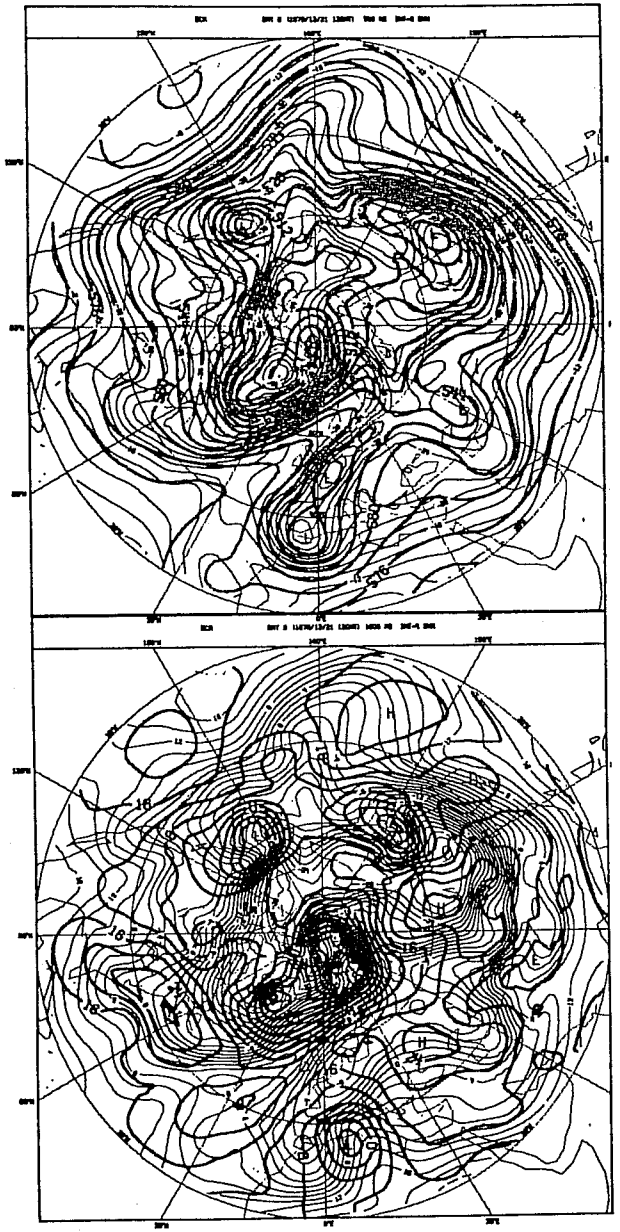

ECA

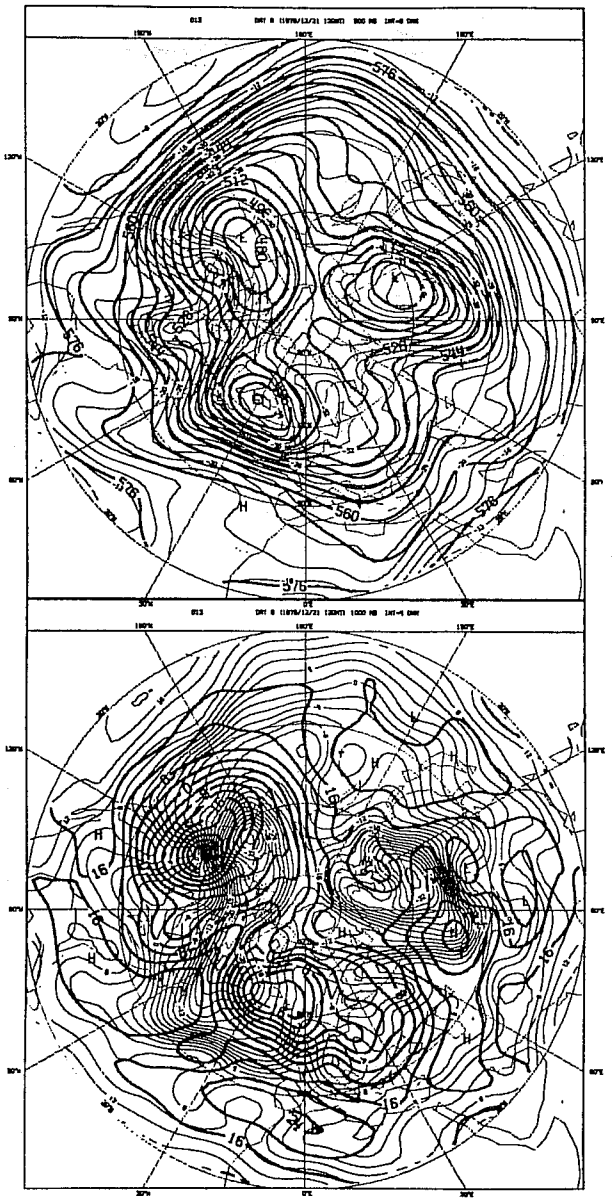

Ø13

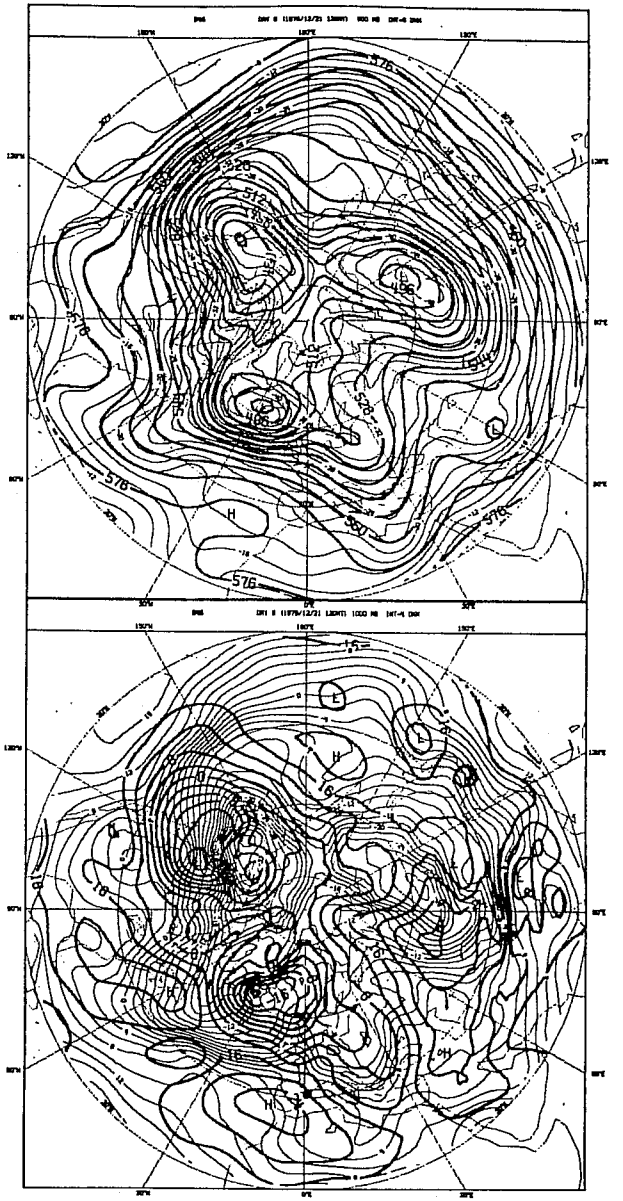

B45

Fig.B3.

DAY 8

Variance by Transient waves

500 MB

1000 MB

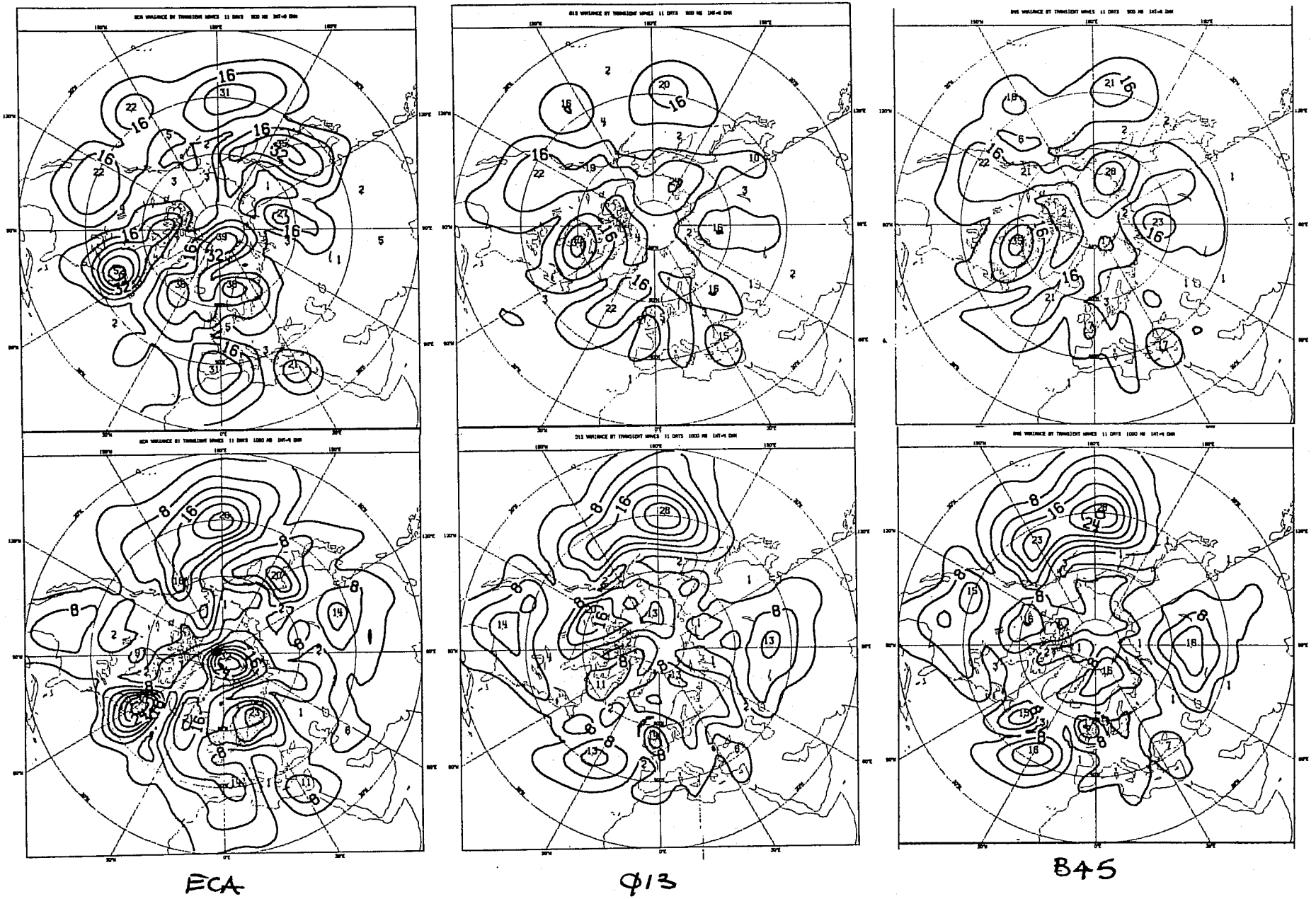

ECA

Φ13

B45

Fig. B4

NO CYCLE

CYCLE (4)

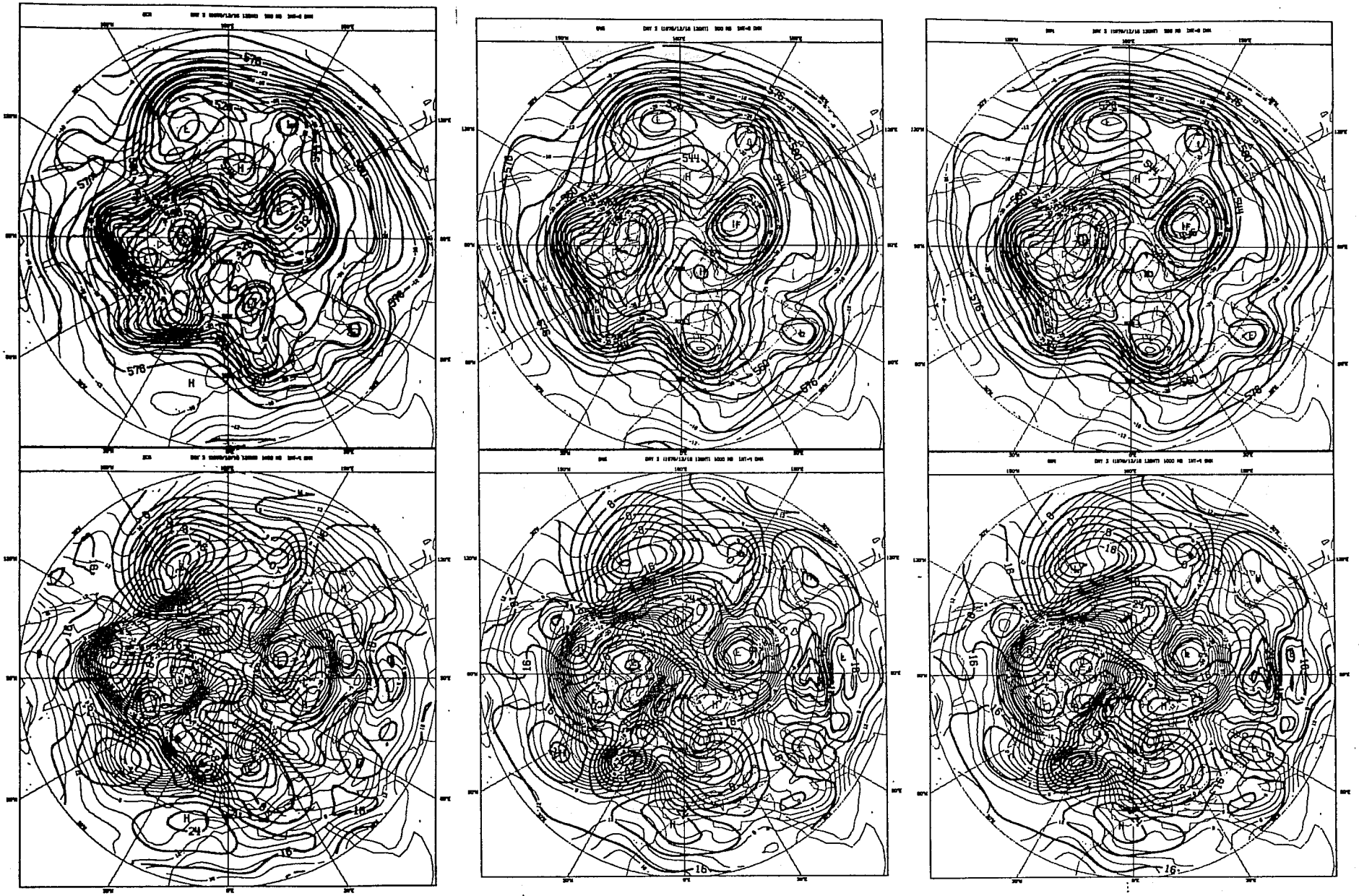

ECA

B45

B54

Fig. B5

DAY 3

NO CYCLE

CYCLE (4)

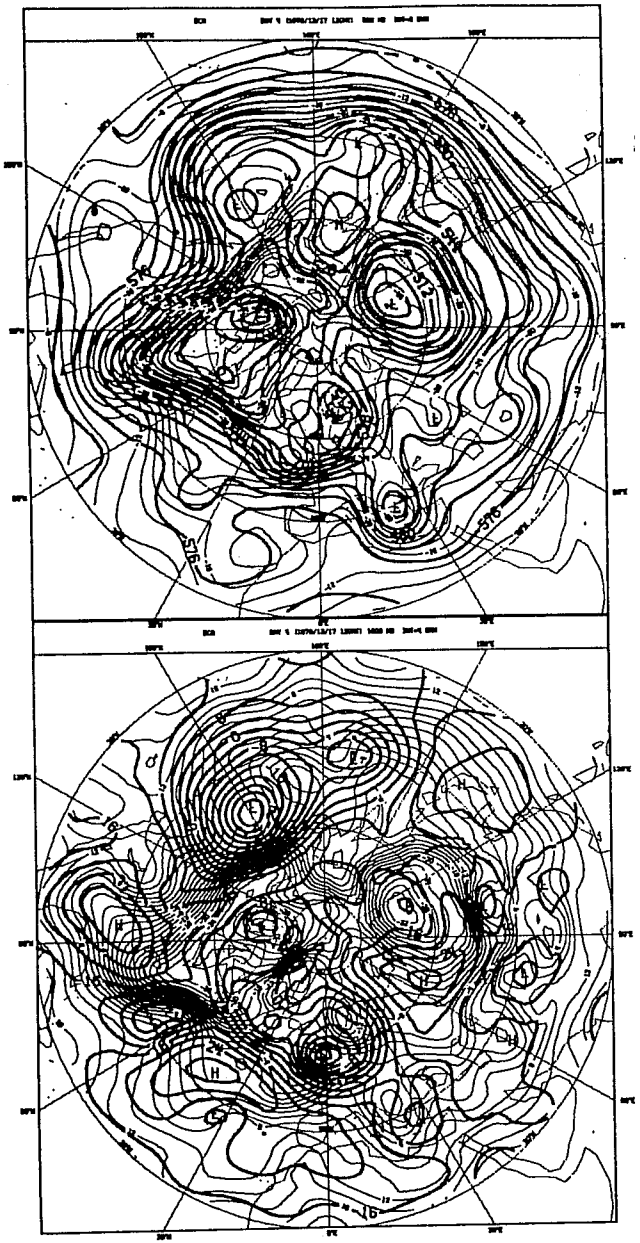

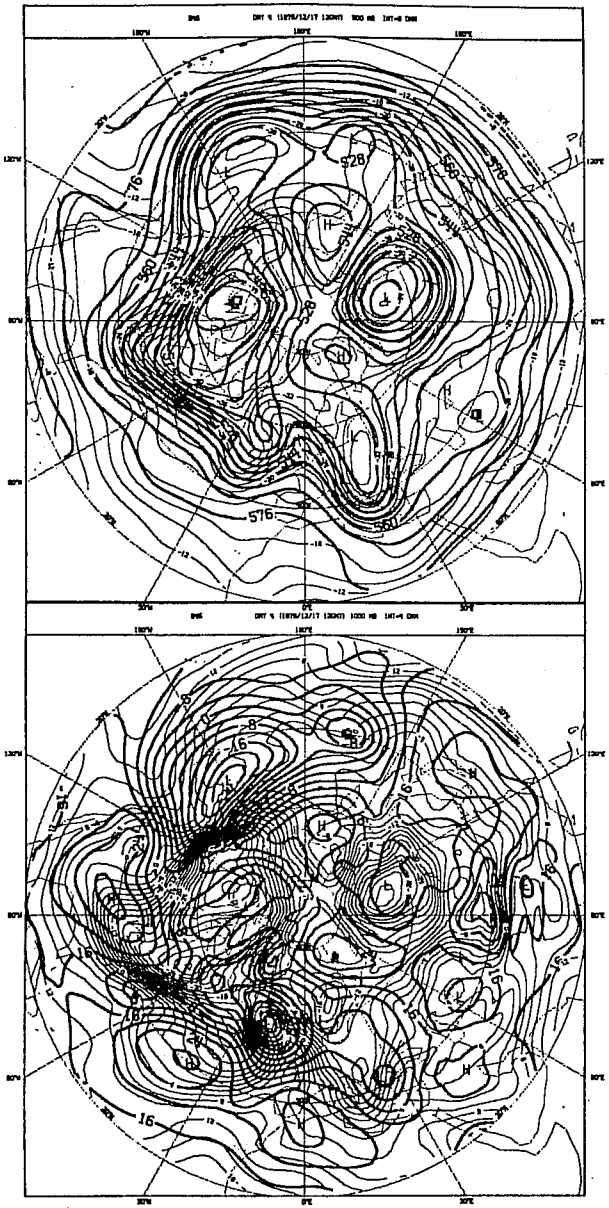

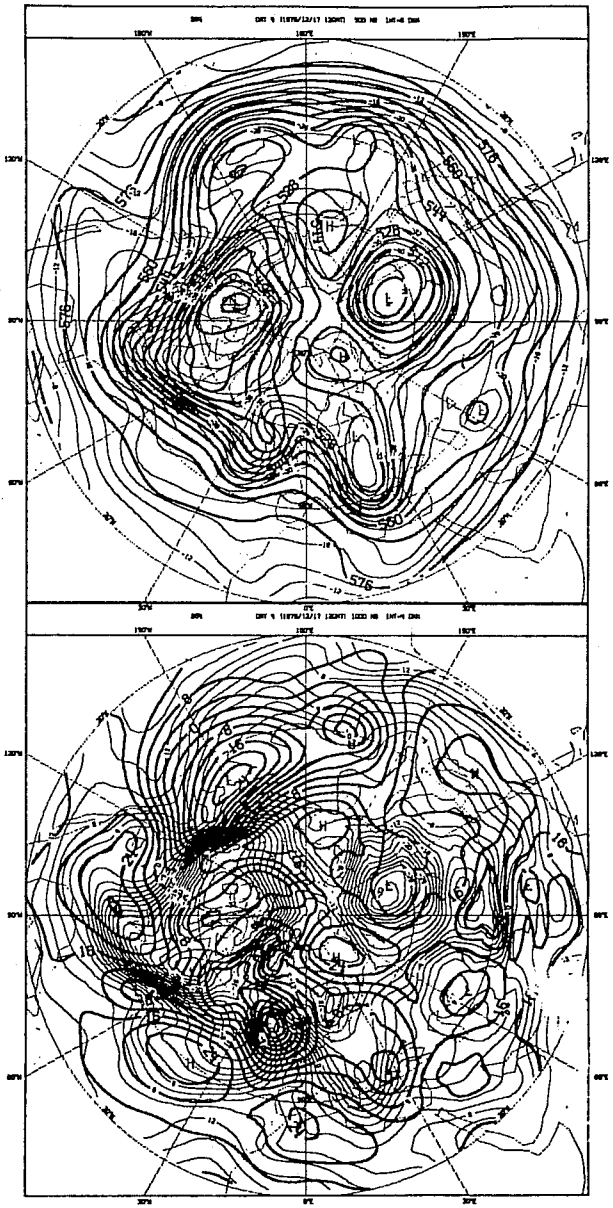

ECA

Fig. B6

B45

B54

DAY 4

NO CYCLE

CYCLE (4)

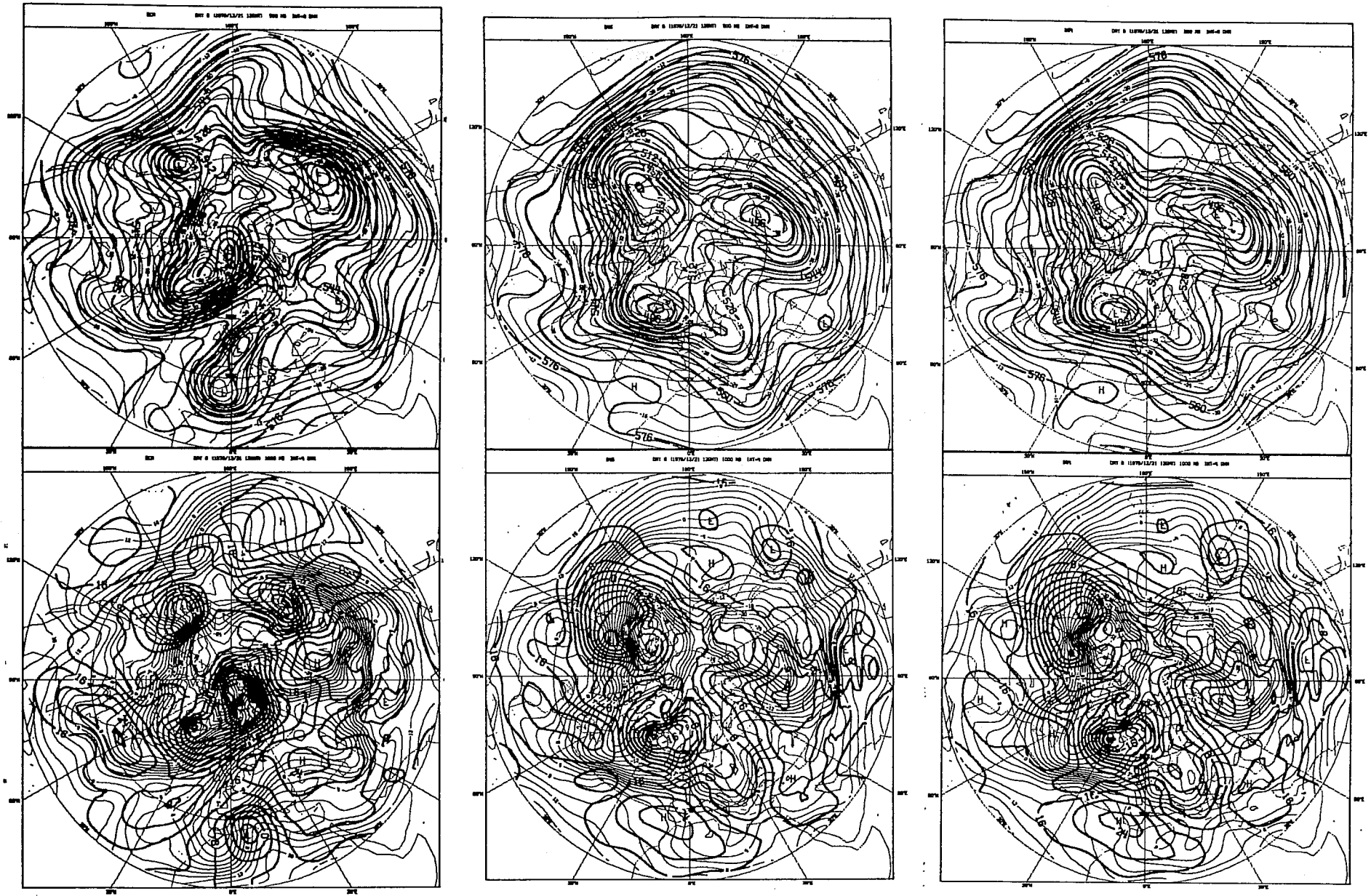

ECA

B45

B54

Fig. B7

DAY 8

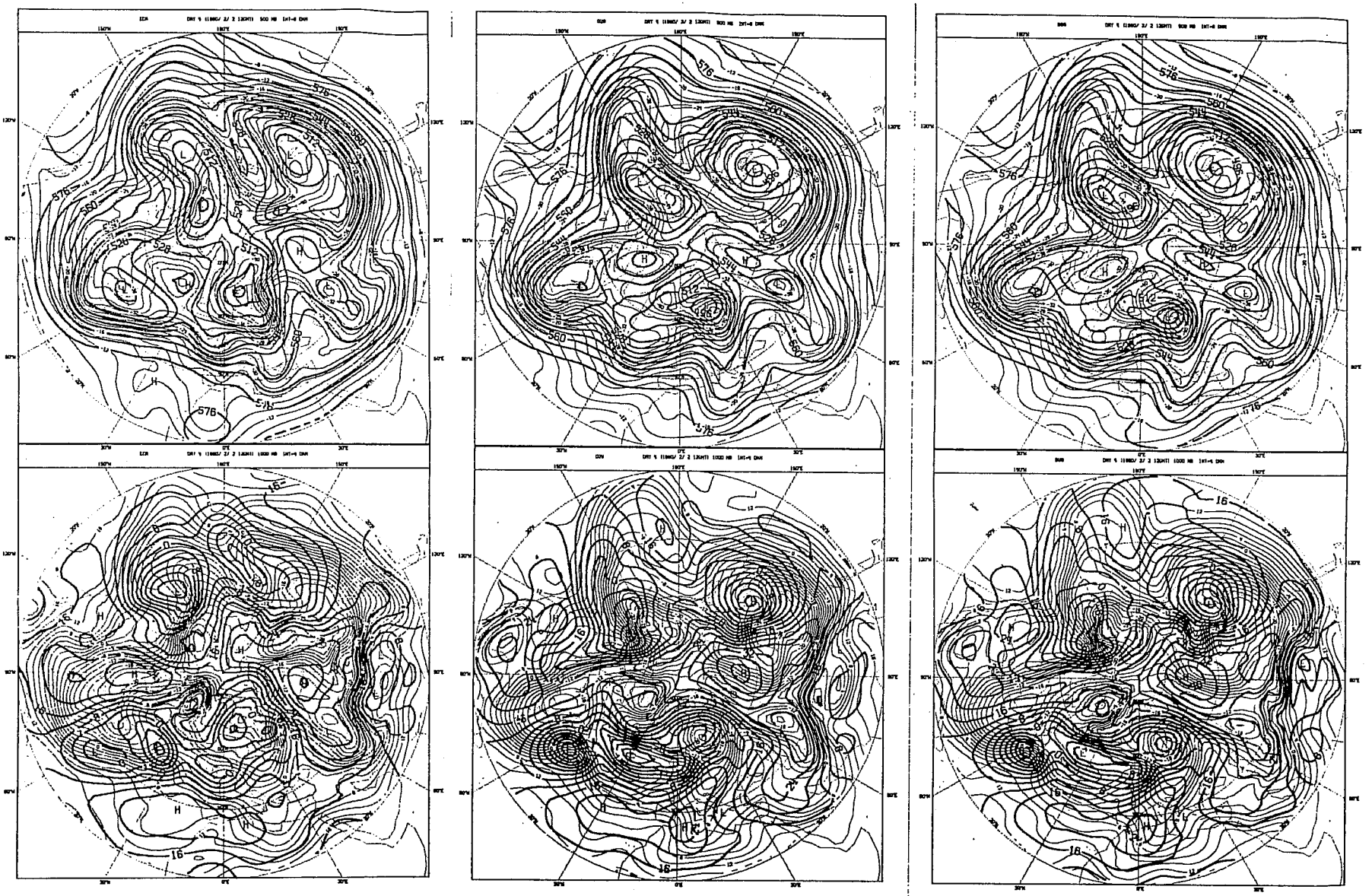

Fig. C1

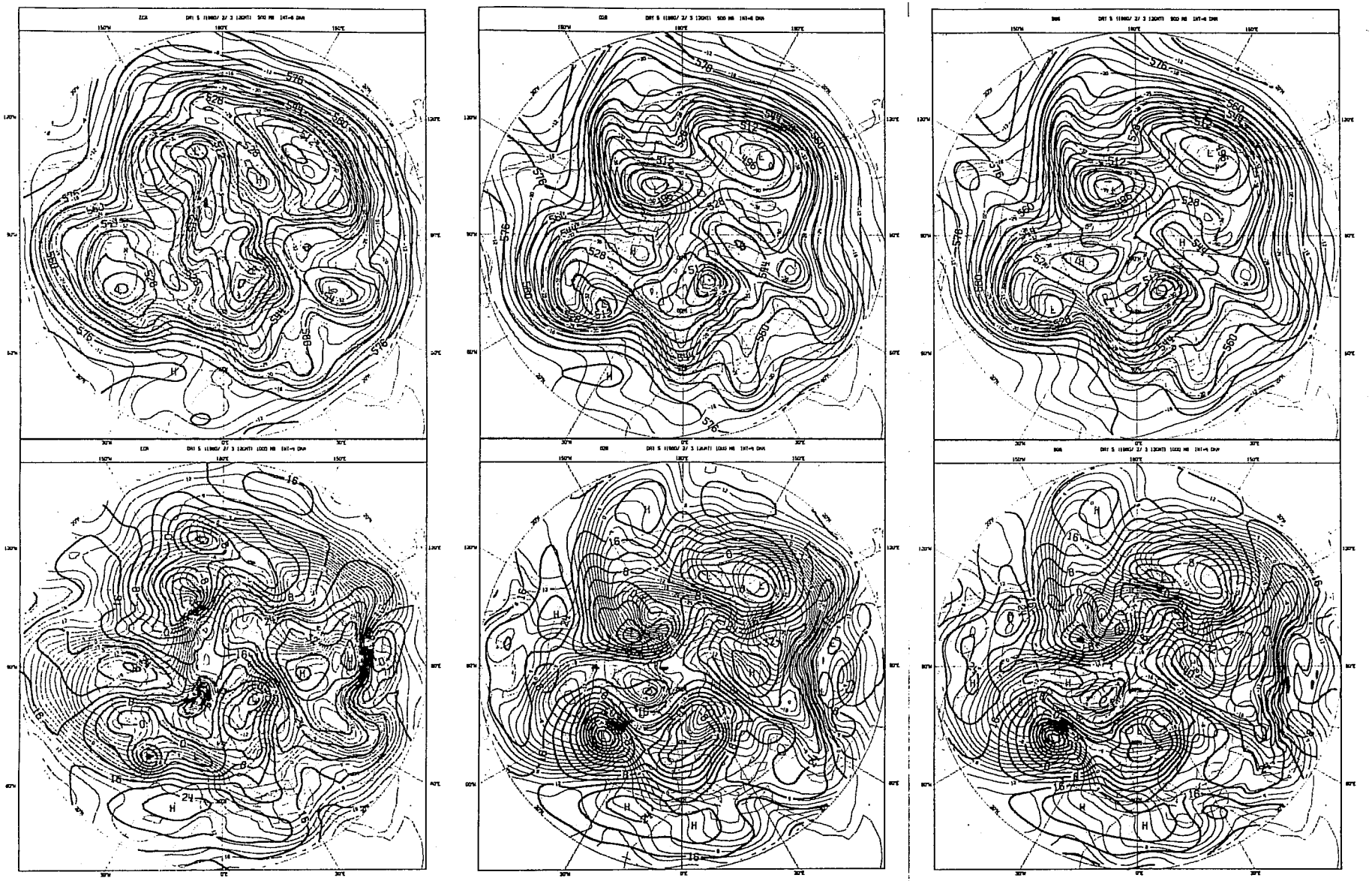

Fig. C2

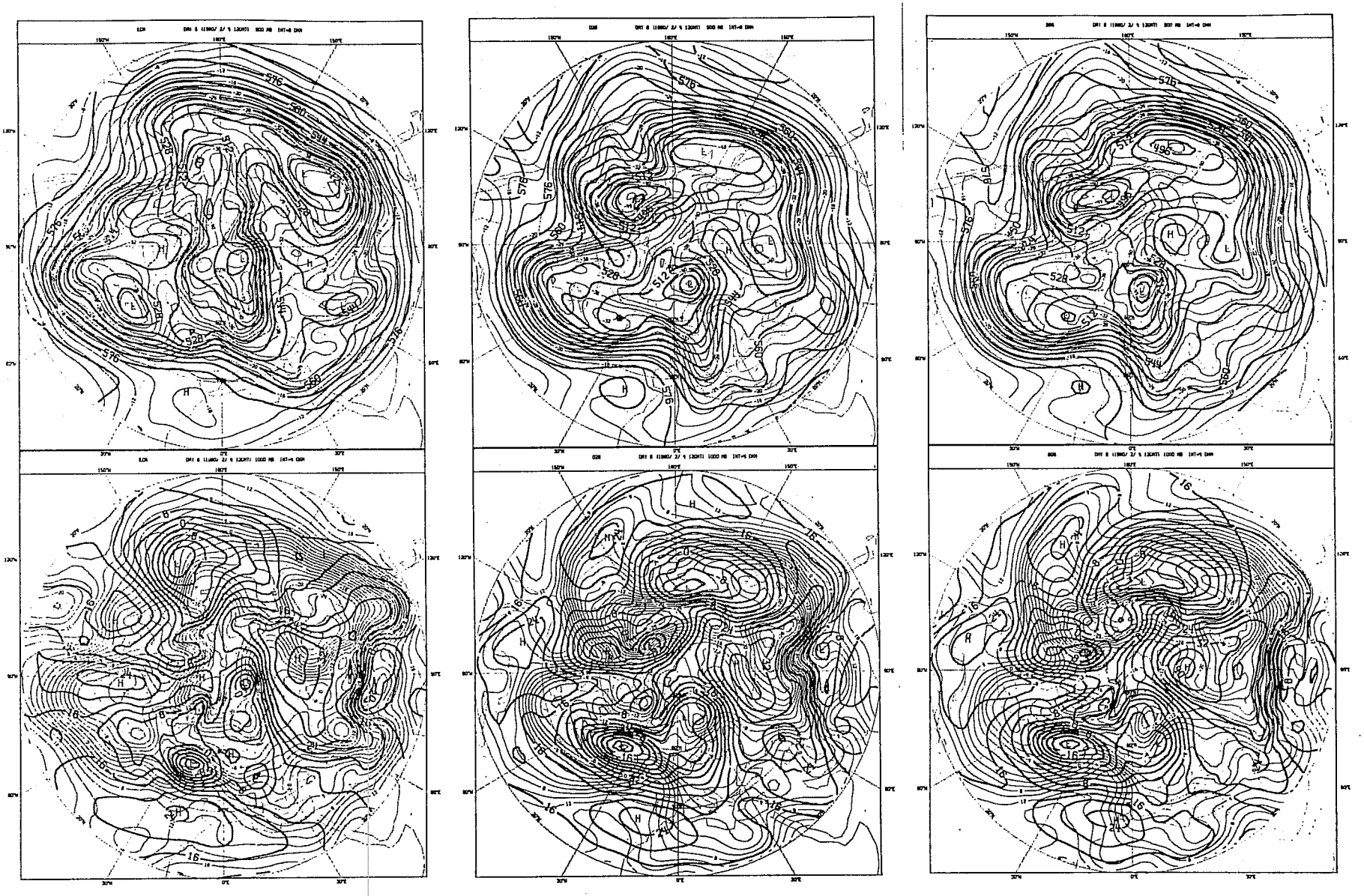

Fig. C3